United States
Environmental Protection
Agency

Office of Air Quality
Planning and Standards
Research Triangle Park, NC 27711

EPA-454/R-92-015
October 1992

Air

EPA

SENSITIVITY ANALYSIS OF A REVISED AREA SOURCE ALGORITHM FOR THE INDUSTRIAL SOURCE COMPLEX SHORT TERM MODEL

EPA-454/R-92-015

SENSITIVITY ANALYSIS OF A REVISED AREA SOURCE ALGORITHM FOR THE INDUSTRIAL SOURCE COMPLEX SHORT TERM MODEL

Office Of Air Quality Planning And Standards
Office Of Air And Radiation
U. S. Environmental Protection Agency
Research Triangle Park, NC 27711

October 1992

This report has been reviewed by the Office Of Air Quality Planning And Standards, U. S. Environmental Protection Agency, and has been approved for publication. Any mention of trade names or commercial products is not intended to constitute endorsement or recommendation for use.

EPA-454/R-92-015

PREFACE

The ability to accurately estimate pollutant concentration due to atmospheric releases from area sources is important to the modeling community, and is of special concern for Superfund where emissions are typically characterized as area sources. Limitations of the Industrial Source Complex (ISC2) model (dated 92273) algorithms for modeling impacts from area sources, especially for receptors located within and nearby the area, have been documented in earlier studies. An improved algorithm for modeling dispersion from area sources has been developed based on a numerical integration of the point source concentration function. Information on this algorithm is provided in three interrelated reports.

In the first report (EPA-454/R-92-014), an evaluation of the algorithm is presented using wind tunnel data collected in the Fluid Modeling Facility of the U.S. Environmental Protection Agency. In the second report (EPA-454/R-92-015), a sensitivity analysis is presented of the algorithm as implemented in the short-term version of ISC2. In the third report (EPA-454/R-92-016), a sensitivity analysis is presented of the algorithm as implemented in the long-term version of ISC2.

The Environmental Protection Agency must conduct a formal and public review before the Agency can recommend for routine use this new algorithm in regulatory analyses. These reports are being released to establish a basis for reviews of the capabilities of this methodology and of the consequences resulting from use of this methodology in routine dispersion modeling of air pollutant impacts. These reports are one part of a larger set of information on the ISC2 models that must be considered before any formal changes can be adopted.

ACKNOWLEDGEMENTS

This report was prepared by Pacific Environmental Services, Inc., under EPA Contract No. 68D00124, with Jawad S. Touma as the Work Assignment Manager.

CONTENTS

1. PURPOSE

The purpose of this study is to evaluate the sensitivity of design concentrations across a range of source characteristics for the new area source algorithm that has been incorporated into the ISC2 Short Term (ISCST2) model (EPA, 1992). Based on the results of an evaluation of area source algorithms performed for EPA by TRC Environmental Consultants (EPA, 1989), the finite line segment algorithm used in the original ISCST model gives physically unrealistic results for receptors located near the edges and corners of the area. The new ISCST2 algorithm, which implements an improved numerical integration approach to the integrated line source algorithm used by the PAL model (Petersen and Rumsey, 1987), is compared to the finite line segment algorithm used by the original ISCST model. Because the new algorithm performs a numerical integration over the source area, it is capable of explicitly handling receptor locations within the area, whereas the finite line segment algorithm is limited to determining impacts at receptors only located outside the area. The integrated line source algorithm, as implemented in the original PAL model, was also examined in the TRC report, and was found to give physically reasonable results for all of the tests performed. The conclusions of the TRC report apply as well to the new area source algorithm implemented in the ISCST2 model since it has been shown during development and testing to give essentially the same results as the original PAL model (Brode, 1992).

2. DESCRIPTION OF THE STUDY

To examine the sensitivity of the design concentrations across a range of source characteristics, five ground-level area sources were modeled, with sizes varying from 10 meters to 1,000 meters in width. An elevated source scenario consisting of a 100-meter wide area with a release height of 10 meters was also modeled. An additional case involving a 1,000 meter wide ground level area was also modeled with receptors located within and nearby the area. The high and high-second-high (HSH) 1-hour, 3-hour and 24-hour averages and high annual averages were determined for each of these source scenarios using a full year of real time meteorological data. All of the sources were modeled as square areas oriented N-S and E-W, since the original ISC algorithm was limited to handling that source geometry. Each scenario was run for one year of National Weather Service (NWS) meteorological data from Pittsburgh, PA (1964); one year of NWS data from Oklahoma City, OK (1988); and one year of NWS data from Seattle, WA (1983).

Each scenario was also run with both the rural and urban mode dispersion options. The only difference between the rural mode and the urban mode that effects the area sources modeled in this study are the lateral and vertical dispersion coefficients,

sigma-y and sigma-z. The dispersion coefficients are somewhat larger for the urban mode to account for the increased dispersive capacity of the atmosphere in the urban environment. The regulatory default option was used for all scenarios. This includes a procedure for calculating averages for periods that include calm hours. A pollutant type of "OTHER" was specified, so that no decay was used for either the rural or the urban mode. For the sake of efficiency, all computer runs involving the original algorithm were performed using the ISCST2 model, rather than the original ISCST model. In this way, the same input runstream file was used for both algorithms. It should also be noted that the results presented in this report for the original finite line segment algorithm reflect a correction to the finite line segment equation as implemented in the original ISCST model. This correction reduces all estimates for the finite line segment algorithm by about 11.4 percent (a factor of 0.886 = SQRT(PI)/2.) relative to the original uncorrected version.

A polar receptor network consisting of ground level receptors at five distances and 36 directions (every 10 degrees) was used to determine design concentrations. Since most area sources are ground-level or low-level releases, the maximum impacts can be expected to occur very near the source. However, the finite line segment algorithm does not allow receptors within the area itself, and is known to provide unreasonable concentration estimates very close to the source. The guidance in the ISC2 User's Guide states that if the source-receptor distance is less than the width of the area, then the area should be subdivided and modeled as multiple sources. Therefore, the first distance ring in the polar network was placed at a downwind distance (measured from the center of the area) of 1.5*XINIT meters, where XINIT is the width of the area. This places the nearest receptors at a distance of about one source width from the edge of the area. Additional distance rings were placed at approximately 2.0, 3.0, 5.0 and 10.0 times the initial distance, for a total of 180 receptors. For the ground level sources, the maximum ground level concentrations are expected to occur at or near the downwind edge of the area, and to decrease beyond that distance. Therefore the maximum concentrations for these source-receptor geometries are expected to occur at the 1.5*XINIT distance. The concentrations at the larger receptor distances were also examined for a few cases in order to compare the algorithms downwind of the maximum concentration.

Additional receptor distances were used for the elevated source to account for the fact that the maximum impact may occur beyond the nearest distance ring. The SCREEN model was run for a 100 meter wide area source with a release height of 10 meters for each stability class using both rural and urban dispersion coefficients. Maximum impacts for the rural coefficients occurred at downwind distances (measured from the downwind edge) ranging from about 60 meters for A stability to 480 meters for F stability, with a peak concentration at 116 meters for C

stability. Maximum impacts for the urban coefficients occurred at downwind distances ranging from 36 meters for A stability to 117 meters for E stability (SCREEN does not perform calculations for F stability in the urban mode), with a peak concentration at 44 meters downwind of the edge for C stability. Additional receptor rings were included at distances of 2.0*XINIT, 2.5*XINIT, and 4.0*XINIT for the elevated release height cases to better represent the peak concentration from the refined model.

In order to assess the sensitivity of the design values for receptors located close to and within an area source, an additional scenario was modeled involving a 1,000 meter wide (extra large) ground-level area source with receptors located within the area and near the edge of the area. For the original finite line segment algorithm, this source was subdivided into 4, 16, 64 and 100 separate areas of equal size. This was necessary because the finite line segment algorithm cannot model impacts at receptor locations within the area being modeled.

An emission rate equivalent to 1.0 g/s for the entire area was used for all scenarios. The area source widths, heights of release, emission rates in g/(sm^2), and receptor distances are shown in Table 1 for each scenario. Table 2 provides the source inputs for the X-Large (XL), Close-in case for the 4-, 16-, 64-, and 100-source treatment used with the finite line segment algorithm. Figure 1 shows the location of the receptors used for the X-Large source with receptors located within and nearby the area.

Table 1. Area Source Scenarios for Sensitivity Analysis

Source Type	Width of Area (m)	Height of Release (m)	Emission Rate (g/(sm^2))	Receptor Distances (m) (measured from the center of the area)
X-Small, Ground-level	10.0	0.0	1.0E-2	15, 30, 50, 75, 150
Small, Ground-level	50.0	0.0	4.0E-4	75, 150, 250, 400, 750
Medium, Ground-level	100.0	0.0	1.0E-4	150, 300, 500, 750, 1500
Large, Ground-level	500.0	0.0	4.0E-6	750, 1500, 2500, 4000, 7500
X-Large, Ground-level	1000.0	0.0	1.0E-6	1500, 3000, 5000, 7500, 15000
Medium, Elevated	100.0	10.0	1.0E-4	150, 200, 250, 300, 400, 500, 750, 1500
X-Large, Close-in, Ground-level	1000.0	0.0	1.0E-6	250, 500, 750, 1000, 1500

Table 2. Area Source Inputs for X-Large, Close-in Scenario (used for the original finite line segment algorithm only)

Scenario Description	Width of Each Side-Area (m)	Height of Release (m)	Emission Rate ($g/(sm^2)$)	Receptor Distances (m) (measured from the center of the 1000m area)
XL, Close-in, 4-sources (2x2)	500.0	0.0	1.0E-6	250, 500, 750, 1000, 1500
XL, Close-in, 16-sources (4x4)	250.0	0.0	1.0E-6	250, 500, 750, 1000, 1500
XL, Close-in, 64-sources (8x8)	125.0	0.0	1.0E-6	250, 500, 750, 1000, 1500
XL, Close-in, 100-sources (10x10)	100.0	0.0	1.0E-6	250, 500, 750, 1000, 1500

3. RESULTS OF THE STUDY

The results of the sensitivity study are presented first for the five ground level sources with receptors located downwind of the area, followed by the results for the elevated source, and then for the ground level source with receptors located within the area.

3.1. Ground Level Sources With Downwind Receptors

Tables 3 through 7 present comparisons of design values (highest and high-second-high (HSH)) obtained from the numerical integration algorithm in ISCST2 with values from the original finite line segment algorithm for the five ground level sources of various widths. The source widths range from the very small (10 meter wide) area source in Table 3 to the very large (1000 meter wide) area source in Table 7. Part A of each table presents the results using rural dispersion coefficients, and part B for each table presents the results using urban dispersion coefficients. The design values are generally located at the receptors located closest to the area source.

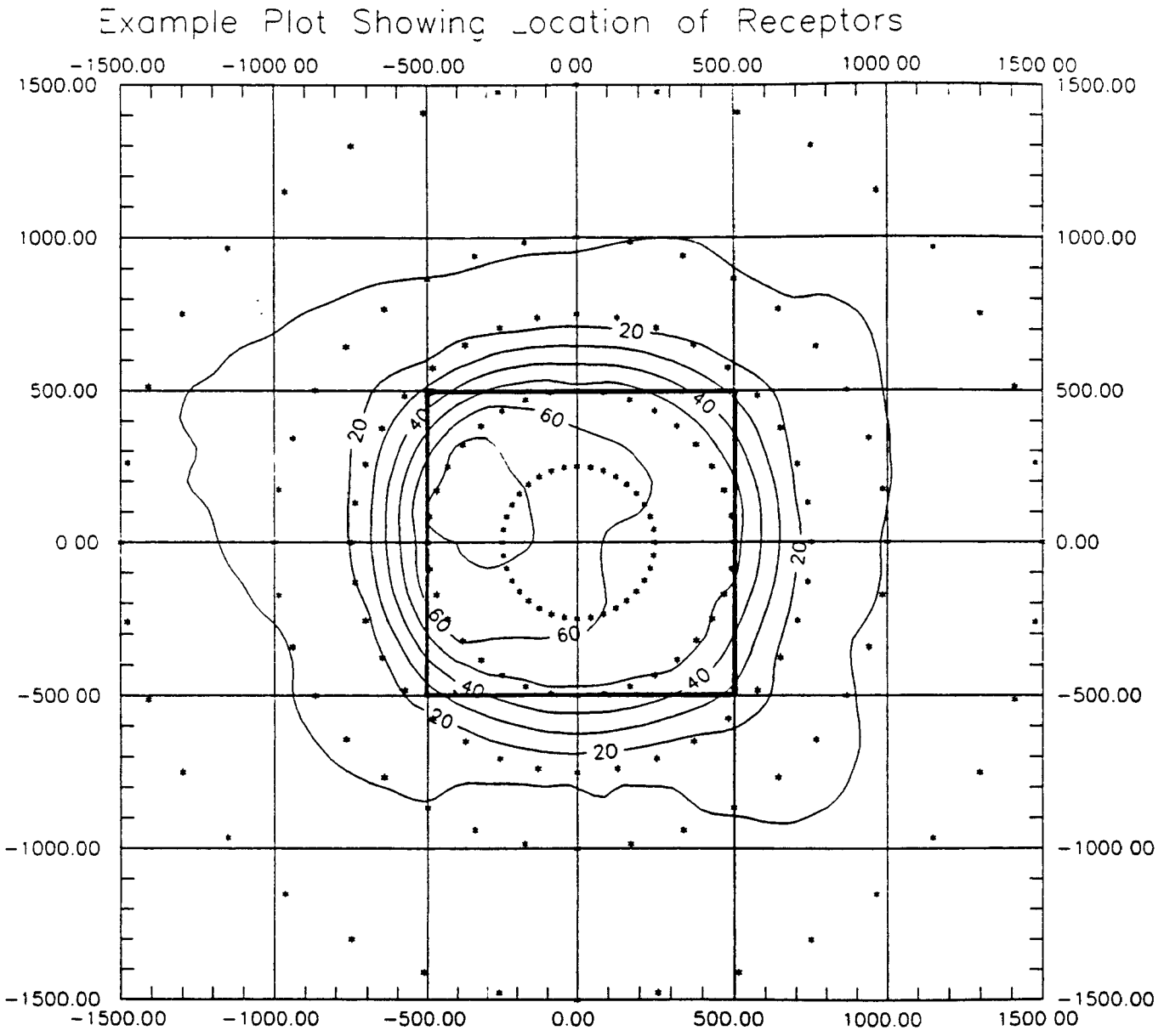

Figure 1. Example Contour Plot Showing Location of Receptors (Asterisks) Relative to the 1000 Meter Wide Ground Level Source for the X-Large Close-in Case

Table 3A

Comparison of Design Concentrations ($\mu g/m^3$) for the Very Small Source (10m Width) - Rural

	Numerical Integration (New)	Finite Line Segment (Old)	Ratio (New/Old)
Pittsburgh 1964			
1-hr High	204857.40000	115807.46520	1.76895
1-hr HSH	169798.00000	114605.51760	1.48159
3-hr High	124283.10000	76954.48688	1.61502
3-hr HSH	118637.60000	69151.30768	1.71562
24-hr High	45466.07000	33218.78914	1.36869
24-hr HSH	31626.08000	24526.59754	1.28946
Annual	4274.40000	3336.20465	1.28122
Okla. City 1988			
1-hr High	238843.70000	208284.60120	1.14672
1-hr HSH	210465.40000	115809.68020	1.81734
3-hr High	125987.90000	76546.80284	1.64589
3-hr HSH	94231.48000	70575.28688	1.33519
24-hr High	40460.68000	28647.34810	1.41237
24-hr HSH	31288.66000	22365.44862	1.39897
Annual	7998.58900	6122.28038	1.30647
Seattle 1983			
1-hr High	205086.10000	115440.48400	1.77655
1-hr HSH	200610.70000	115108.32260	1.74280
3-hr High	101556.20000	68040.57378	1.49258
3-hr HSH	83307.44000	57482.91804	1.44926
24-hr High	29787.68000	21684.13234	1.37371
24-hr HSH	26249.53000	20813.33610	1.26119
Annual	6305.98900	4814.46818	1.30980

Table 3B

Comparison of Design Concentrations ($\mu g/m^3$) for the Very Small Source (10m Width) - Urban

	Numerical Integration (New)	Finite Line Segment (Old)	Ratio (New/Old)
Pittsburgh 1964			
1-hr High	80215.95000	45519.26004	1.76224
1-hr HSH	66346.86000	45478.96476	1.45885
3-hr High	48728.32000	30147.93972	1.61631
3-hr HSH	46834.78000	27583.64308	1.69792
24-hr High	19892.41000	13936.16512	1.42739
24-hr HSH	14349.51000	10413.21116	1.37801
Annual	1997.23900	1467.77152	1.36073
Okla. City 1988			
1-hr High	81917.46000	45525.68354	1.79937
1-hr HSH	81917.46000	45478.96476	1.80122
3-hr High	49956.39000	31022.20022	1.61034
3-hr HSH	39824.69000	29865.37660	1.33347
24-hr High	17721.98000	12418.28232	1.42709
24-hr HSH	14468.18000	10112.44960	1.43073
Annual	3756.77800	2802.65190	1.34044
Seattle 1983			
1-hr High	80292.38000	45476.18272	1.76559
1-hr HSH	78857.11000	45359.85978	1.73848
3-hr High	41170.05000	28419.30942	1.44866
3-hr HSH	36746.55000	23697.29268	1.55066
24-hr High	13349.30000	9560.20580	1.39634
24-hr HSH	11331.30000	8472.34222	1.33745
Annual	2855.42500	2124.37549	1.34412

Table 4A

Comparison of Design Concentrations ($\mu g/m^3$) for the Small Source (50m Width) - Rural

	Numerical Integration (New)	Finite Line Segment (Old)	Ratio (New/Old)
Pittsburgh 1964			
1-hr High	11092.09000	6560.99480	1.69061
1-hr HSH	9191.13000	6168.35947	1.49004
3-hr High	6724.00100	4147.70179	1.62114
3-hr HSH	6413.65800	3721.89817	1.72322
24-hr High	2420.26400	1771.20083	1.36645
24-hr HSH	1652.91800	1277.19381	1.29418
Annual	220.33050	169.14086	1.30265
Okla. City 1988			
1-hr High	47791.59000	41656.92024	1.14727
1-hr HSH	11390.75000	6238.70521	1.82582
3-hr High	16237.42000	14119.49092	1.15000
3-hr HSH	5086.67400	3822.66295	1.33066
24-hr High	2492.74500	2175.89373	1.14562
24-hr HSH	1635.14000	1172.49785	1.39458
Annual	412.03130	314.56136	1.30986
Seattle 1983			
1-hr High	23028.41000	17203.88728	1.33856
1-hr HSH	10855.31000	6195.51182	1.75212
3-hr High	7676.13800	5734.62791	1.33856
3-hr HSH	4574.56900	3153.53271	1.45062
24-hr High	1536.58300	1123.35231	1.36785
24-hr HSH	1325.26800	1047.97143	1.26460
Annual	316.63400	241.19002	1.31280

Table 4B

Comparison of Design Concentrations ($\mu g/m^3$) for the Small Source (50m Width) - Urban

	Numerical Integration (New)	Finite Line Segment (Old)	Ratio (New/Old)
Pittsburgh 1964			
1-hr High	3343.59000	1919.71392	1.74171
1-hr HSH	2770.22400	1912.22279	1.44869
3-hr High	2030.04800	1271.85743	1.59613
3-hr HSH	1951.02400	1163.47837	1.67689
24-hr High	827.10080	585.66788	1.41224
24-hr HSH	593.45340	433.78206	1.36809
Annual	82.16215	60.43786	1.35945
Okla. City 1988			
1-hr High	3413.99300	1920.01073	1.77811
1-hr HSH	3413.99300	1918.13064	1.77985
3-hr High	2080.32700	1308.67605	1.58964
3-hr HSH	1658.01400	1260.04616	1.31584
24-hr High	736.45720	521.36608	1.41255
24-hr HSH	598.99680	422.03928	1.41929
Annual	154.78950	116.41287	1.32966
Seattle 1983			
1-hr High	3344.33000	1917.92331	1.74372
1-hr HSH	3284.12400	1913.23637	1.71653
3-hr High	1715.47200	1199.00785	1.43074
3-hr HSH	1531.42300	999.57545	1.53207
24-hr High	548.15180	395.33116	1.38656
24-hr HSH	467.42150	352.87032	1.32463
Annual	116.43890	87.09868	1.33686

Table 5A

Comparison of Design Concentrations ($\mu g/m^3$) for the Medium Source (100m Width) - Rural

	Numerical Integration (New)	Finite Line Segment (Old)	Ratio (New/Old)
Pittsburgh 1964			
1-hr High	4189.18800	3280.49740	1.27700
1-hr HSH	2617.63200	1752.36890	1.49377
3-hr High	1914.47100	1395.96654	1.37143
3-hr HSH	1825.38300	1178.79022	1.54852
24-hr High	684.94450	502.12854	1.36408
24-hr HSH	464.41880	358.64412	1.29493
Annual	61.57570	47.03294	1.30920
Okla. City 1988			
1-hr High	23913.31000	20828.46012	1.14811
1-hr HSH	3243.66700	1772.68931	1.82980
3-hr High	8055.44500	7006.82734	1.14966
3-hr HSH	1447.85100	1088.95336	1.32958
24-hr High	1132.80900	990.78899	1.14334
24-hr HSH	459.60370	331.32874	1.38715
Annual	113.15580	87.97547	1.28622
Seattle 1983			
1-hr High	11590.70000	8601.94258	1.34745
1-hr HSH	3090.86700	2298.72700	1.34460
3-hr High	3863.56600	2867.31396	1.34745
3-hr HSH	1301.83300	900.30447	1.44599
24-hr High	540.42210	411.73129	1.31256
24-hr HSH	411.38410	329.97918	1.24670
Annual	87.45323	66.63176	1.31249

Table 5B

Comparison of Design Concentrations ($\mu g/m^3$) for the Medium Source (100m Width) - Urban

	Numerical Integration (New)	Finite Line Segment (Old)	Ratio (New/Old)
Pittsburgh 1964			
1-hr High	876.43690	509.18588	1.72125
1-hr HSH	727.42470	507.27877	1.43397
3-hr High	531.82200	337.44054	1.57605
3-hr HSH	511.08630	308.65821	1.65583
24-hr High	216.17090	154.80414	1.39642
24-hr HSH	154.20440	113.56970	1.35780
Annual	21.22755	15.62494	1.35857
Okla. City 1988			
1-hr High	894.73940	509.26040	1.75694
1-hr HSH	894.73940	508.77886	1.75860
3-hr High	544.71500	347.26876	1.56857
3-hr HSH	433.97790	334.37011	1.29790
24-hr High	192.38550	137.62654	1.39788
24-hr HSH	155.82930	110.70676	1.40759
Annual	40.05390	30.38232	1.31833
Seattle 1983			
1-hr High	875.88820	508.70665	1.72179
1-hr HSH	860.01120	507.51108	1.69457
3-hr High	449.45410	318.22462	1.41238
3-hr HSH	401.30460	265.16793	1.51340
24-hr High	141.42290	102.67934	1.37733
24-hr HSH	121.11490	92.36754	1.31123
Annual	29.62306	22.44348	1.31990

Table 6A

Comparison of Design Concentrations ($\mu g/m^3$) for the Large Source (500m Width) - Rural

	Numerical Integration (New)	Finite Line Segment (Old)	Ratio (New/Old)
Pittsburgh 1964			
1-hr High	845.68710	656.09948	1.28896
1-hr HSH	339.78180	288.96367	1.17586
3-hr High	292.36470	235.58102	1.24104
3-hr HSH	113.26060	105.08270	1.07782
24-hr High	51.30783	39.73355	1.29130
24-hr HSH	25.66165	20.97978	1.22316
Annual	3.37200	2.61144	1.29124
Okla. City 1988			
1-hr High	4787.69200	4165.69202	1.14931
1-hr HSH	184.33330	103.10914	1.78775
3-hr High	1600.98900	1393.02679	1.14929
3-hr HSH	82.02331	63.83916	1.28484
24-hr High	206.67020	180.55466	1.14464
24-hr HSH	25.46798	18.97512	1.34218
Annual	6.31944	4.92970	1.28191
Seattle 1983			
1-hr High	2352.58300	1720.38873	1.36747
1-hr HSH	447.87980	440.01303	1.01788
3-hr High	784.19450	573.46279	1.36747
3-hr HSH	158.06740	146.67128	1.07770
24-hr High	107.69580	79.55786	1.35368
24-hr HSH	30.89734	24.21862	1.27577
Annual	4.67383	3.63307	1.28647

Table 6B

Comparison of Design Concentrations ($\mu g/m^3$) for the Large Source (500m Width) - Urban

	Numerical Integration (New)	Finite Line Segment (Old)	Ratio (New/Old)
Pittsburgh 1964			
1-hr High	46.24926	28.04318	1.64922
1-hr HSH	38.69476	27.93455	1.38519
3-hr High	27.97519	18.58977	1.50487
3-hr HSH	26.82369	17.02197	1.57583
24-hr High	11.19910	8.42143	1.32983
24-hr HSH	7.76747	5.90910	1.31449
Annual	1.03987	0.79235	1.31239
Okla. City 1988			
1-hr High	47.18597	28.04283	1.68264
1-hr HSH	47.18597	28.00716	1.68478
3-hr High	28.60593	20.49336	1.39586
3-hr HSH	22.65347	18.46705	1.22670
24-hr High	9.96523	8.46159	1.17770
24-hr HSH	7.90206	5.80201	1.36195
Annual	1.97723	1.55787	1.26919
Seattle 1983			
1-hr High	99.66319	86.12153	1.15724
1-hr HSH	59.07021	53.74087	1.09917
3-hr High	36.47066	36.53461	0.99825
3-hr HSH	23.86000	20.50081	1.16386
24-hr High	12.35849	10.86709	1.13724
24-hr HSH	6.40791	5.65684	1.13277
Annual	1.40481	1.09953	1.27764

Table 7A

Comparison of Design Concentrations ($\mu g/m^3$) for the Very Large Source (1000m Width) - Rural

	Numerical Integration (New)	Finite Line Segment (Old)	Ratio (New/Old)
Pittsburgh 1964			
1-hr High	424.38890	328.04974	1.29367
1-hr HSH	170.89860	144.48206	1.18284
3-hr High	144.60010	114.75047	1.26013
3-hr HSH	56.96619	50.98467	1.11732
24-hr High	22.94715	17.84420	1.28597
24-hr HSH	9.44751	8.56149	1.10349
Annual	1.04146	0.84477	1.23284
Okla. City 1988			
1-hr High	2394.39400	2082.84601	1.14958
1-hr HSH	59.10365	51.25244	1.15319
3-hr High	800.29010	696.35383	1.14926
3-hr HSH	27.27462	24.09787	1.13183
24-hr High	102.04460	89.10697	1.14519
24-hr HSH	7.88571	6.07173	1.29876
Annual	1.95303	1.57807	1.23760
Seattle 1983			
1-hr High	1183.58100	860.19419	1.37595
1-hr HSH	224.21050	214.98834	1.04290
3-hr High	394.52700	286.73140	1.37595
3-hr HSH	77.40852	71.66283	1.08018
24-hr High	54.09274	39.77379	1.36001
24-hr HSH	11.31509	10.96250	1.03216
Annual	1.43274	1.16327	1.23164

Table 7B

Comparison of Design Concentrations ($\mu g/m^3$) for the Very Large Source (1000m Width) - Urban

	Numerical Integration (New)	Finite Line Segment (Old)	Ratio (New/Old)
Pittsburgh 1964			
1-hr High	14.40249	8.85869	1.62580
1-hr HSH	12.09639	8.80733	1.37345
3-hr High	8.68877	5.87223	1.47964
3-hr HSH	8.31132	5.37184	1.54720
24-hr High	3.43113	2.64040	1.29947
24-hr HSH	2.34182	1.89132	1.23819
Annual	0.31041	0.24362	1.27414
Okla. City 1988			
1-hr High	14.69298	11.47803	1.28010
1-hr HSH	14.69298	10.76066	1.36544
3-hr High	11.63643	10.25001	1.13526
3-hr HSH	8.39101	7.41392	1.13179
24-hr High	4.67000	4.19282	1.11381
24-hr HSH	2.39467	1.78293	1.34311
Annual	0.59116	0.47608	1.24172
Seattle 1983			
1-hr High	50.83767	43.07947	1.18009
1-hr HSH	29.93746	26.87695	1.11387
3-hr High	18.61257	18.36330	1.01357
3-hr HSH	10.46676	8.99064	1.16418
24-hr High	5.38388	4.81261	1.11870
24-hr HSH	2.83220	2.82427	1.00281
Annual	0.41316	0.33395	1.23719

Overall, the new integrated line source algorithm predicts higher design concentrations than the original finite line segment algorithm. The average ratio of the numerical integration results over the finite line segment results (averaged over all three cities and for all averaging periods) ranges from about 1.5 (i.e., 50 percent higher for the integration method) for the 10 meter wide area to about 1.2 for the 1000 meter wide area. This trend toward smaller ratios for larger areas is illustrated in Figures 2 and 3, which show the average ratios (averaged across the three meteorological data locations) for the five ground-level sources for downwind receptors only, for rural and urban dispersion, respectively. Included in these figures are the average ratios for each of the averaging periods. Note that only the high-second-high (HSH) results are used for the short term averages presented in these figures. The patterns are nearly identical for the 10-meter and 50-meter wide areas for both rural and urban dispersion, but the pattern shifts as the size of the area increases. Figure 4 shows the ratios by averaging period, averaged across all of the ground level sources. As can be seen from these figures, the ratios tend to be largest for the 1-hour averages, and then decrease with longer averaging periods. The average ratios for the 24-hour HSH values and the high annual values are about the same. The ratios are generally larger for the cases with urban dispersion coefficients than for the cases with rural dispersion coefficients.

The most notable feature about these results is that the numerical integration method produces larger concentration estimates than the original finite line segment algorithm. One possible explanation for part of this difference is that the finite line segment algorithm allows the vertical dispersion coefficient, sigma-z, to grow from the upwind edge of the area. This is done by adding a vertical virtual distance (XZ) equal to the width of the area (XINIT) to the downwind distance when calculating sigma-z. The downwind distance is measured from the downwind edge of the area. In effect, for vertical dispersion, the finite line segment is located at the upwind edge of the area, whereas for lateral dispersion the finite line segment is located at the downwind edge. Since the numerical integration method integrates over the area, the vertical dispersion coefficient for each element of the integration will be representative of the actual distance from that element of the area to the receptor location. Thus, for the portion of the area that is closest to the receptor, and therefore having the greatest impact on the receptor, the distance used for sigma-z will essentially be the distance from the downwind edge of the area to the receptor location. The result of this difference will be a smaller overall "effective" vertical dispersion coefficient for the numerical integration method than for the finite line source algorithm. Since these are ground level

releases and ground level receptors, a smaller effective vertical dispersion coefficient would result in larger ground level concentrations, other factors being equal.

To test this hypothesis, the 10 meter wide ground level source was modeled again for the Oklahoma City 1988 data with a version of the finite line segment algorithm that used a vertical virtual distance of one half the source width (XZ = XINIT/2). In other words, the source-receptor distance for calculation of sigma-z was measured from the center of the area. The ratios of the numerical integration (new) algorithm to the finite line segment (old) algorithm are presented below for the original XZ=XINIT and the modified XZ=XINIT/2 versions for both rural and urban dispersion coefficients. The ratios for the XZ=XINIT/2 case are much closer to 1.0 than the original XZ=XINIT case, especially for the longer averaging periods. These results provide an indication that a significant part of the discrepancies between the two algorithms are related to the treatment of the vertical dispersion coefficients, specifically the use of a vertical virtual distance equal to the width of the area for the finite line segment algorithm. In addition, since the urban dispersion coefficients are larger than the rural coefficients, this factor also explains in part why the ratios are larger for the urban cases than for the rural cases.

Rural Dispersion Coefficients; 10-meter Ground Level Area; Oklahoma City, OK 1988 Data

	Ratio New/Old with XZ=XINIT	Ratio New/Old with XZ=XINIT/2
1-Hr High	1.15	1.15
1-Hr HSH	1.81	1.41
3-Hr High	1.65	1.28
3-Hr HSH	1.34	1.04
24-Hr High	1.41	1.10
24-Hr HSH	1.40	1.09
Annual	1.31	1.01

Urban Dispersion Coefficients; 10-meter Ground Level Area; Oklahoma City, OK 1988 Data

	Ratio New/Old with XZ=XINIT	Ratio New/Old with XZ=XINIT/2
1-Hr High	1.80	1.33
1-Hr HSH	1.80	1.33
3-Hr High	1.61	1.19
3-Hr HSH	1.33	0.99
24-Hr High	1.43	1.06
24-Hr HSH	1.43	1.06
Annual	1.34	0.99

Another notable feature of the results is that the ratios show a larger variation from site to site and across averaging periods for the cases with rural dispersion coefficients than for the cases with urban dispersion coefficients. One of the major factors in causing this variability for the rural cases is thought to be the influence of limited mixing effects for very low mixing heights. This is particularly noticeable for the Oklahoma City cases, which show very large differences between the high and HSH results for rural dispersion. The hourly interpolation scheme used for urban mixing heights reduces the likelihood of very low mixing heights for the urban cases.

In addition to examining the design values, which all occurred at receptors located on the nearest distance ring for the ground level sources, the results at distances located further downwind were examined briefly to determine whether or not the results converge with distance. Figures 5 and 6 present the high concentration values versus distance downwind for the 10 meter wide ground level area source for the Oklahoma City data for the case with rural dispersion coefficients. The HSH short term values are presented in Figure 5, and the high annual average values are presented in Figure 6. These figures show that the two algorithms converge to nearly identical answers at a distance of about 15 source widths for this example. The longer period averages converge to within a few percent at a distance of about 5 source widths downwind. This general pattern was also apparent for other cases that were examined.

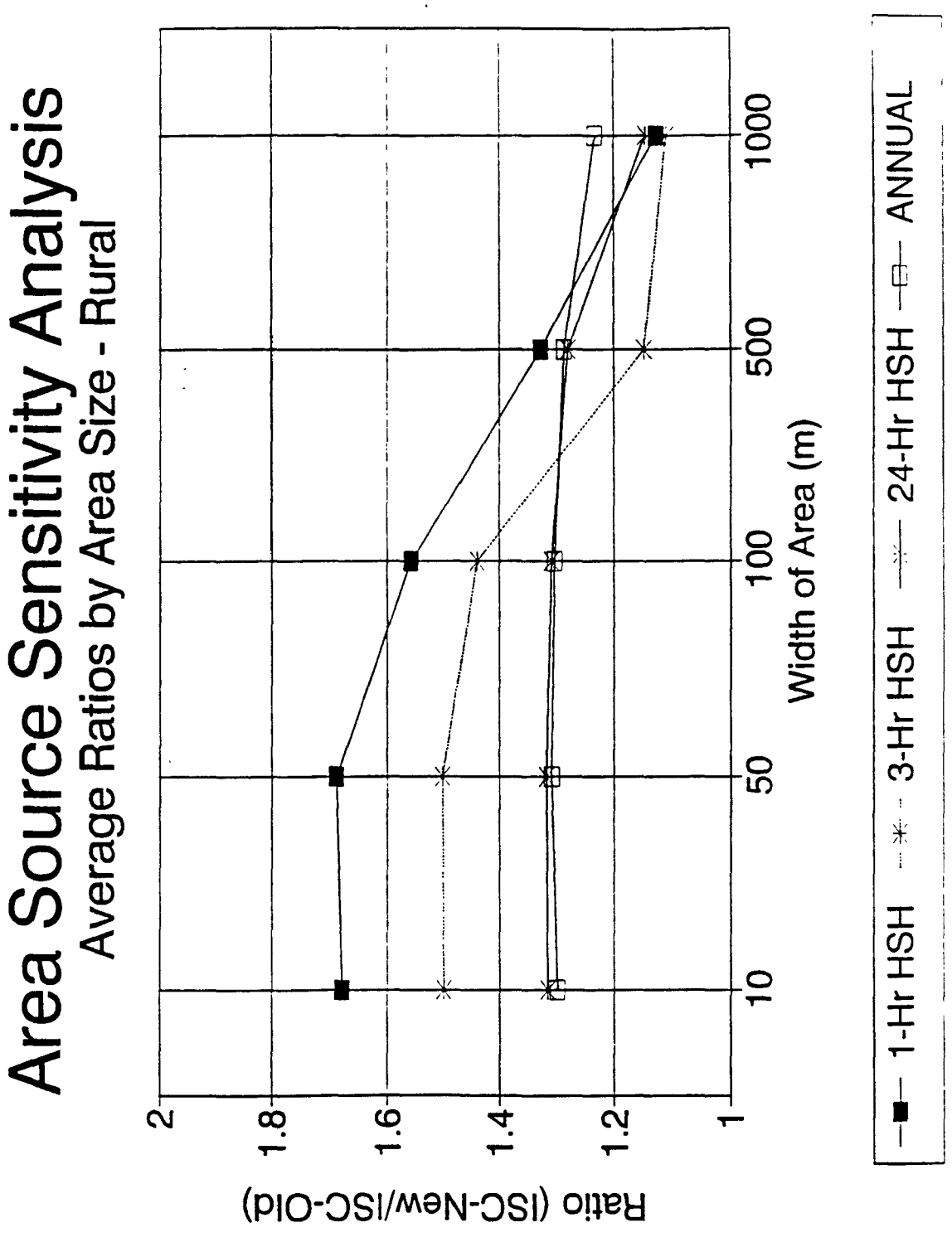

Figure 2. Average Ratios (New/Old) by Area Size for Ground Level Sources - Rural Dispersion Coefficients

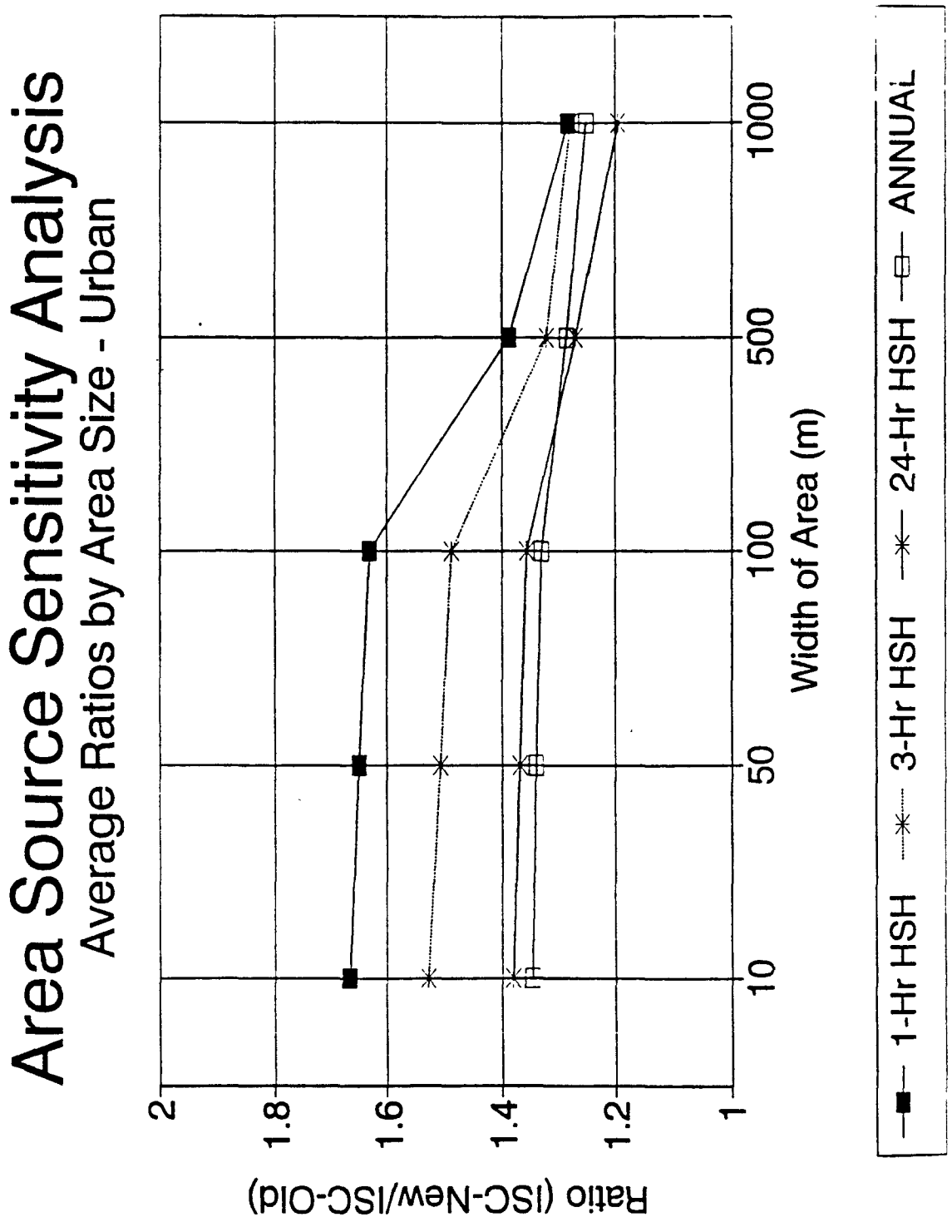

Figure 3. Average Ratios (New/Old) by Area Size for Ground Level Sources - Urban Dispersion Coefficients

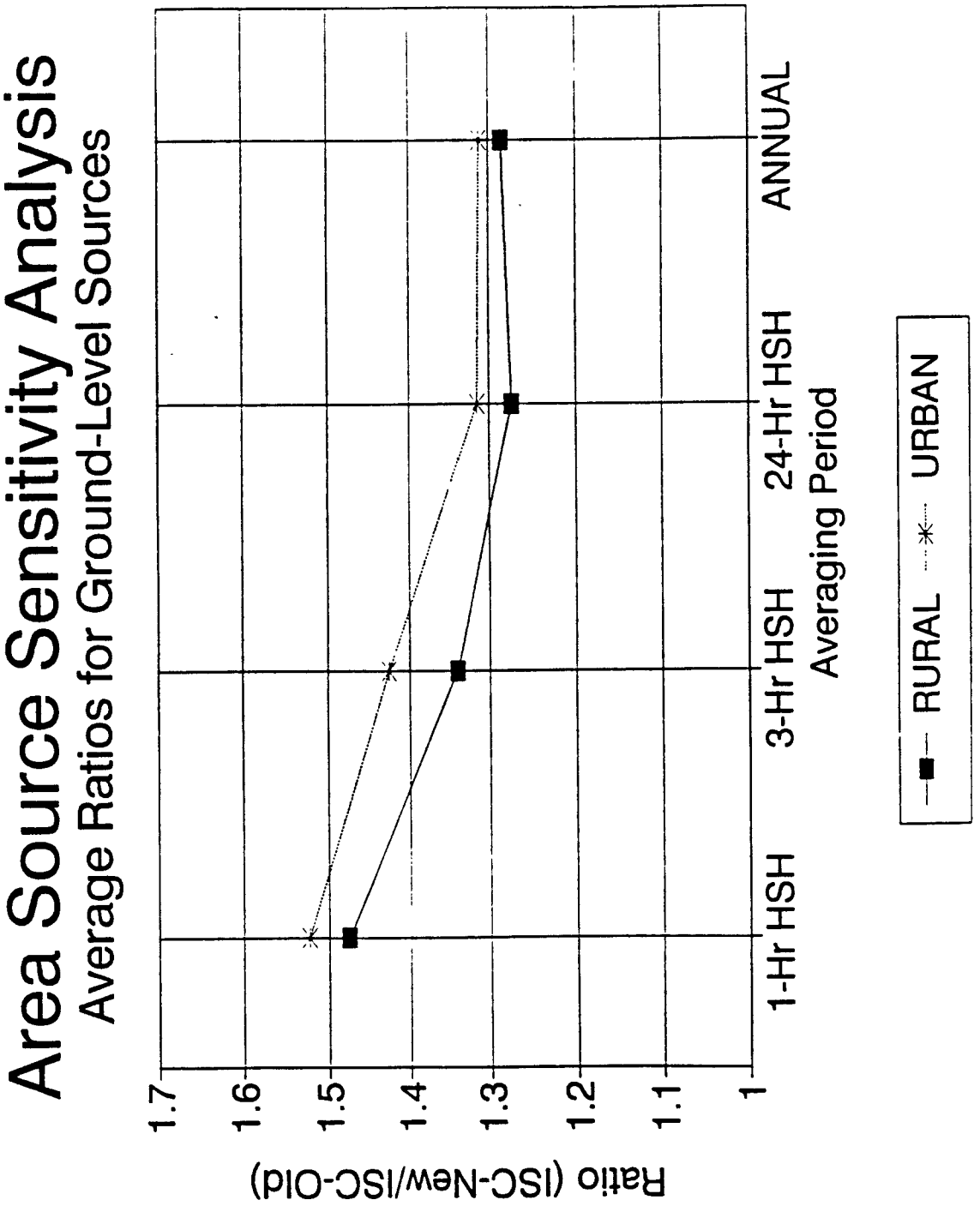

Figure 4. Average Ratios (New/Old) by Averaging Period for All Ground Level Sources Combined

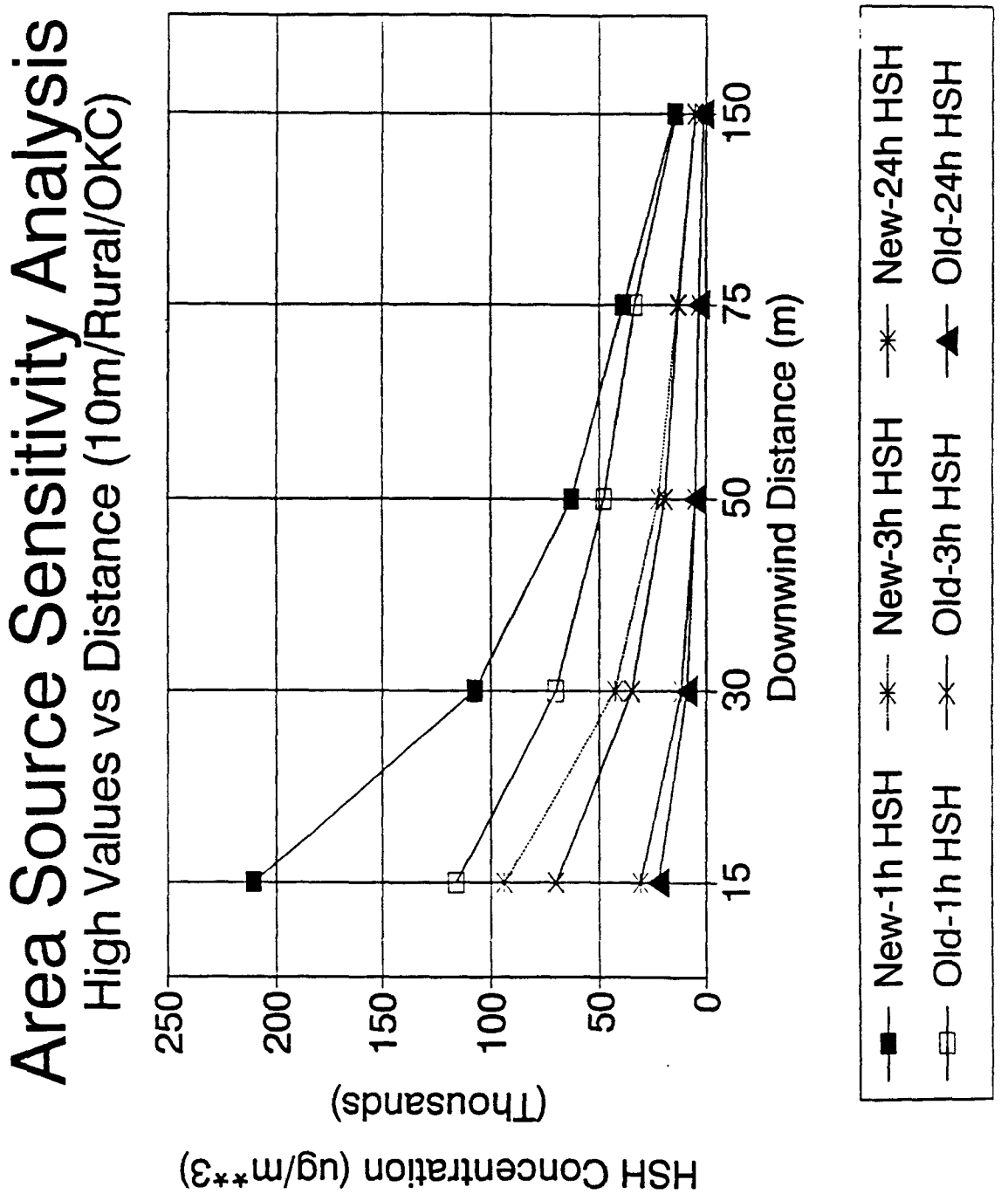

Figure 5. High (HSH) Short Term Values Versus Distance for the 10 Meter Wide Ground Level Source for Rural Dispersion and Oklahoma City Data

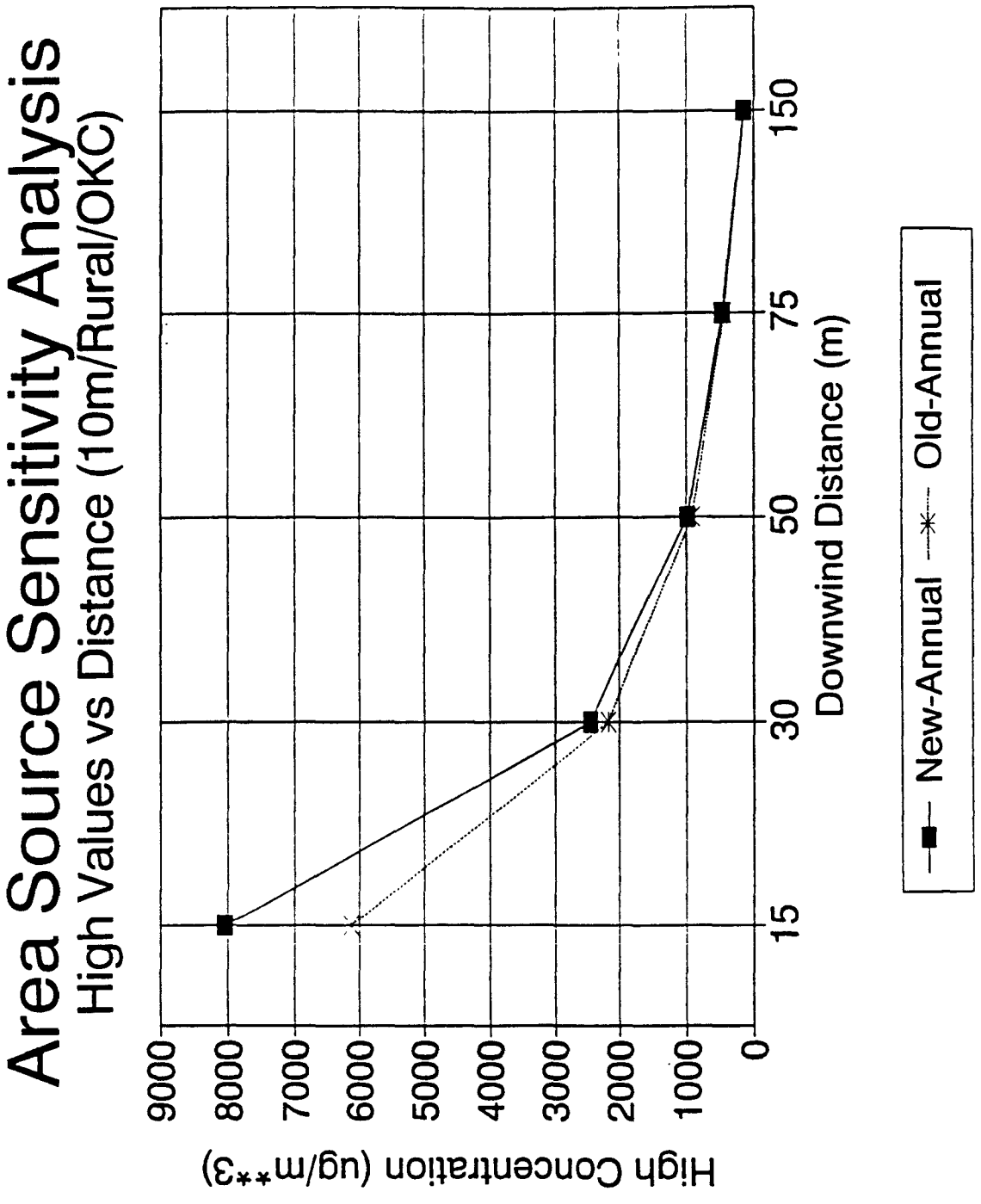

Figure 6. High Annual Average Values Versus Distance for the 10 Meter Wide Ground Level Source for Rural Dispersion and Oklahoma City Data

3.2. Elevated Area Source

Tables 8A and 8B present comparisons of design values obtained from the numerical integration algorithm and from the finite line segment algorithm for the 100 meter wide elevated source (10 meter release height). Part A of the table presents the results using rural dispersion coefficients, and part B presents the results using urban dispersion coefficients. The ratios for the elevated source are smaller than the corresponding ratios for the 100-meter ground level source (see Tables 5A and 5B). In fact, the ratios for the rural dispersion case for longer averaging periods are actually less than 1.0, indicating that the numerical integration algorithm estimates smaller concentrations than the finite line segment algorithm. The ratios follow a similar trend as the ground level sources with a decrease for longer averaging periods. Urban ratios are larger than rural ratios. This trend is shown in Figure 7, which depicts the average ratios for each averaging period (averaged across the three meteorological data locations).

One possible explanation for the lower ratios of design values for the elevated source than for the ground level sources is related to the differences in treatment of the vertical dispersion parameter described in the previous section. The ground level concentrations will tend to be smaller for the numerical integration algorithm since it uses a smaller "effective" vertical dispersion parameter than the finite line segment algorithm, and since the receptors are located off the plume centerline vertically. To test this hypothesis, the modified finite line segment algorithm with a vertical virtual distance of one half the source width (XZ=XINIT/2) was run on the 100 meter wide elevated source for the Oklahoma City 1988 data. Once again, the ratios are much closer to 1.0, especially for longer averaging periods, for the XZ=XINIT/2 case than for the XZ=XINIT case. The ratios for the XZ=XINIT/2 cases are also very similar to the corresponding ratios for the 10 meter ground level source presented above. The results suggest that the use of XZ=XINIT/2 for the finite line segment algorithm may better represent an "effective" vertical dispersion coefficient that the XZ=XINIT currently in use.

Rural Dispersion Coefficients;
100-meter Elevated Area (10m Release Height);
Oklahoma City, OK 1988 Data

	Ratio New/Old with XZ=XINIT	Ratio New/Old with XZ=XINIT/2
1-Hr High	1.02	1.06
1-Hr HSH	1.12	1.22
3-Hr High	1.01	1.06
3-Hr HSH	0.99	1.03
24-Hr High	0.92	1.13
24-Hr HSH	0.93	1.04
Annual	0.84	1.02

Urban Dispersion Coefficients;
10-meter Elevated Area (10m Release Height);
Oklahoma City, OK 1988 Data

	Ratio New/Old with XZ=XINIT	Ratio New/Old with XZ=XINIT/2
1-Hr High	1.34	1.24
1-Hr HSH	1.34	1.24
3-Hr High	1.22	1.14
3-Hr HSH	1.02	0.94
24-Hr High	1.13	1.03
24-Hr HSH	1.09	0.97
Annual	1.12	0.98

Table 8A

Comparison of Design Concentrations ($\mu g/m^3$) for the Medium Elevated Source (100m Width) - Rural

	Numerical Integration (New)	Finite Line Segment (Old)	Ratio (New/Old)
Pittsburgh 1964			
1-hr High	462.32990	393.69871	1.17432
1-hr HSH	422.63290	381.90658	1.10664
3-hr High	234.75510	214.93128	1.09223
3-hr HSH	200.89060	187.96933	1.06874
24-hr High	91.53203	107.91631	0.84818
24-hr HSH	74.36944	85.41618	0.87067
Annual	11.16831	14.37888	0.77672
Okla. City 1988			
1-hr High	720.21940	705.65284	1.02064
1-hr HSH	507.60260	451.47096	1.12433
3-hr High	240.07310	238.51368	1.00654
3-hr HSH	200.39990	202.80062	0.98816
24-hr High	86.47166	93.92442	0.92065
24-hr HSH	67.74000	72.81362	0.93032
Annual	20.13812	24.07448	0.83649
Seattle 1983			
1-hr High	502.80920	416.25104	1.20795
1-hr HSH	437.91930	385.72169	1.13532
3-hr High	265.34210	253.70769	1.04586
3-hr HSH	218.36560	202.80062	1.07675
24-hr High	101.61880	93.92442	1.08192
24-hr HSH	88.98233	72.81362	1.22206
Annual	21.29089	26.61255	0.80003

Table 8B

Comparison of Design Concentrations ($\mu g/m^3$) for the Medium Elevated Source (100m Width) - Urban

	Numerical Integration (New)	Finite Line Segment (Old)	Ratio (New/Old)
Pittsburgh 1964			
1-hr High	440.36300	333.21034	1.32158
1-hr HSH	387.56370	332.92531	1.16412
3-hr High	264.93450	221.74347	1.19478
3-hr HSH	253.21430	201.67743	1.25554
24-hr High	116.70530	103.46557	1.12796
24-hr HSH	88.28399	79.45618	1.11110
Annual	13.34216	11.61218	1.14898
Okla. City 1988			
1-hr High	517.93870	386.55693	1.33988
1-hr HSH	517.93870	386.55693	1.33988
3-hr High	319.70040	261.90585	1.22067
3-hr HSH	257.91310	253.84751	1.01602
24-hr High	121.18880	107.13822	1.13114
24-hr HSH	96.71584	88.77676	1.08943
Annual	27.83596	24.78361	1.12316
Seattle 1983			
1-hr High	502.52200	386.02931	1.30177
1-hr HSH	493.15130	386.01780	1.27754
3-hr High	262.68700	239.52381	1.09671
3-hr HSH	241.21780	204.08399	1.18195
24-hr High	102.85800	87.11106	1.18077
24-hr HSH	90.25307	77.30210	1.16754
Annual	23.19134	19.54454	1.18659

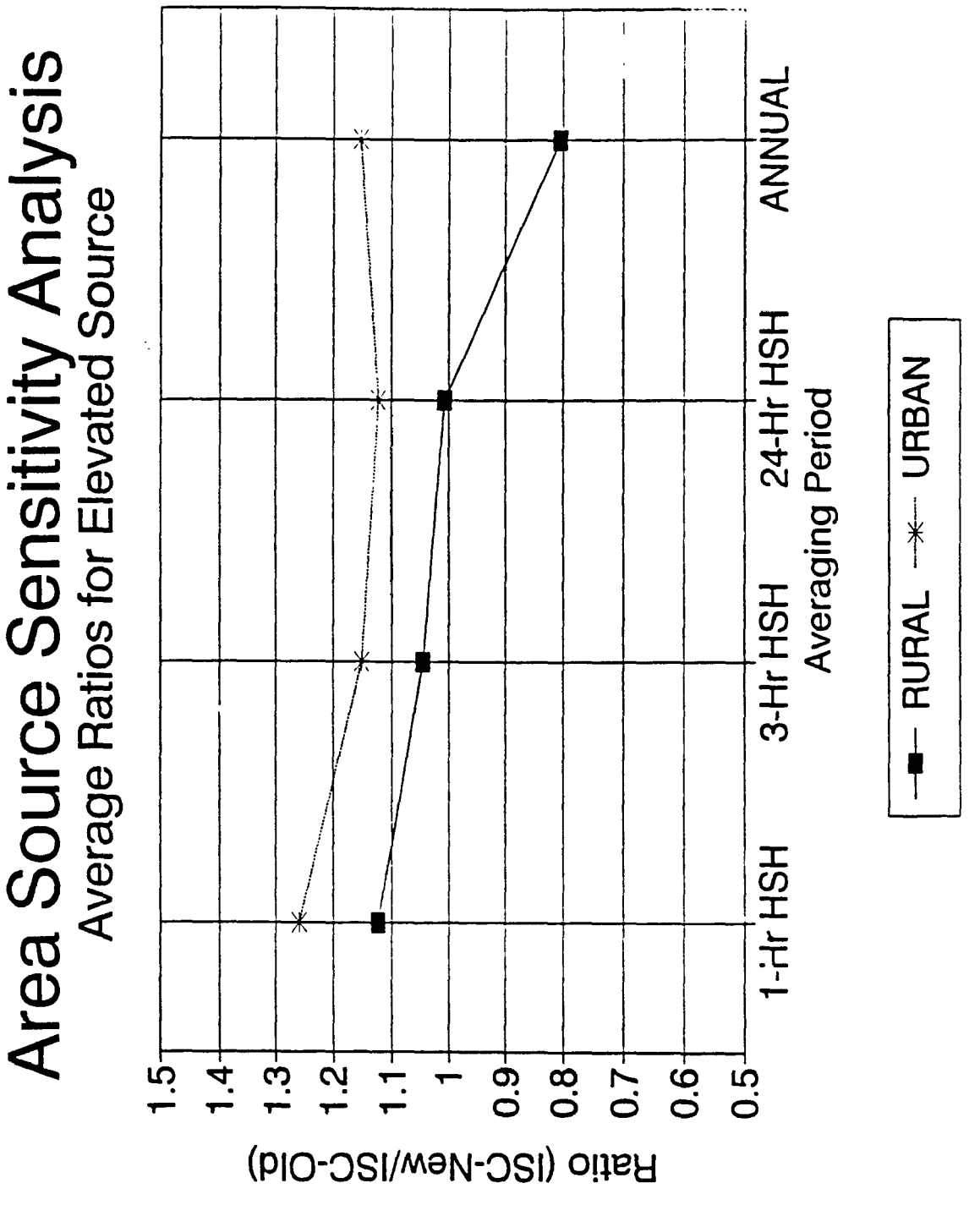

Figure 7. Average Ratios (New/Old) by Averaging Period for 100 Meter Wide Elevated Source (Release Height of 10 Meters)

3.3. Ground-level Sources With Receptors Within and Nearby the Area

Tables 9A and 9B present comparisons of design values from the numerical integration algorithm and from the finite line segment algorithm for the 1000 meter wide ground level source with receptors located within and nearby the area. Parts A and B of the table present the results using rural and urban dispersion coefficients, respectively. The results for the finite line segment algorithm are presented for each of the subdivided multiple-source scenarios examined using 4, 16, 64 and 100 areas of equal size. The ratios for the cases with receptors within and nearby the area are generally larger than the corresponding ratios for the other ground level cases (see Tables 1 through 7). In addition, the trend is for larger ratios for longer averaging periods, which is the reverse of the trend seen for the other ground level sources. This trend is shown in Figure 8, which shows the average ratios (averaged over the three meteorological data locations) for each averaging period. As with the other sources examined, the ratios are larger for the case with urban dispersion coefficients than for the case with rural dispersion coefficients. The results in Tables 9A and 9B also show that, in general, the design values for the old finite line segment algorithm tend to increase as the number of subdivided areas increases. Since the impact at any receptor located within the area does not include any contribution from the subarea in which the receptor is located, as the number of subareas increases and the size of the subarea decreases, the amount of contribution not accounted for will tend to decrease. In principal, as the number of subareas approaches infinity and the individual subareas approach point sources, the two algorithms should converge, although no attempt has been made to verify this.

The reason for the ratios increasing with longer averaging periods is also relatively simple. For the high 1-hour averages, the amount of contribution from the subarea containing the receptor location that is not accounted for will depend only on the amount of the subarea upwind of the receptor for a single wind direction. For the highest 1-hour average, it is likely that the receptors are located near the upwind edge of the subarea, where the lost contribution will be relatively small. In fact, the high 1-hour values for the rural dispersion cases (Table 9A) are quite similar for the two algorithms. For longer period averages, the amount of contribution lost for the local subarea will vary as the wind direction varies from hour to hour, and the relative amount lost for the entire averaging period will tend to be larger than for the high 1-hour values. This trend should increase as the length of the averaging period increases and the wind direction variation becomes larger. This trend is clearly seen in Tables 9A and 9B.

The receptor locations for the design values are also included in Tables 9A and 9B for the numerical integration algorithm and for the finite line segment case based on 100 sources. The locations are given as direction (in degrees) and distance (in meters). Thus, a location of (40,500) means a receptor located along the 40 degree direction radial, measured clockwise from North, at a distance of 500 meters from the center of the area. The receptor locations show better agreement between the algorithms for the longer averaging periods. A more complete picture is provided in Figures 9 through 44, which display contour plots of high concentrations across the receptor grid for the numerical integration algorithm and for the finite line segment algorithm based on 100 sources. Contour plots are given for the HSH 1-hour, HSH 24-hour, and annual average concentrations. The 3-hour average results were not included in the contour plots since they are not expected to provide any significantly different results. The rural results are presented first, followed by the urban results, with the numerical integration algorithm results and finite line segment (100-source) results for the same location and averaging period on facing pages to facilitate comparison. The four grid squares at the center of the diagrams (between X = -500 to 500 and Y = -500 to 500) define the location of the 1000 meter wide area source. The source location and the distribution of receptor points was shown in Figure 1 in Section 2.

Generally, the contour patterns between the two algorithms compare better for the longer averaging periods than for the 1-hour averages. Some of the contour plots exhibit isolated peaks and valleys, and some discontinuities (or "kinks") in the contours. These may be due to the limited number of data points (180) on which the plots are based, or may be an artifact of the interpolation scheme used to generate a uniform grid of data by the contouring program prior to determining the contours, or the method used in contouring the data. Therefore, the fine-scale details should not be given much credence in these plots, although the overall patterns should be fairly reliable. The numerical integration algorithm, which explicitly handles receptors located within the area, generally shows reasonable patterns across the area source itself, whereas the finite line segment algorithm with the 100-source subdivided treatment of the area shows some unusual patterns over the area. This is particularly noticeable for 1-hour averages, such as in Figures 10, 16, 34 and 40. These unusual patterns for the finite line segment algorithm are indicative of an inability of that algorithm to adequately model the concentration distributions within the area, even when the area is subdivided into 100 areas. In a few cases the patterns are surprisingly similar, such as Figures 21 and 22. But the overall conclusion evident from these contour diagrams is that the numerical integration algorithm is far superior to the finite line segment algorithm in handling receptors within and nearby the area.

Table 9A

Comparison of Design Concentrations (ug/m^3) for the 1000m Wide Area
With Receptors Located Within and Nearby the Area - Rural

	Numerical Integration (New)	Finite Line Segment (Old) 4 Sources	Finite Line Segment (Old) 16 Sources	Finite Line Segment (Old) 64 Sources	Finite Line Segment (Old) 100 Sources	Ratio New/Old-100
Pittsburgh 1964						
1-hr High	432.55590 (40,750)	491.85377	441.24368	446.04837	442.15387 (40,750)	0.97829
1-hr HSH	207.18820 (280,500)	204.15247	198.70738	194.18373	191.51714 (50,750)	1.08183
3-hr High	177.47750 (20,500)	173.71970	159.83803	162.11036	163.52689 (40,750)	1.08531
3-hr HSH	134.43460 (360,500)	75.71328	76.33872	75.61375	76.89537 (50,750)	1.74828
24-hr High	78.94704 (320,500)	31.03172	31.18236	35.64745	41.16997 (330,500)	1.91759
24-hr HSH	74.63991 (290,500)	18.91487	25.78640	32.86131	38.21827 (320,500)	1.95299
Annual	30.06087 (20,250)	4.05184	8.33124	11.77271	12.17878 (30,250)	2.46830
Okla. City 1988						
1-hr High	2395.17100 (150,750)	2927.43792	2474.81064	2408.71504	2437.45954 (20,750)	0.98265
1-hr HSH	210.16090 (60,500)	83.93556	108.08660	118.18593	134.81013 (300,500)	1.55894
3-hr High	806.08260 (180,500)	978.66585	828.29845	805.65300	815.66666 (20,750)	0.98825
3-hr HSH	186.00090 (50,250)	41.81989	72.52082	94.45699	92.22968 (100,250)	2.01671
24-hr High	118.92130 (180,500)	126.18350	110.04926	106.62629	107.93943 (140,750)	1.10174
24-hr HSH	57.16613 (290,250)	14.75862	20.69101	26.84766	27.59182 (310,500)	2.07185
Annual	24.85228 (340,250)	4.37314	7.19887	10.00716	10.42655 (330,250)	2.38356
Seattle 1983						
1-hr High	1246.38900 (140,750)	1286.65097	1303.16601	1327.30242	1239.79929 (140,750)	1.00532
1-hr HSH	553.65640 (210,250)	323.04225	431.29435	474.10294	516.40297 (210,250)	1.07214
3-hr High	416.00020 (140,750)	431.85155	434.38879	442.98414	413.88205 (140,750)	1.00512
3-hr HSH	201.34430 (190,500)	109.09121	150.80349	165.82801	182.86048 (210,250)	1.10108
24-hr High	81.90249 (140,500)	60.53212	60.87819	62.42380	60.34736 (140,500)	1.35718
24-hr HSH	71.92862 (150,250)	25.36595	27.34034	34.48674	33.90401 (210,250)	2.12154
Annual	31.43343 (300,250)	4.62616	8.59221	12.18340	12.83955 (330,250)	2.44817

Note: Values in parentheses are receptor locations given as direction (degrees from North) and downwind distance (meters).

Table 98

Comparison of Design Concentrations (ug/m^3) for the 1000m Wide Area With Receptors Located Within and Nearby the Area - Urban

	Numerical Integration (New)	Finite Line Segment (Old) 4 Sources	Finite Line Segment (Old) 16 Sources	Finite Line Segment (Old) 64 Sources	Finite Line Segment (Old) 100 Sources	Ratio New/Old-100
Pittsburgh 1964						
1-hr High	75.36378 (50,500)	22.87120	28.72459	32.04270	35.76426 (150,500)	2.10724
1-hr HSH	74.17054 (280,500)	18.60340	24.24223	30.78414	32.90812 (270,500)	2.25387
3-hr High	56.60395 (180,250)	13.61754	17.48827	21.21428	22.21074 (120,500)	2.54850
3-hr HSH	47.63224 (320,500)	12.52957	15.82253	18.05589	21.24188 (300,500)	2.24237
24-hr High	30.56433 (320,500)	6.51216	9.00127	11.00509	12.41048 (330,500)	2.46278
24-hr HSH	29.19938 (290,500)	5.43449	7.70050	10.10606	11.65855 (320,500)	2.50455
Annual	12.77044 (30,250)	1.23812	2.64040	3.85130	3.99965 (30,250)	3.19289
Okla. City 1988						
1-hr High	75.31821 (300,500)	22.87172	28.47258	32.14429	36.81676 (300,500)	2.04576
1-hr HSH	75.28640 (310,500)	22.68481	28.47258	32.14429	36.81676 (300,500)	2.04489
3-hr High	69.43607 (20,500)	15.77947	19.90494	26.64702	27.92990 (360,500)	2.48608
3-hr HSH	61.00494 (340,250)	12.86407	17.21320	22.08193	24.01311 (60,500)	2.54049
24-hr High	23.90601 (330,500)	5.35411	6.27145	8.12755	8.86338 (310,500)	2.69716
24-hr HSH	23.47807 (320,250)	4.44532	5.85526	7.77340	8.61436 (330,500)	2.72546
Annual	10.75157 (340,250)	1.39736	2.33758	3.34950	3.52936 (330,250)	3.04632
Seattle 1983						
1-hr High	75.13278 (60,500)	57.73794	58.11319	53.95553	53.85180 (130,750)	1.39518
1-hr HSH	75.09218 (60,500)	32.12452	31.32098	31.46416	36.41715 (60,500)	2.06200
3-hr High	49.30389 (70,500)	23.58462	24.22136	24.01670	26.12551 (120,500)	1.88719
3-hr HSH	48.29193 (70,500)	16.09491	16.10262	19.32749	20.61560 (90,500)	2.34249
24-hr High	28.92939 (140,250)	8.86869	10.03667	11.42896	11.89885 (360,500)	2.43128
24-hr HSH	27.20447 (290,250)	5.13370	6.26770	8.39970	8.94196 (60,250)	3.04234
Annual	13.39305 (300,250)	1.42362	2.73066	4.00072	4.24711 (330,250)	3.15345

Note: Values in parentheses are receptor locations given as direction (degrees from North) and downwind distance (meters).

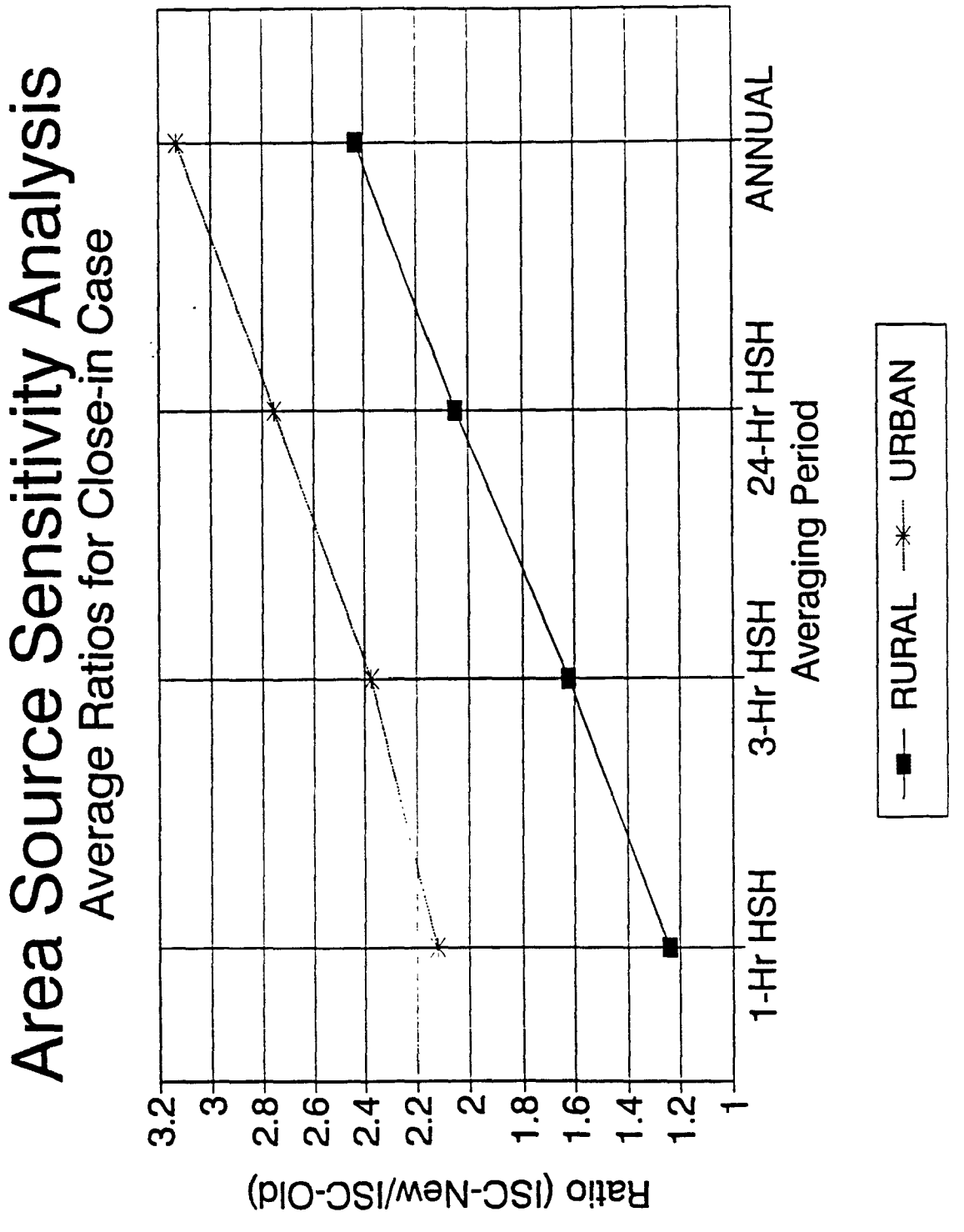

Figure 8. Average Ratios (New/Old) by Averaging Period for the 1000 Meter Wide Ground Level Source with Close-in Receptors

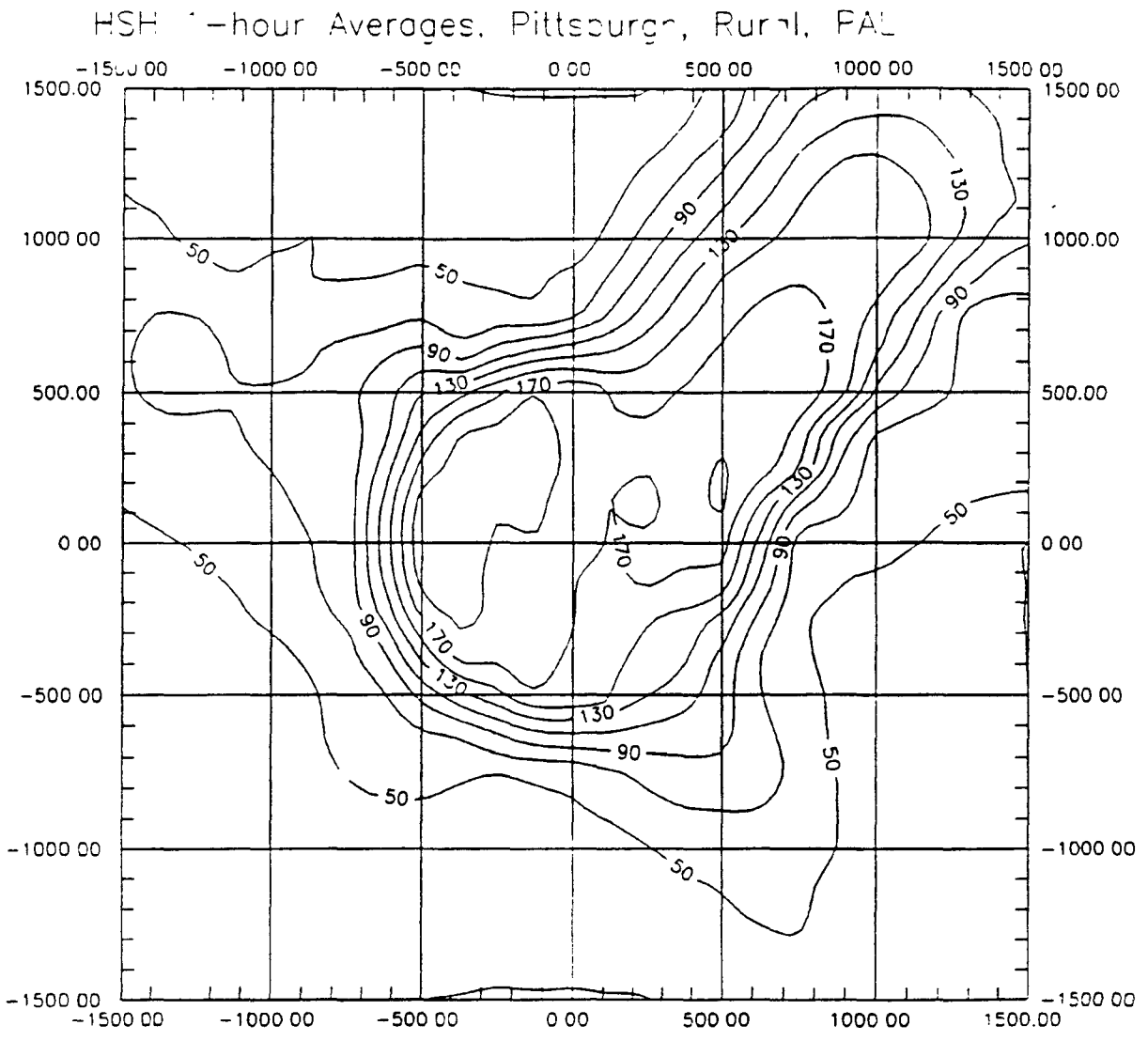

Figure 9. Contour Diagram of HSH 1-hour Average Rural Concentrations ($\mu g/m^3$) from the Numerical Integration Algorithm for the 1000 Meter Wide Ground Level Source with Close-in Receptors Using Pittsburgh 1964 Data.

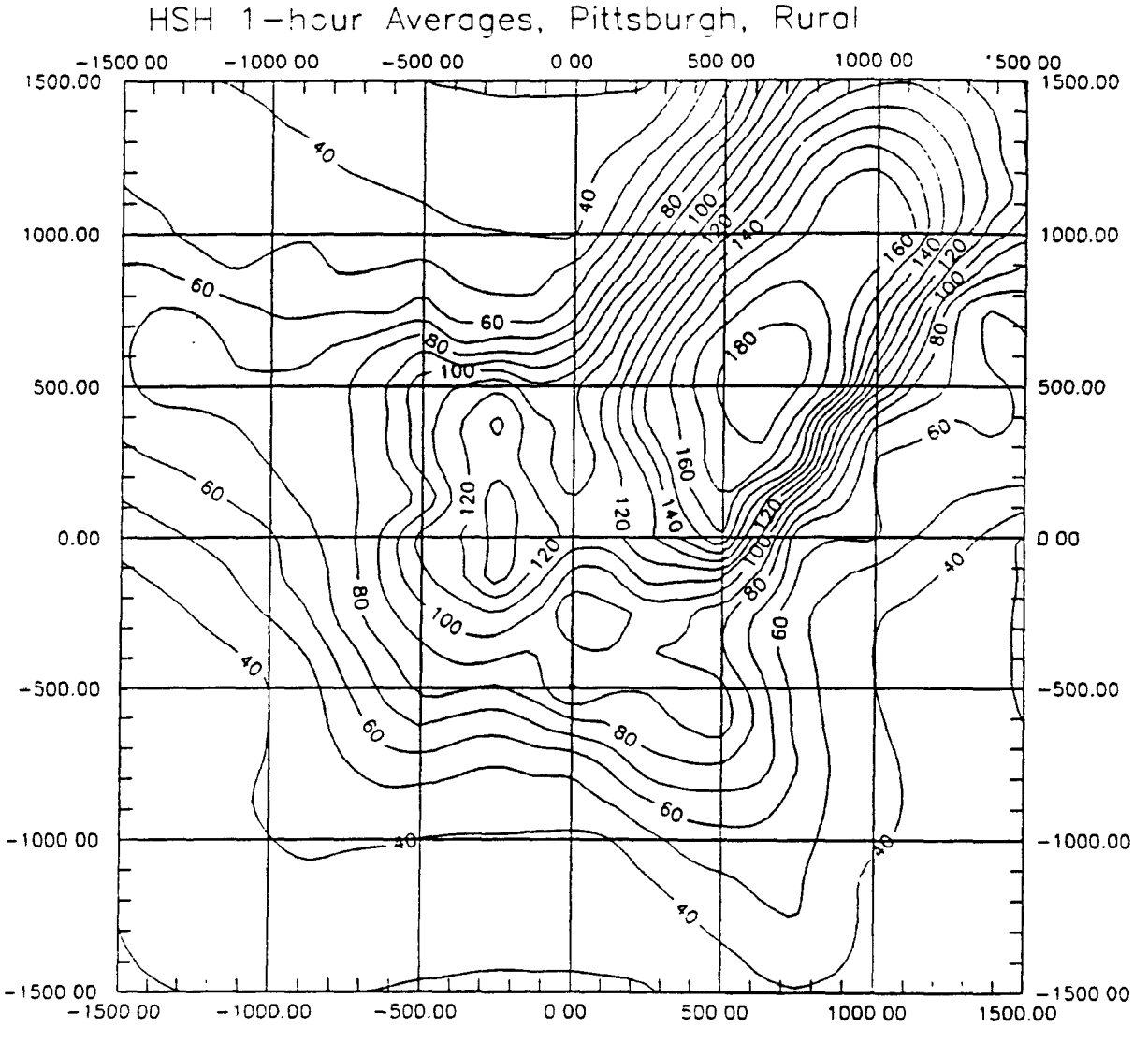

Figure 10. Contour Diagram of HSH 1-hour Average Rural Concentrations ($\mu g/m^3$) from the Finite Line Segment Algorithm for the 1000 Meter Wide Ground Level Source with Close-in Receptors Using Pittsburgh 1964 Data.

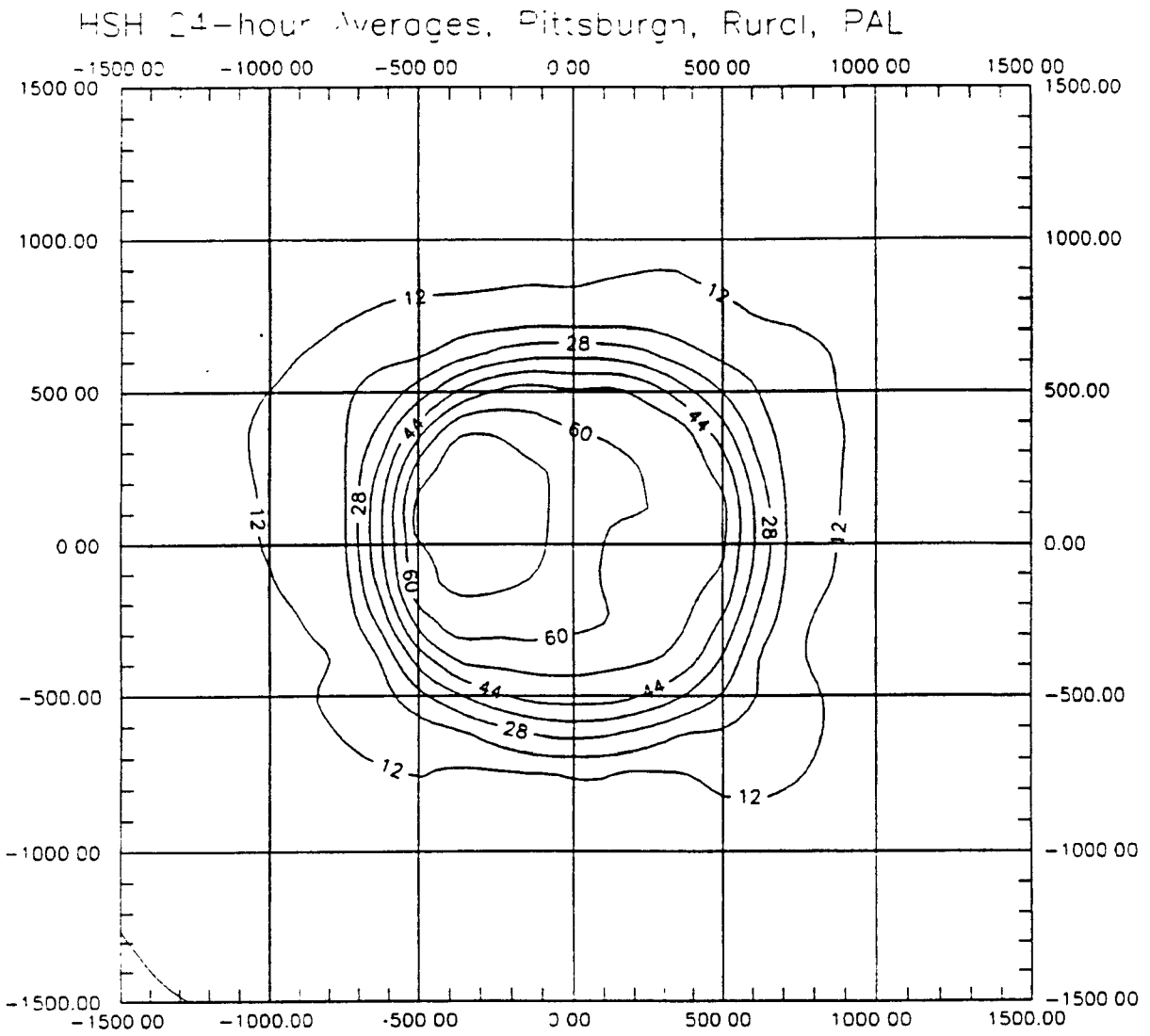

Figure 11. Contour Diagram of HSH 24-hour Average Rural Concentrations ($\mu g/m^3$) from the Numerical Integration Algorithm for the 1000 Meter Wide Ground Level Source with Close-in Receptors Using Pittsburgh 1964 Data.

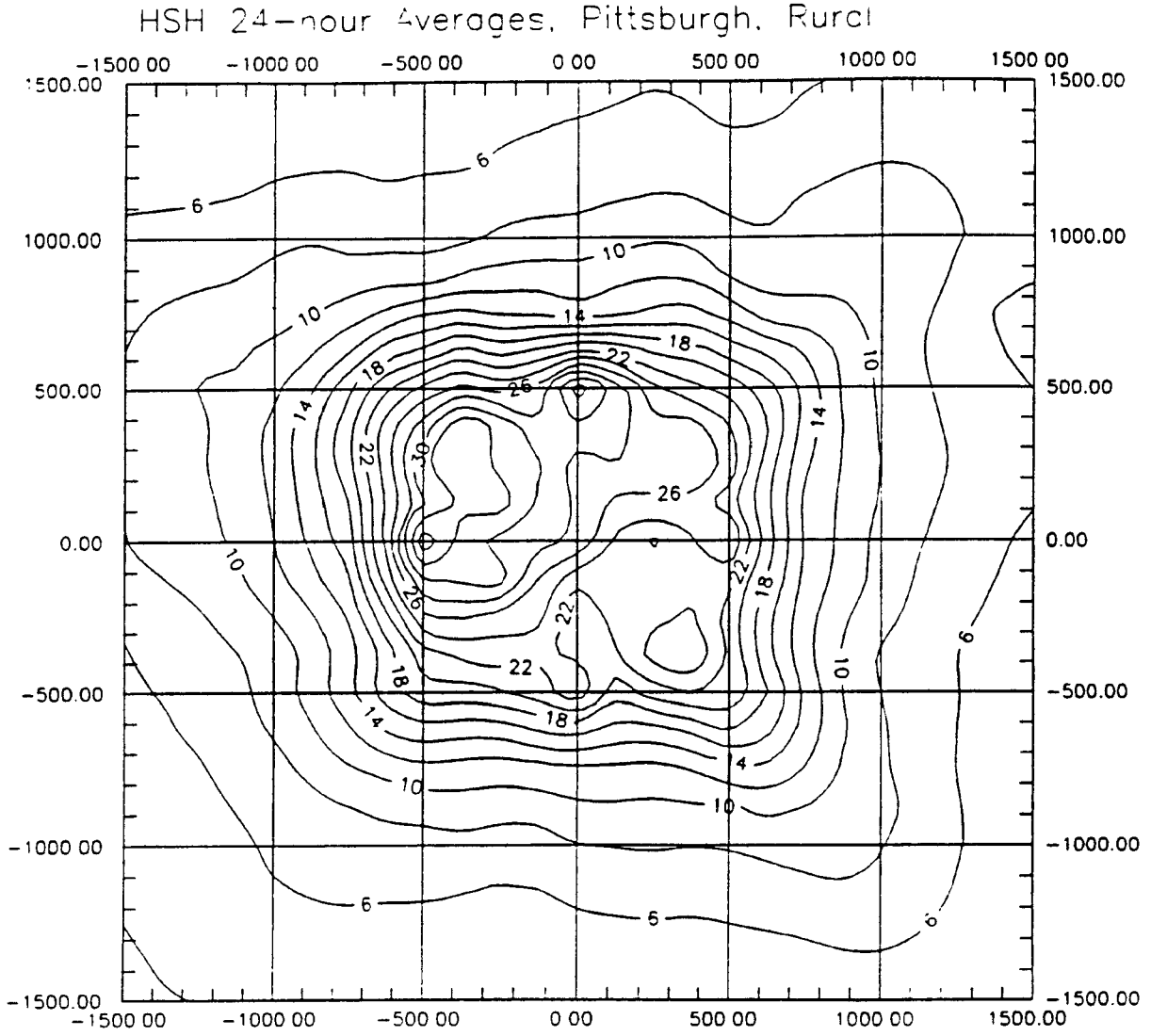

Figure 12. Contour Diagram of HSH 24-hour Average Rural Concentrations ($\mu g/m^3$) from the Finite Line Segment Algorithm for the 1000 Meter Wide Ground Level Source with Close-in Receptors Using Pittsburgh 1964 Data.

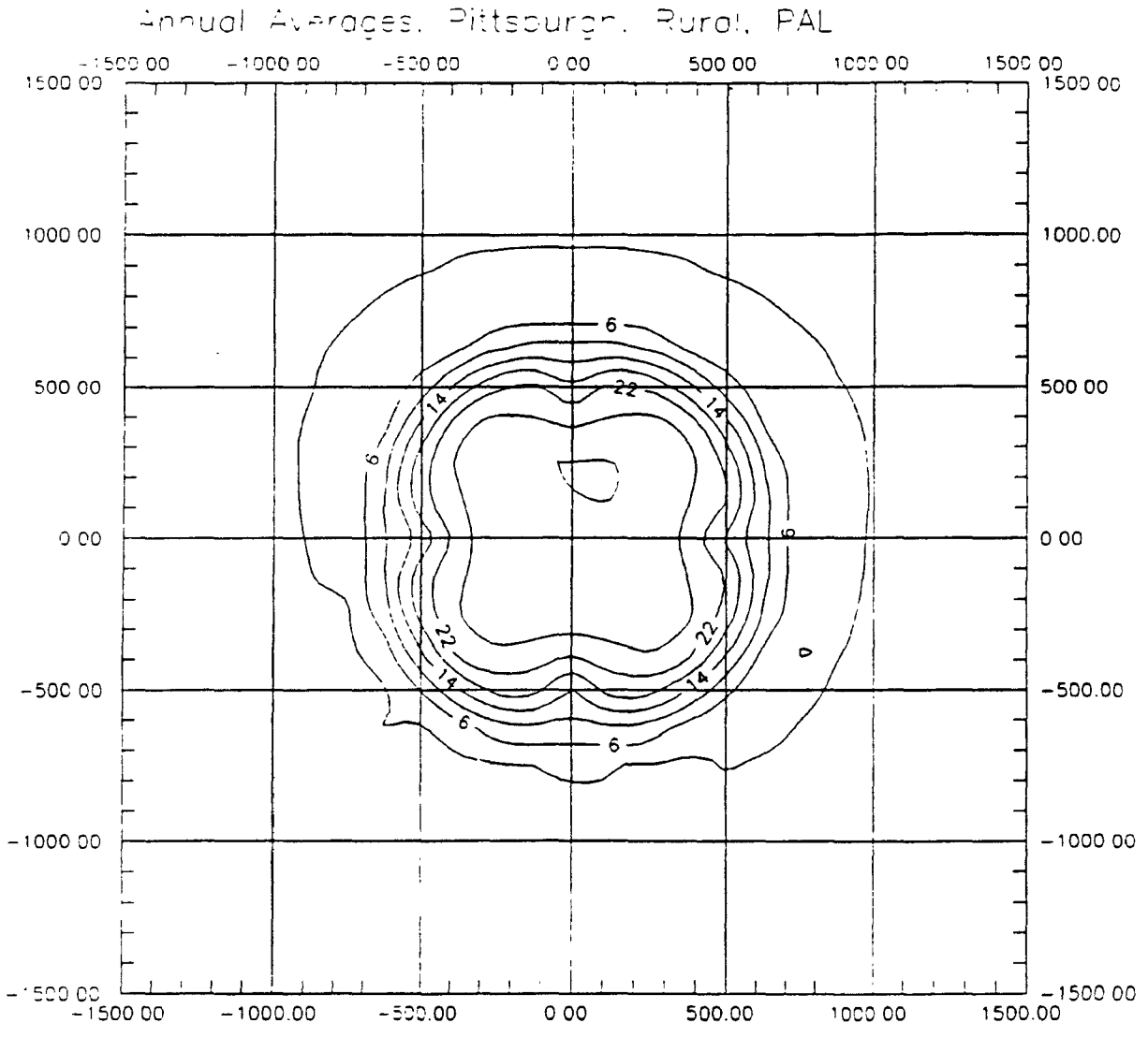

Figure 13. Contour Diagram of Annual Average Rural Concentrations ($\mu g/m^3$) from the Numerical Integration Algorithm for the 1000 Meter Wide Ground Level Source with Close-in Receptors Using Pittsburgh 1964 Data.

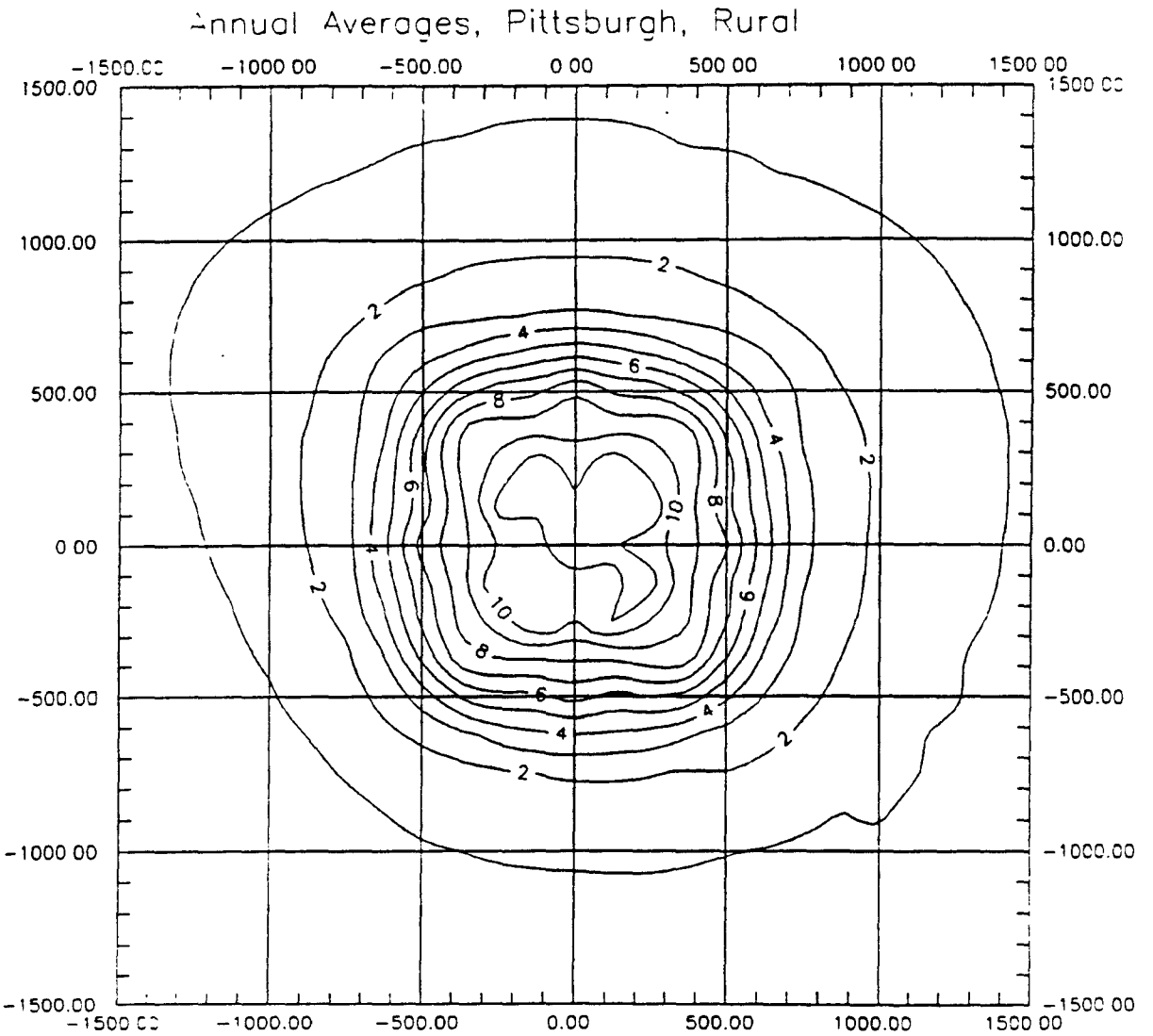

Figure 14. Contour Diagram of Annual Average Rural Concentrations ($\mu g/m^3$) from the Finite Line Segment Algorithm for the 1000 Meter Wide Ground Level Source with Close-in Receptors Using Pittsburgh 1964 Data.

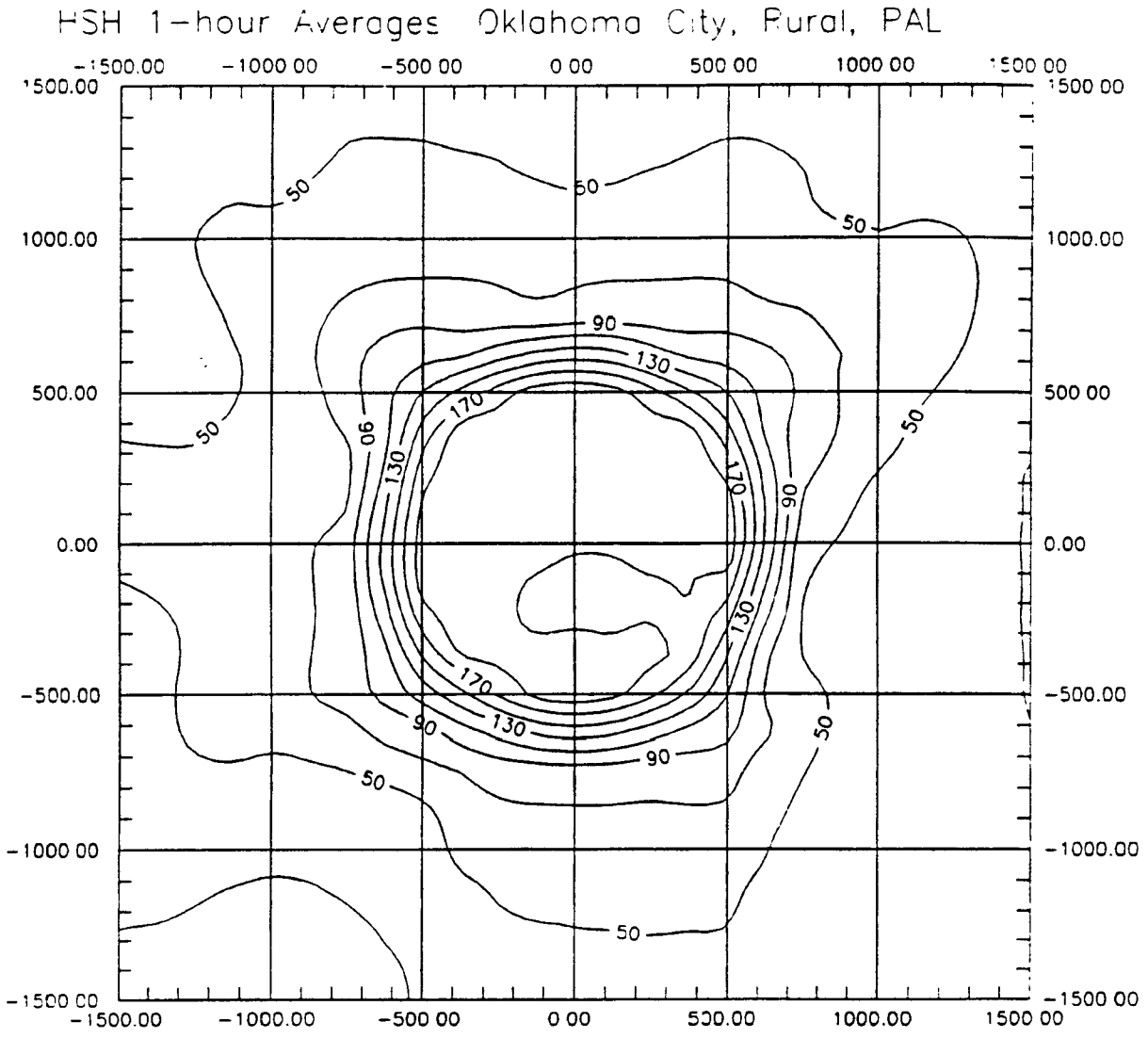

Figure 15. Contour Diagram of HSH 1-hour Average Rural Concentrations ($\mu g/m^3$) from the Numerical Integration Algorithm for the 1000 Meter Wide Ground Level Source with Close-in Receptors Using Oklahoma City 1988 Data.

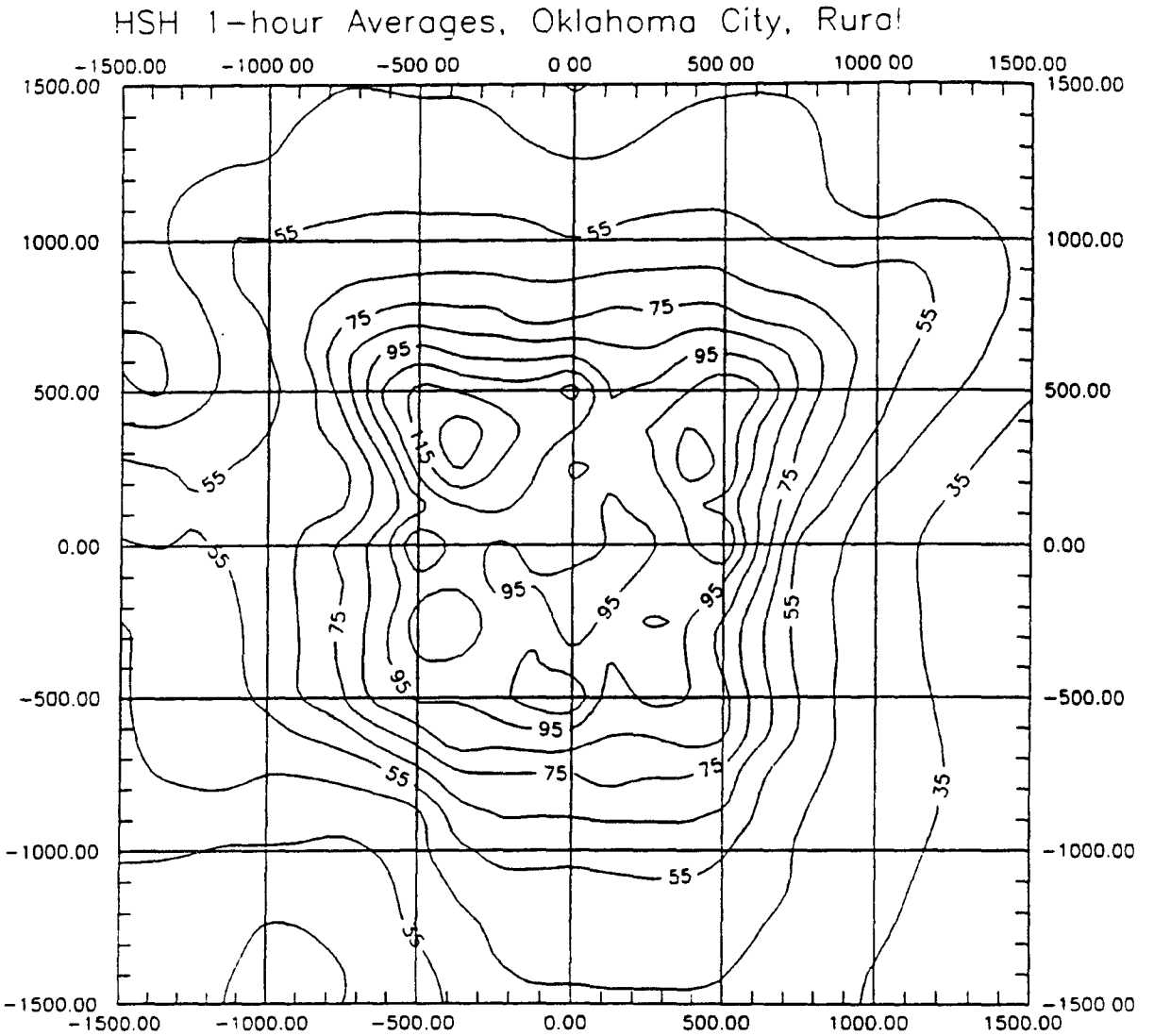

Figure 16. Contour Diagram of HSH 1-hour Average Rural Concentrations ($\mu g/m^3$) from the Finite Line Segment Algorithm for the 1000 Meter Wide Ground Level Source with Close-in Receptors Using Oklahoma City 1988 Data.

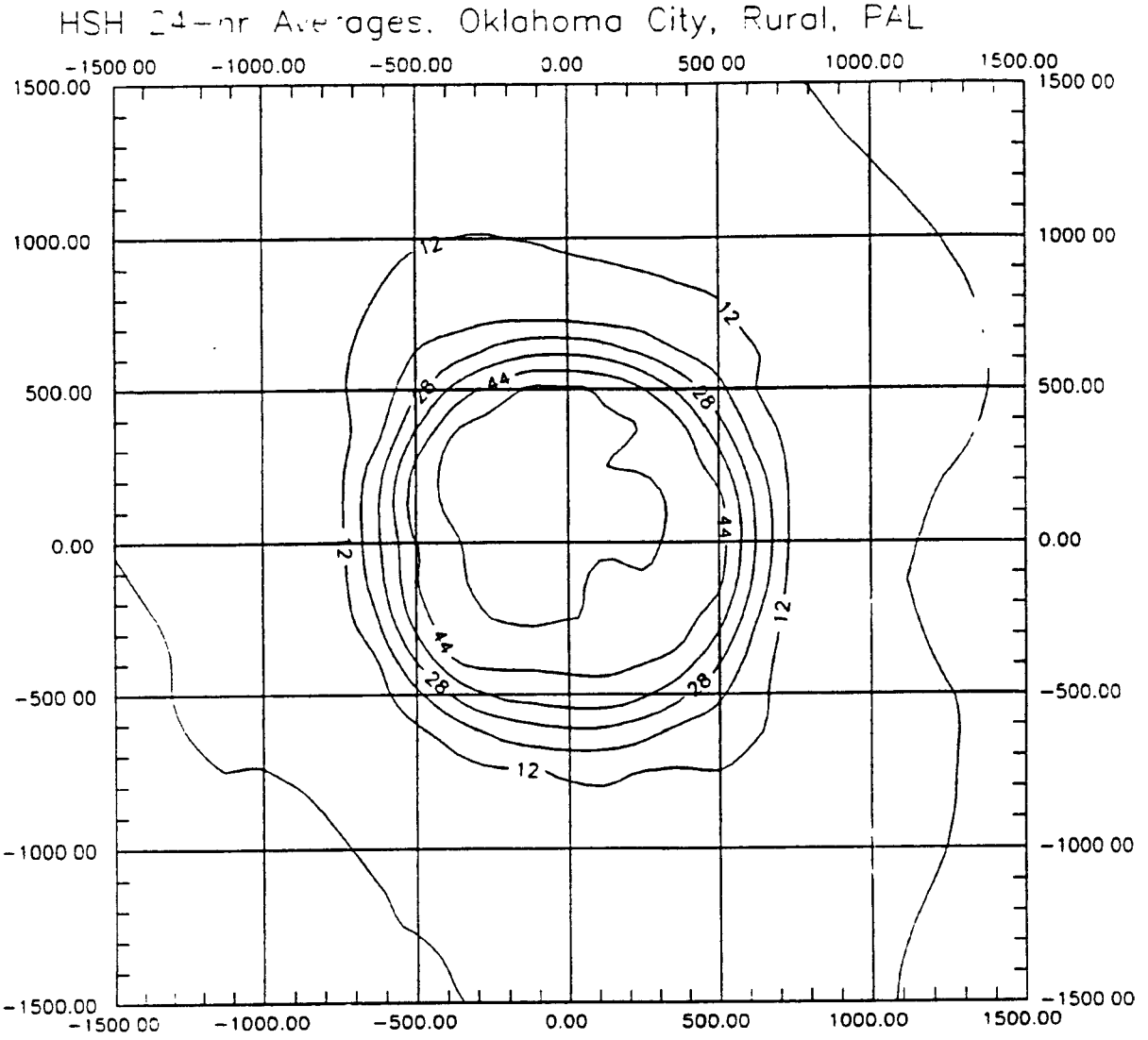

Figure 17. Contour Diagram of HSH 24-hour Average Rural Concentrations ($\mu g/m^3$) from the Numerical Integration Algorithm for the 1000 Meter Wide Ground Level Source with Close-in Receptors Using Oklahoma City 1988 Data.

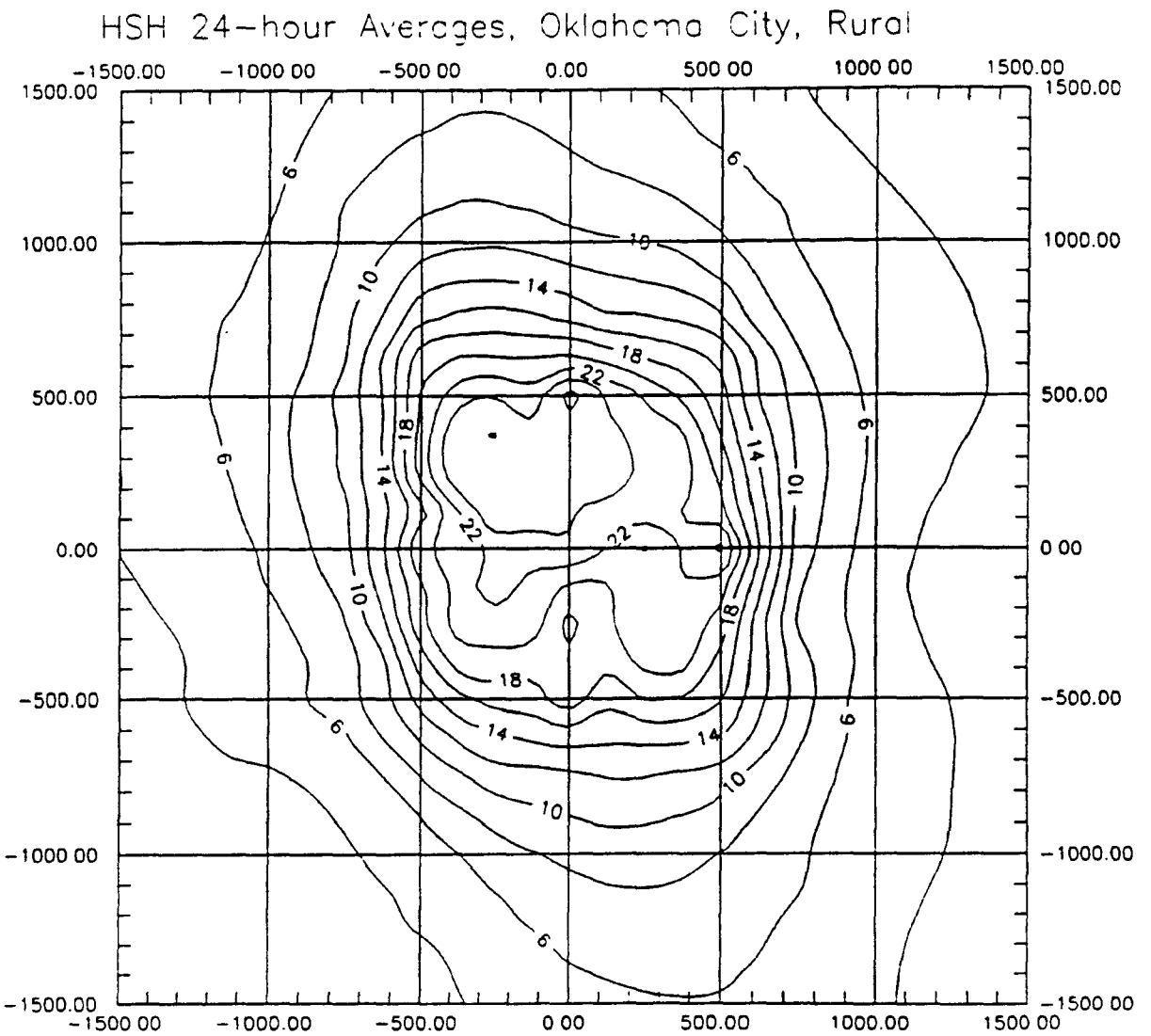

Figure 18. Contour Diagram of HSH 24-hour Average Rural Concentrations ($\mu g/m^3$) from the Finite Line Segment Algorithm for the 1000 Meter Wide Ground Level Source with Close-in Receptors Using Oklahoma City 1988 Data.

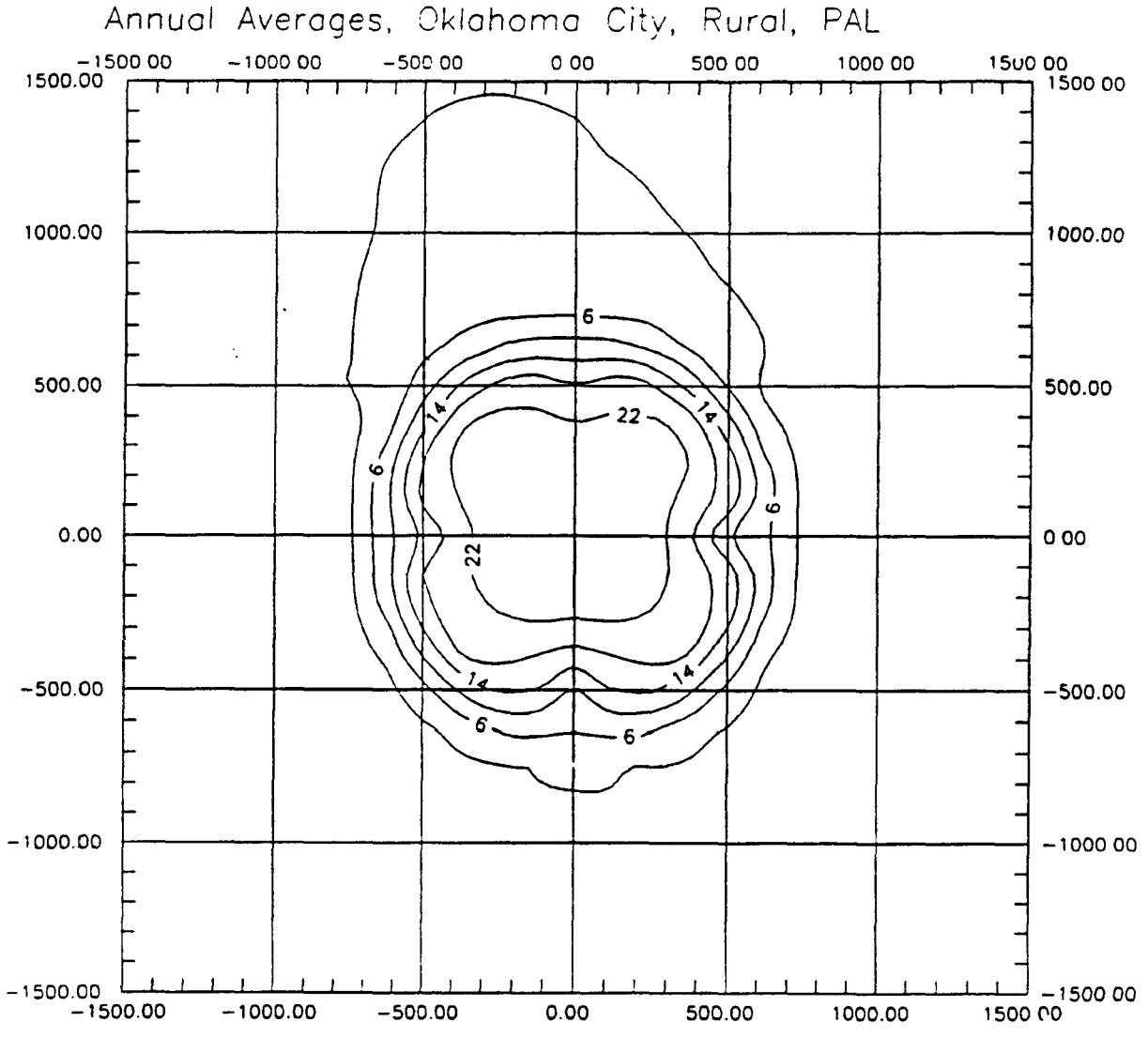

Figure 19. Contour Diagram of Annual Average Rural Concentrations ($\mu g/m^3$) from the Numerical Integration Algorithm for the 1000 Meter Wide Ground Level Source with Close-in Receptors Using Oklahoma City 1988 Data.

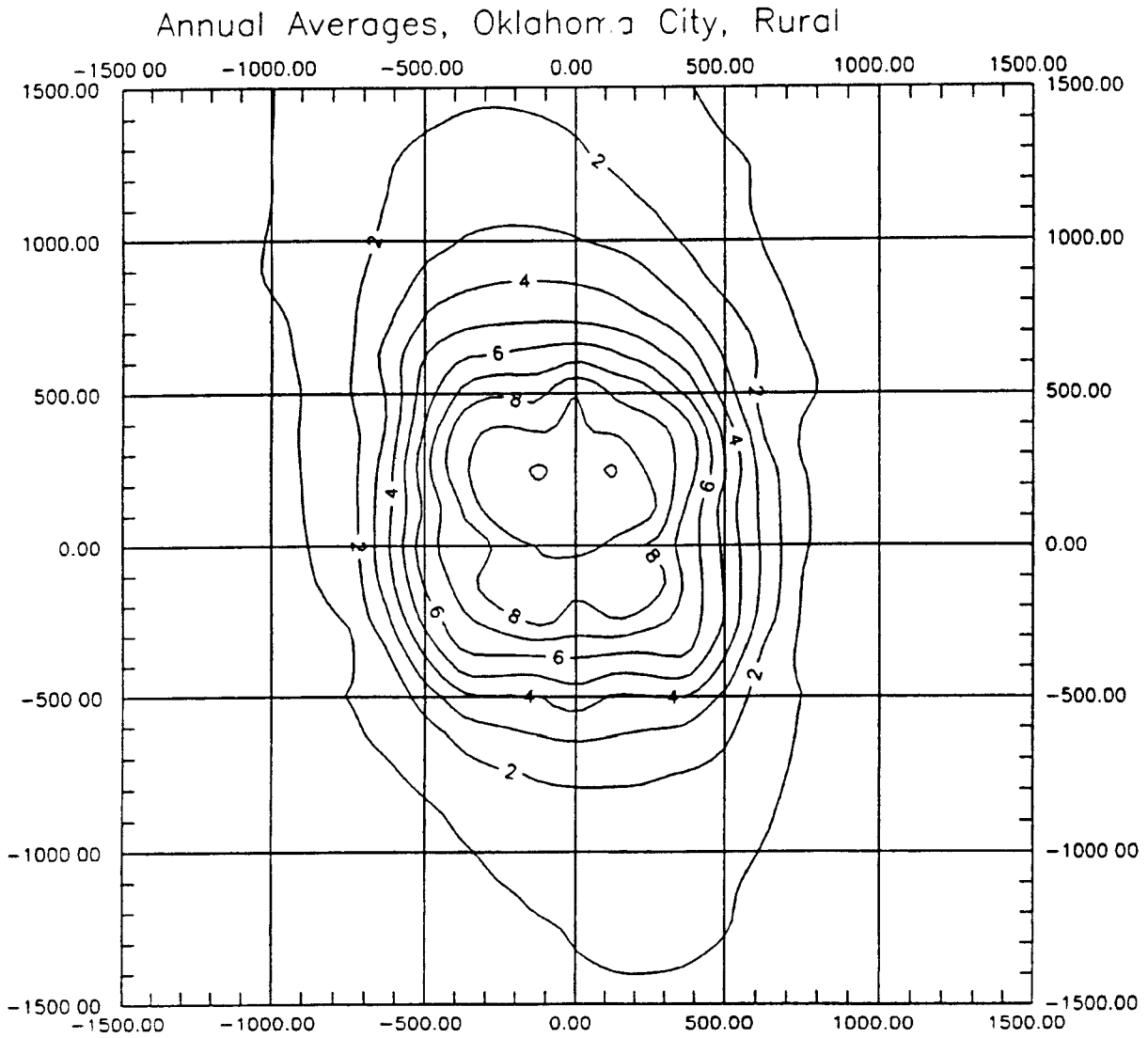

Figure 20. Contour Diagram of Annual Average Rural Concentrations ($\mu g/m^3$) from the Finite Line Segment Algorithm for the 1000 Meter Wide Ground Level Source with Close-in Receptors Using Oklahoma City 1988 Data.

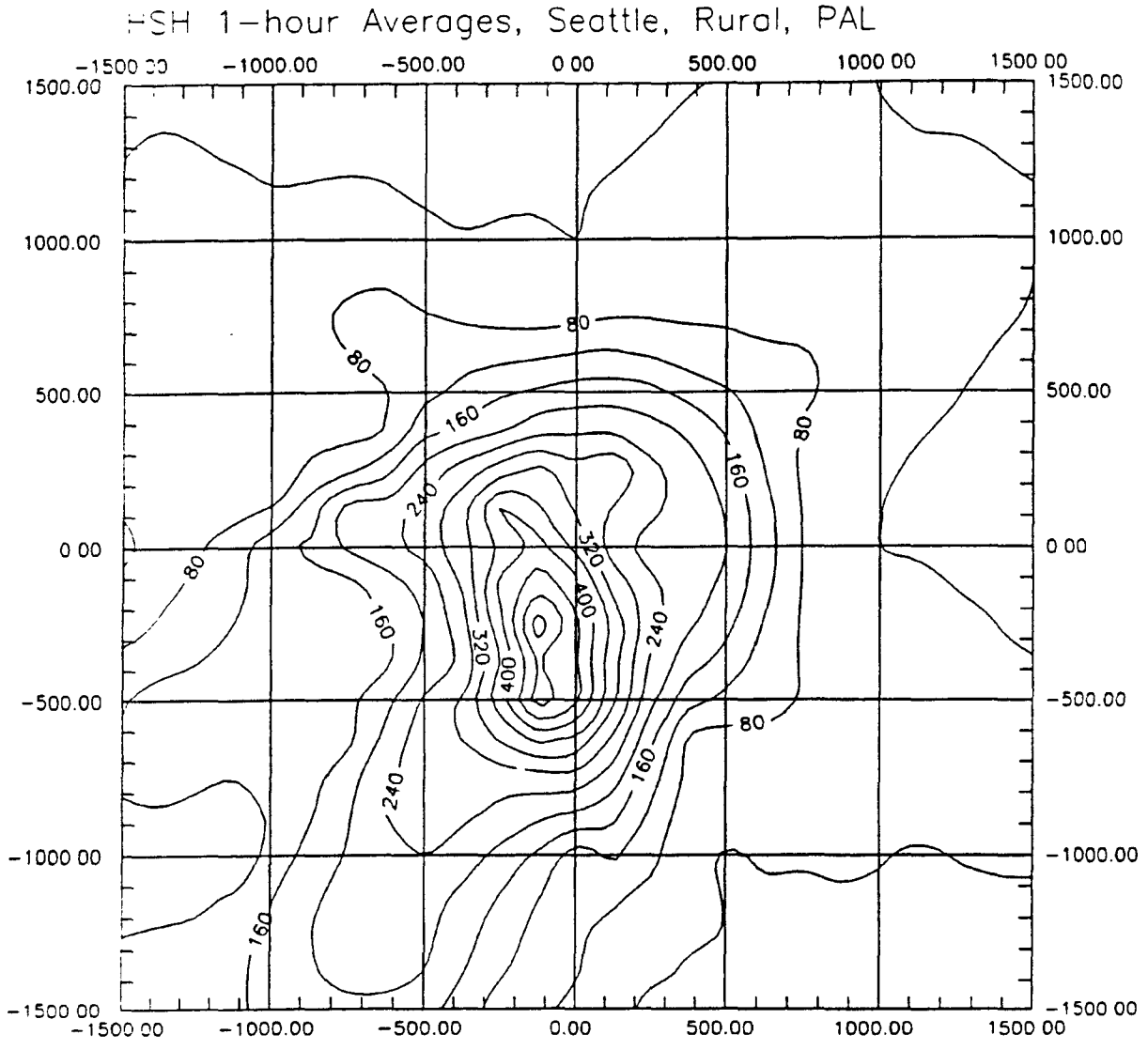

Figure 21. Contour Diagram of HSH 1-hour Average Rural Concentrations ($\mu g/m^3$) from the Numerical Integration Algorithm for the 1000 Meter Wide Ground Level Source with Close-in Receptors Using Seattle 1983 Data.

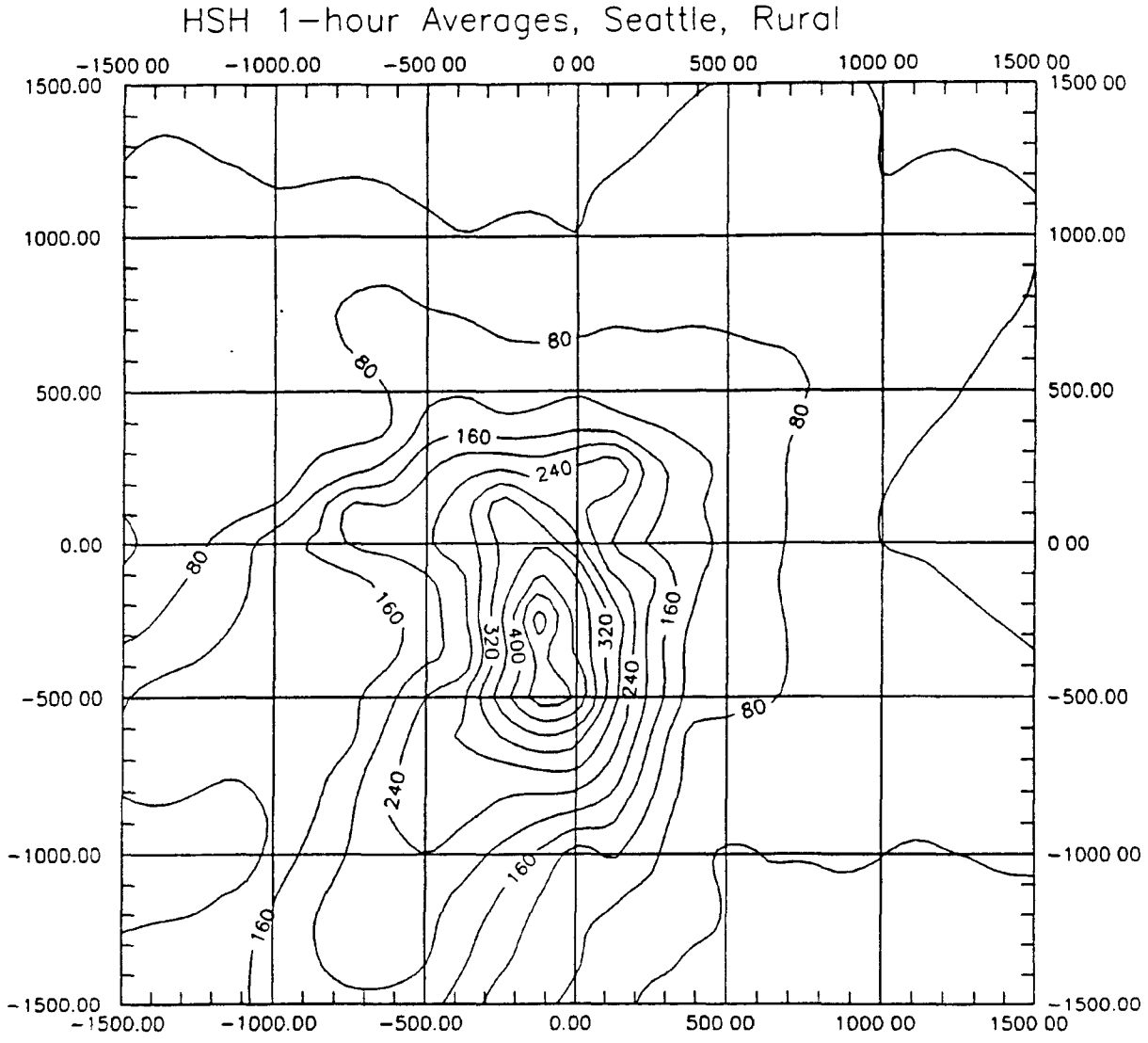

Figure 22. Contour Diagram of HSH 1-hour Average Rural Concentrations ($\mu g/m^3$) from the Finite Line Segment Algorithm for the 1000 Meter Wide Ground Level Source with Close-in Receptors Using Seattle 1983 Data.

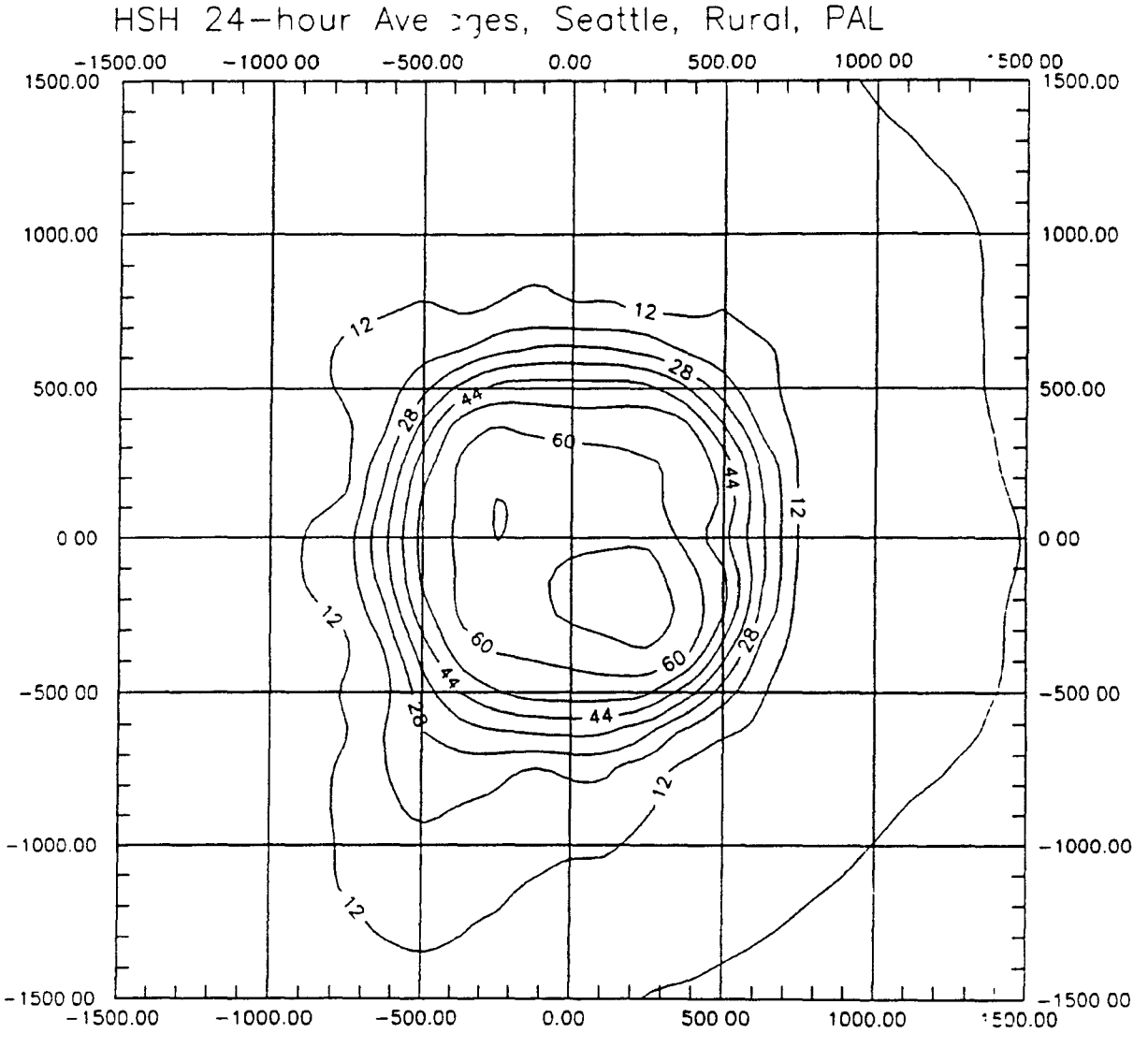

Figure 23. Contour Diagram of HSH 24-hour Average Rural Concentrations ($\mu g/m^3$) from the Numerical Integration Algorithm for the 1000 Meter Wide Ground Level Source with Close-in Receptors Using Seattle 1983 Data.

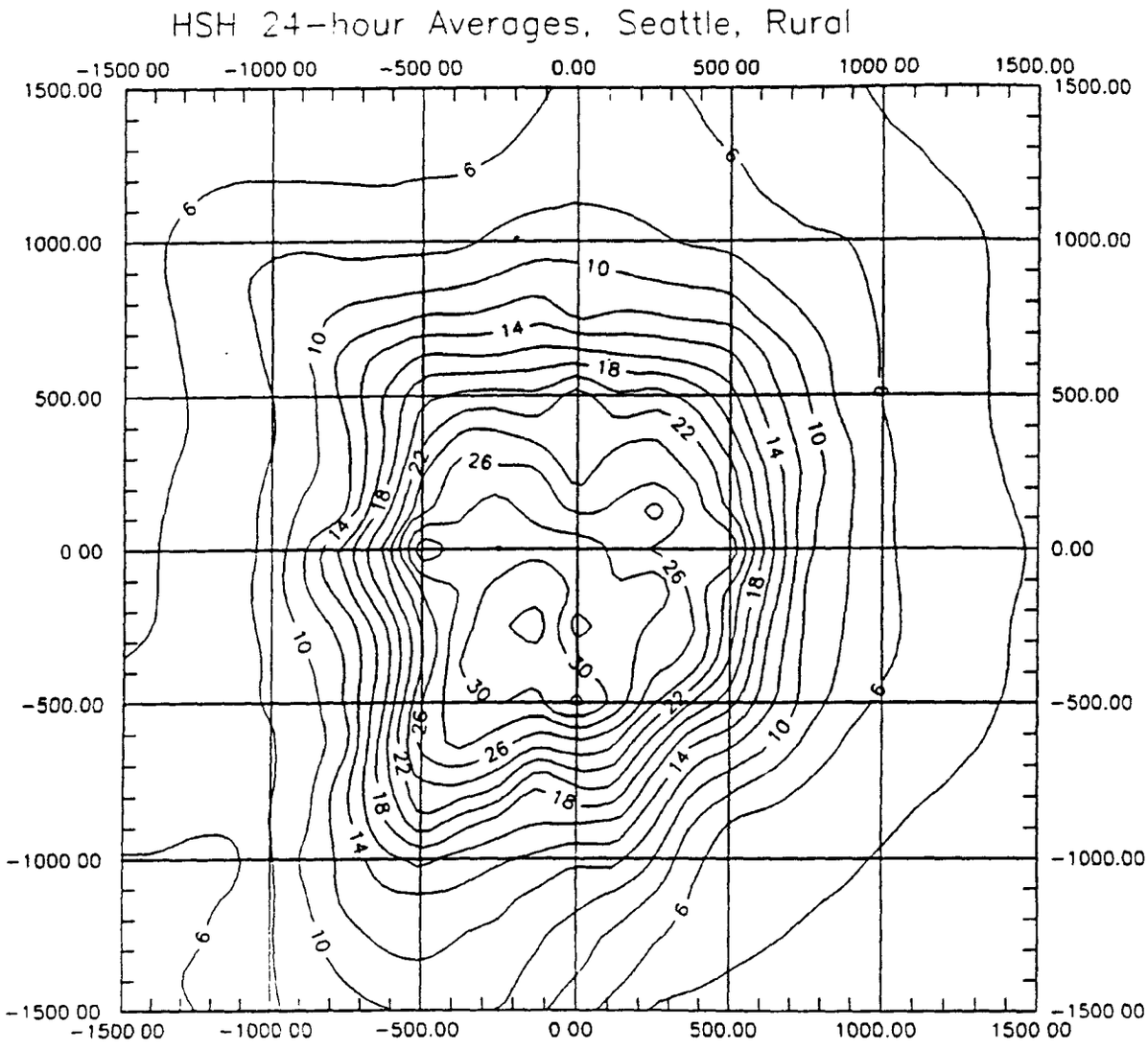

Figure 24. Contour Diagram of HSH 24-hour Average Rural Concentrations ($\mu g/m^3$) from the Finite Line Segment Algorithm for the 1000 Meter Wide Ground Level Source with Close-in Receptors Using Seattle 1983 Data.

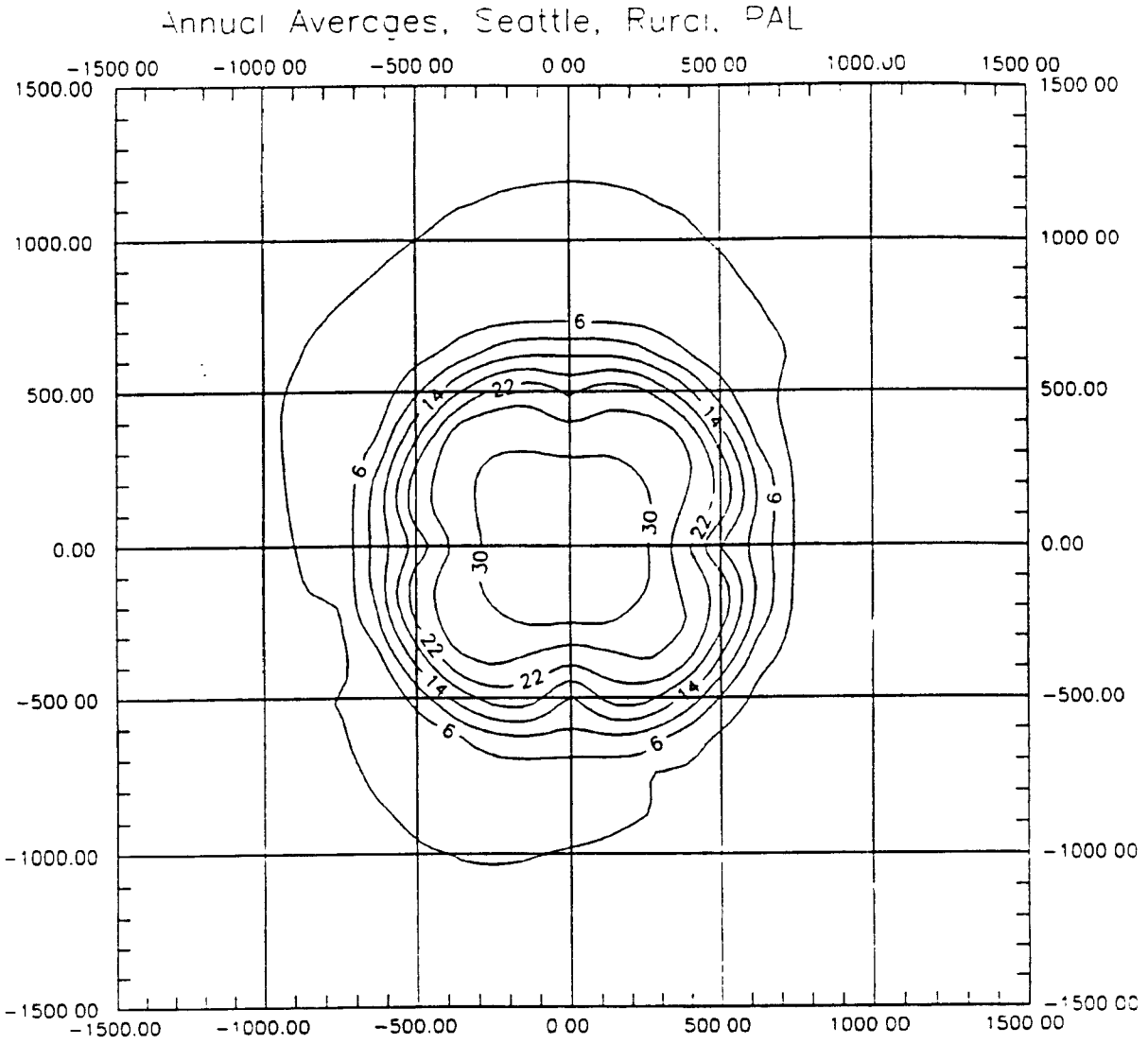

Figure 25. Contour Diagram of Annual Average Rural Concentrations ($\mu g/m^3$) from the Numerical Integration Algorithm for the 1000 Meter Wide Ground Level Source with Close-in Receptors Using Seattle 1983 Data.

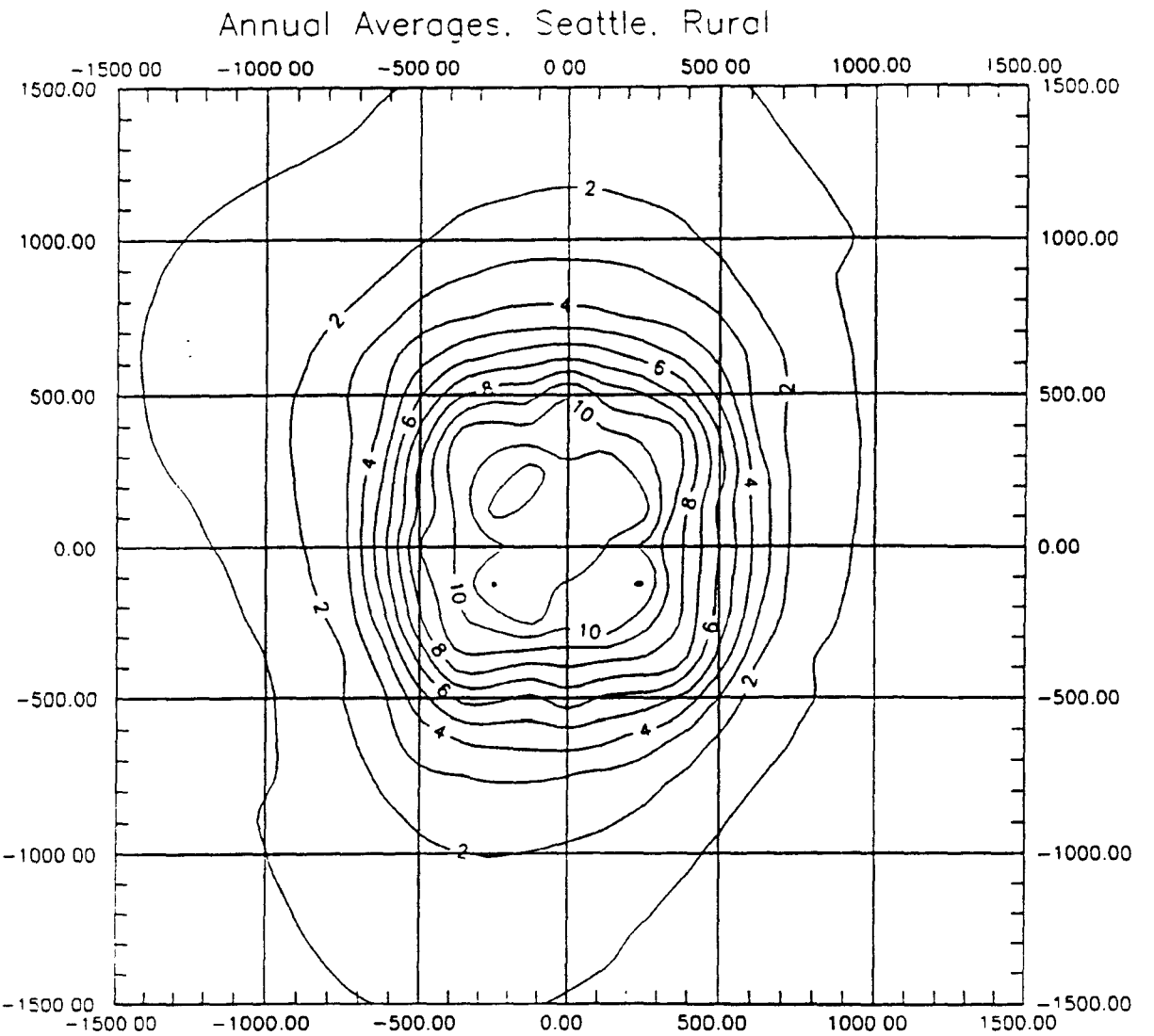

Figure 26. Contour Diagram of Annual Average Rural Concentrations ($\mu g/m^3$) from the Finite Line Segment Algorithm for the 1000 Meter Wide Ground Level Source with Close-in Receptors Using Seattle 1983 Data.

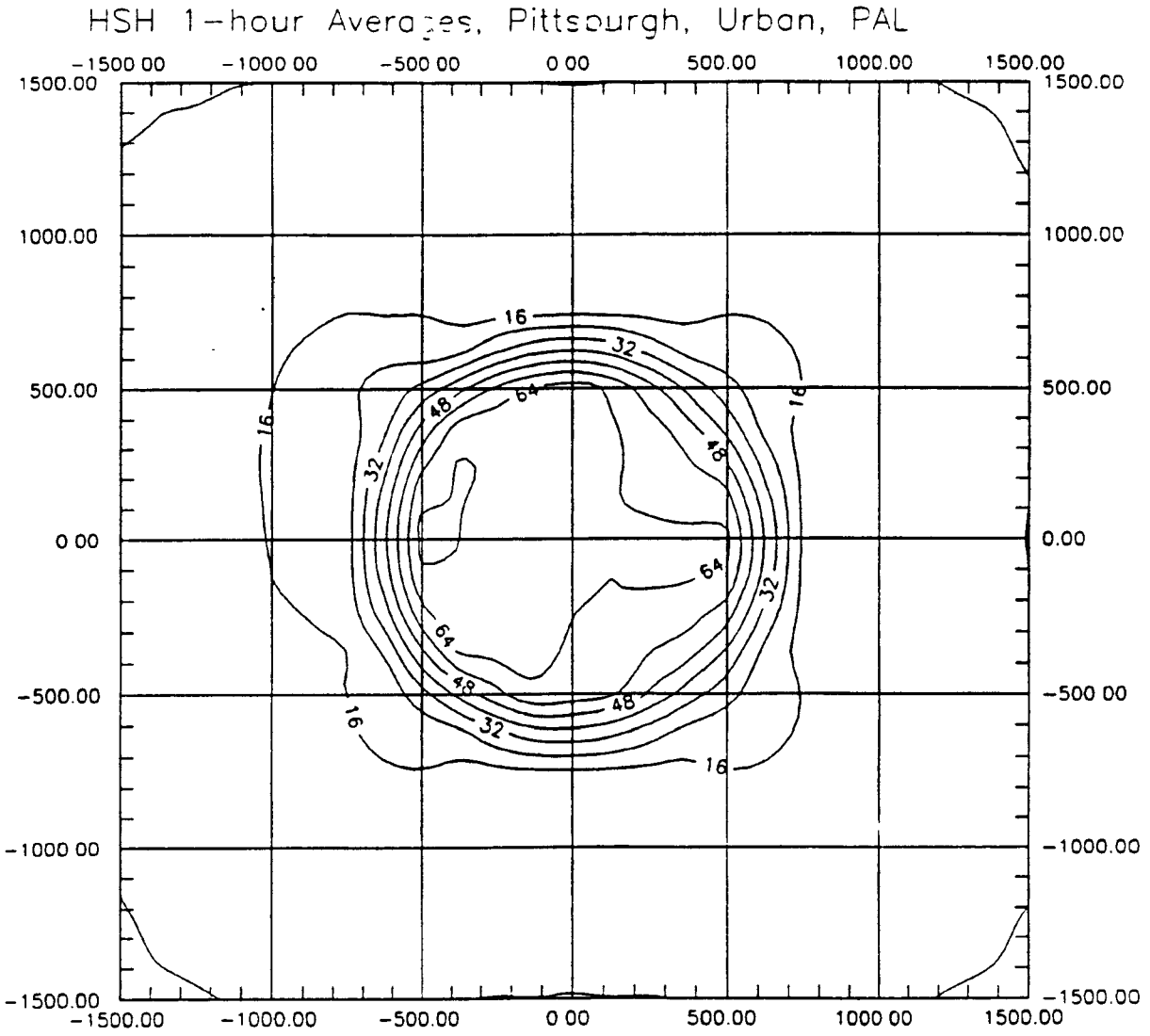

Figure 27. Contour Diagram of HSH 1-hour Average Urban Concentrations ($\mu g/m^3$) from the Numerical Integration Algorithm for the 1000 Meter Wide Ground Level Source with Close-in Receptors Using Pittsburgh 1964 Data.

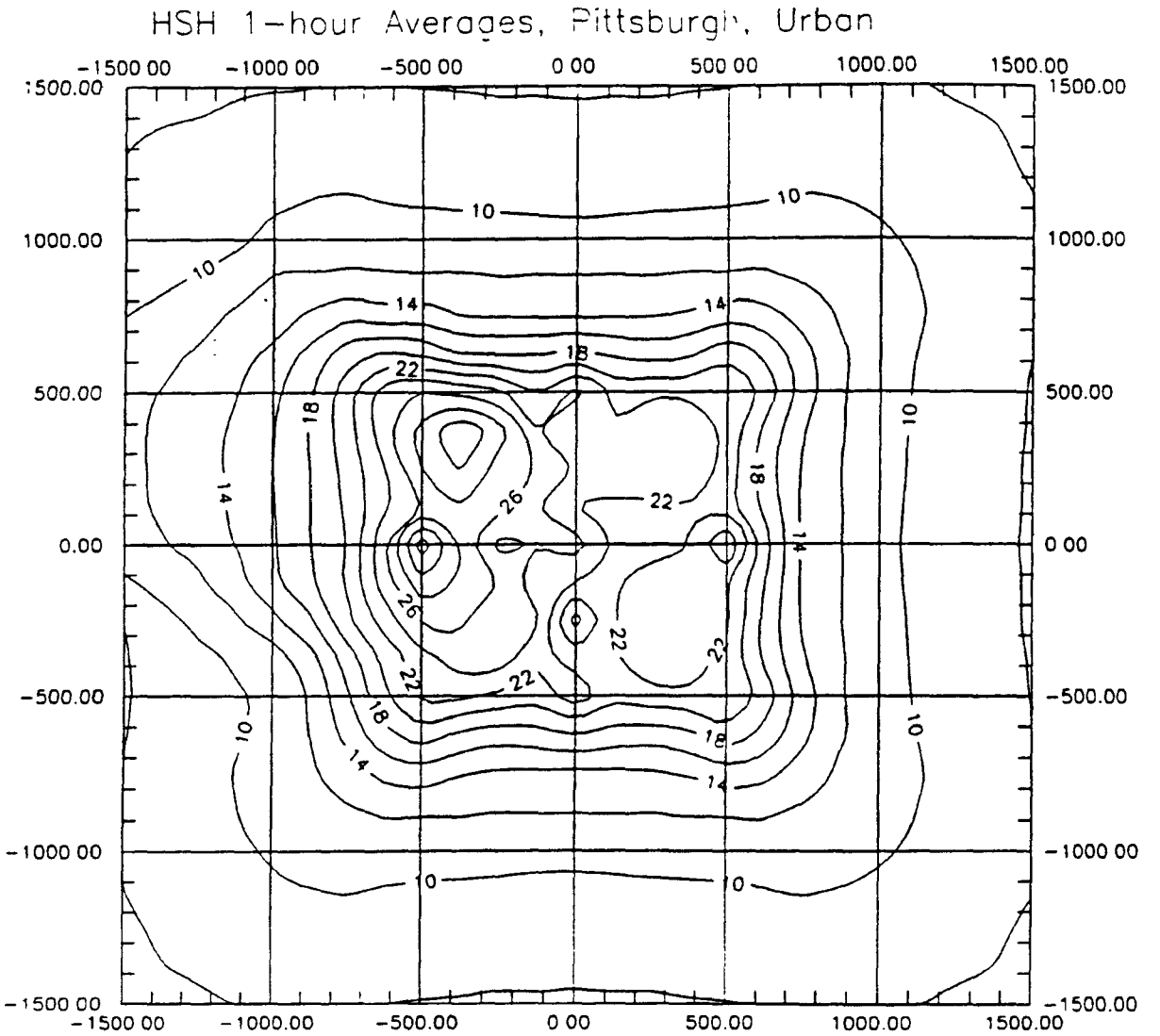

Figure 28. Contour Diagram of HSH 1-hour Average Urban Concentrations ($\mu g/m^3$) from the Finite Line Segment Algorithm for the 1000 Meter Wide Ground Level Source with Close-in Receptors Using Pittsburgh 1964 Data.

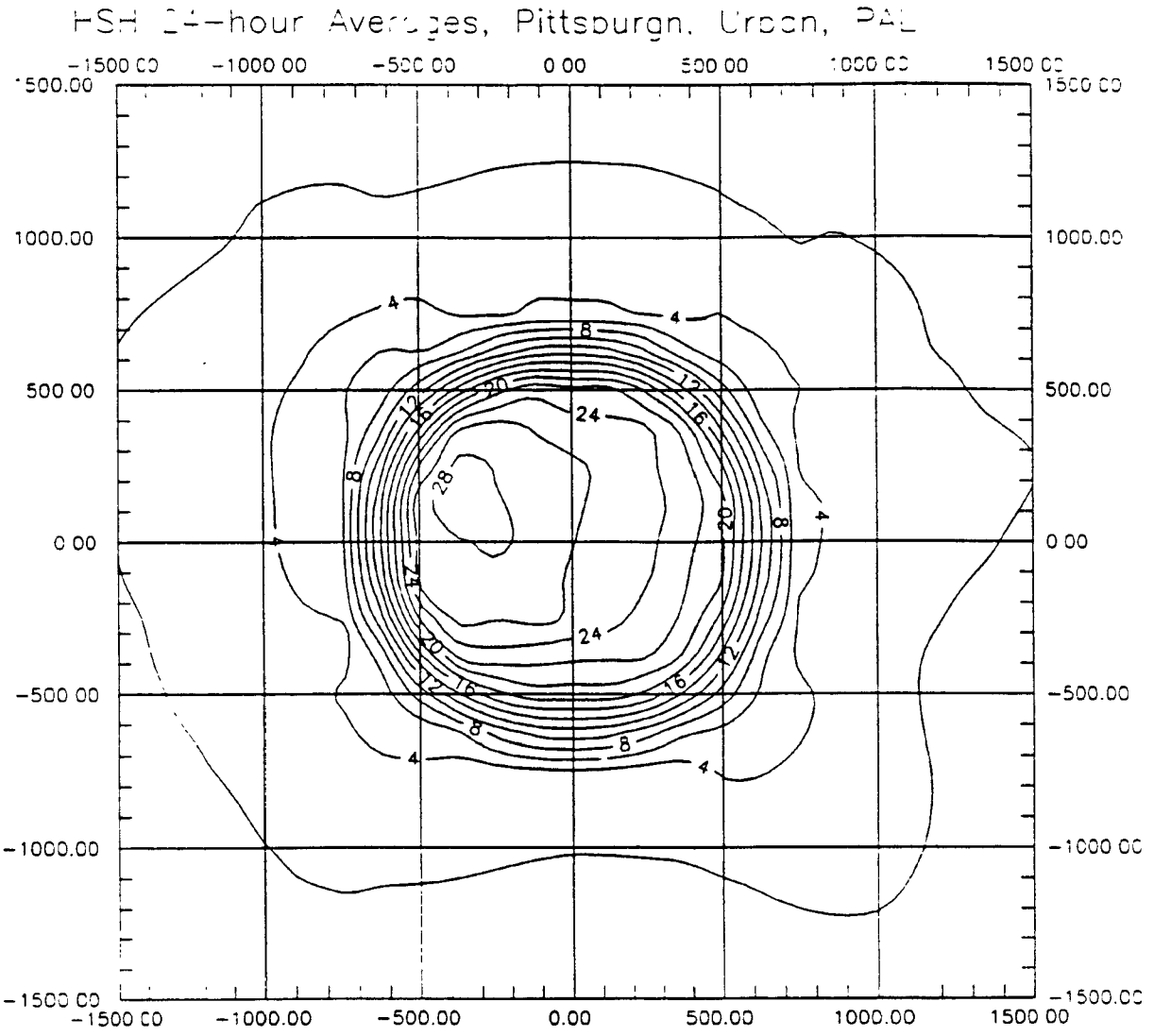

Figure 29. Contour Diagram of HSH 24-hour Average Urban Concentrations ($\mu g/m^3$) from the Numerical Integration Algorithm for the 1000 Meter Wide Ground Level Source with Close-in Receptors Using Pittsburgh 1964 Data.

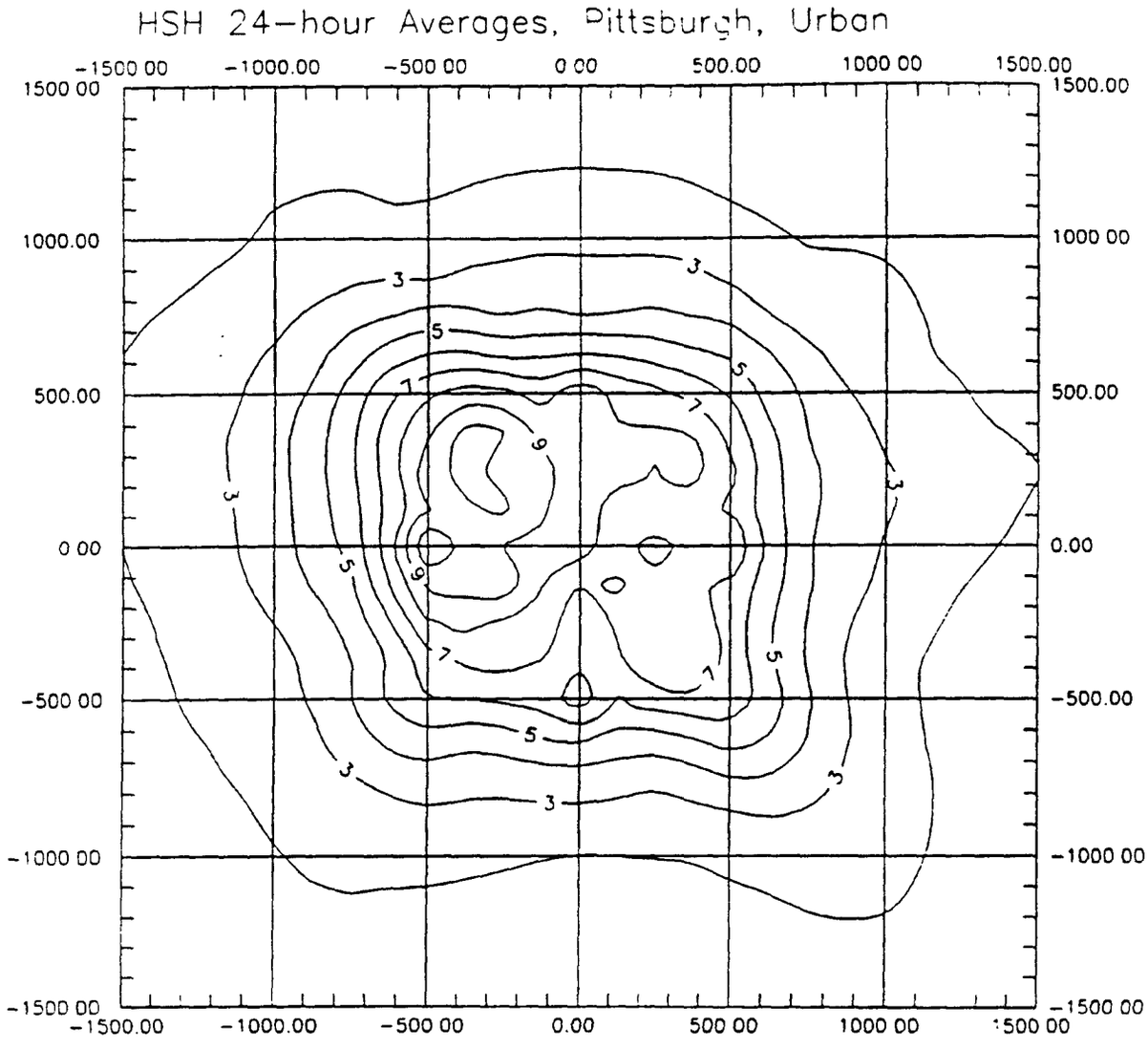

Figure 30. Contour Diagram of HSH 24-hour Average Urban Concentrations ($\mu g/m^3$) from the Finite Line Segment Algorithm for the 1000 Meter Wide Ground Level Source with Close-in Receptors Using Pittsburgh 1964 Data.

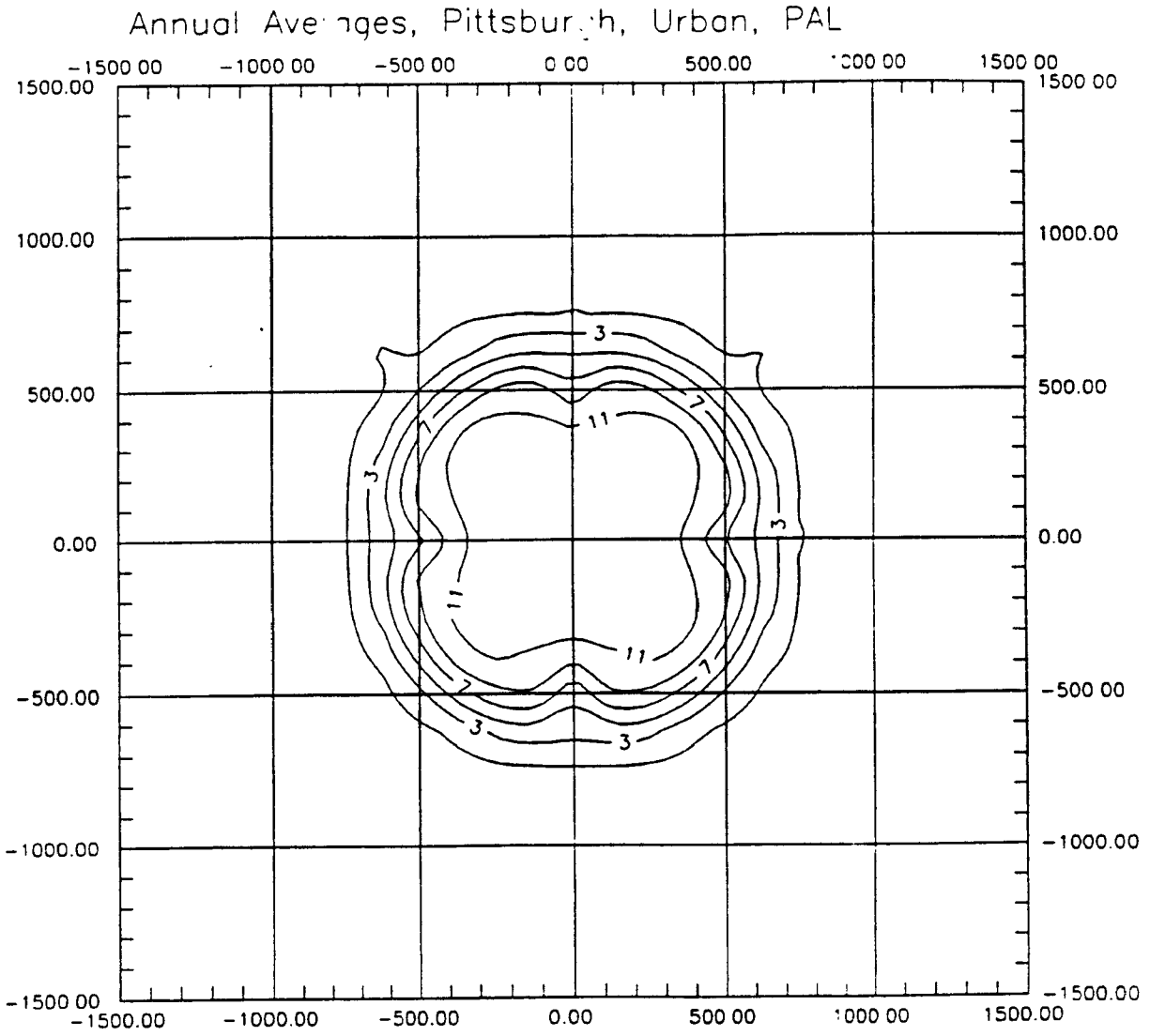

Figure 31. Contour Diagram of Annual Average Urban Concentrations ($\mu g/m^3$) from the Numerical Integration Algorithm for the 1000 Meter Wide Ground Level Source with Close-in Receptors Using Pittsburgh 1964 Data.

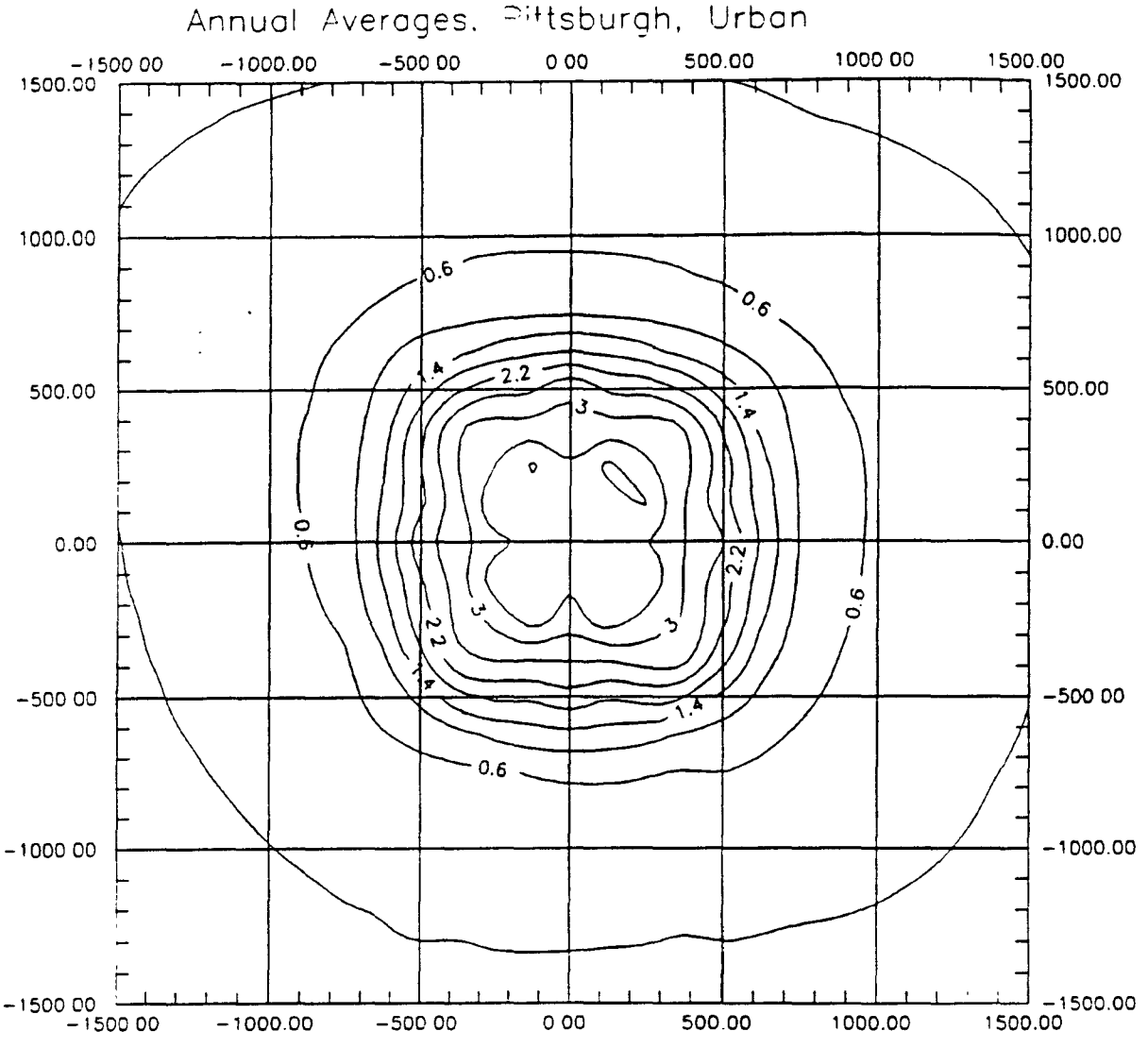

Figure 32. Contour Diagram of Annual Average Urban Concentrations ($\mu g/m^3$) from the Finite Line Segment Algorithm for the 1000 Meter Wide Ground Level Source with Close-in Receptors Using Pittsburgh 1964 Data.

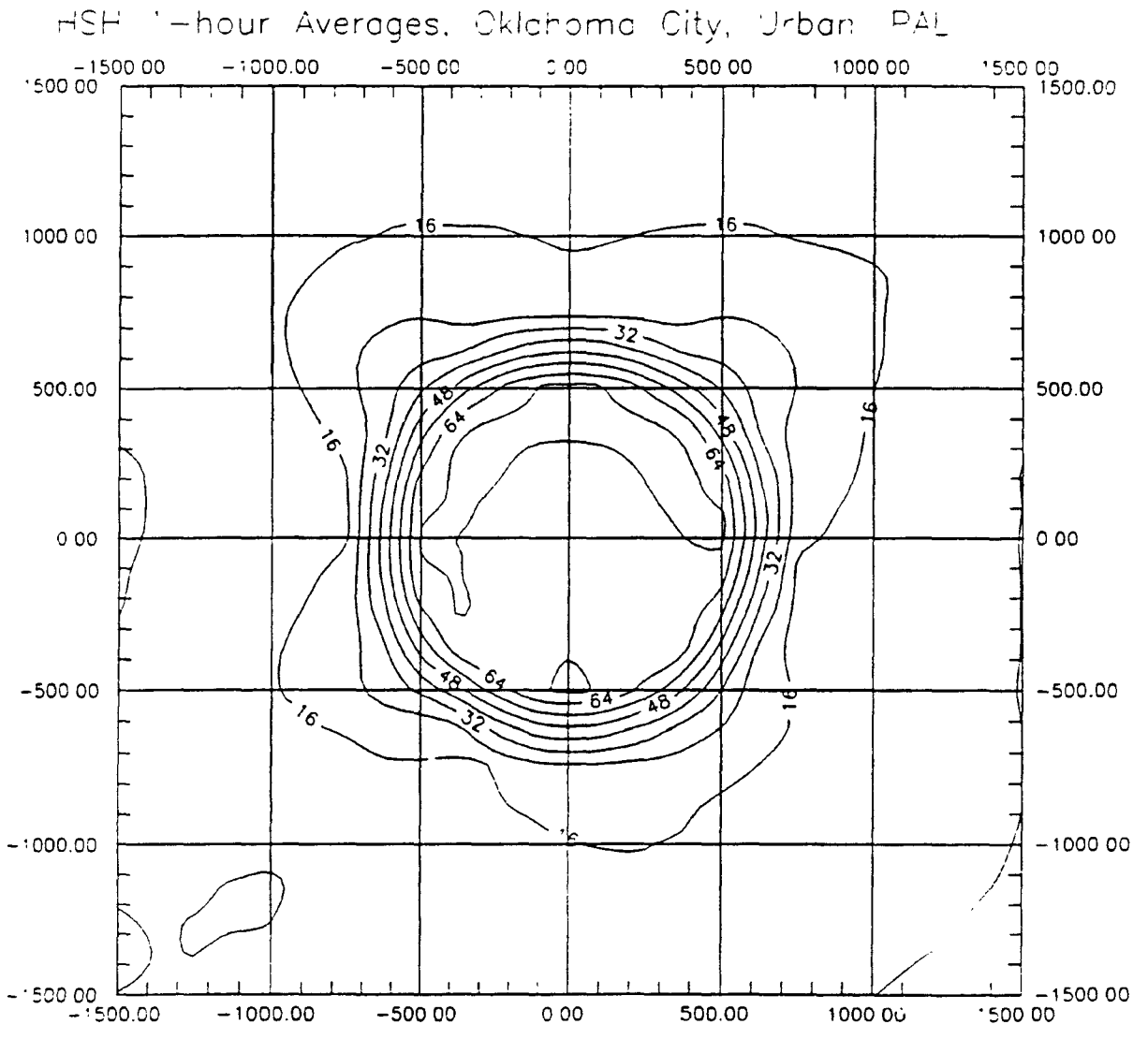

Figure 33. Contour Diagram of HSH 1-hour Average Urban Concentrations ($\mu g/m^3$) from the Numerical Integration Algorithm for the 1000 Meter Wide Ground Level Source with Close-in Receptors Using Oklahoma City 1988 Data.

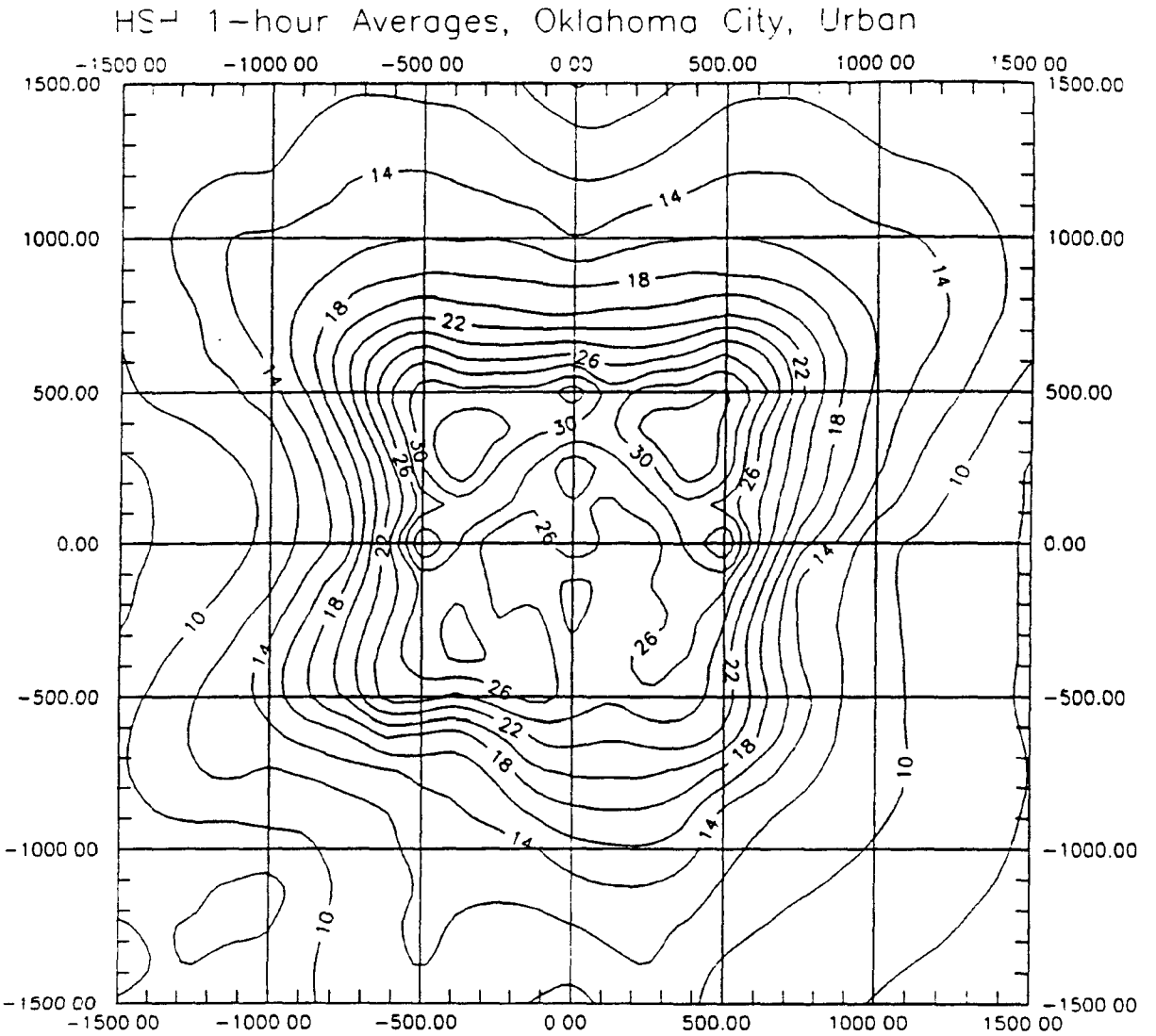

Figure 34. Contour Diagram of HSH 1-hour Average Urban Concentrations ($\mu g/m^3$) from the Finite Line Segment Algorithm for the 1000 Meter Wide Ground Level Source with Close-in Receptors Using Oklahoma City 1988 Data.

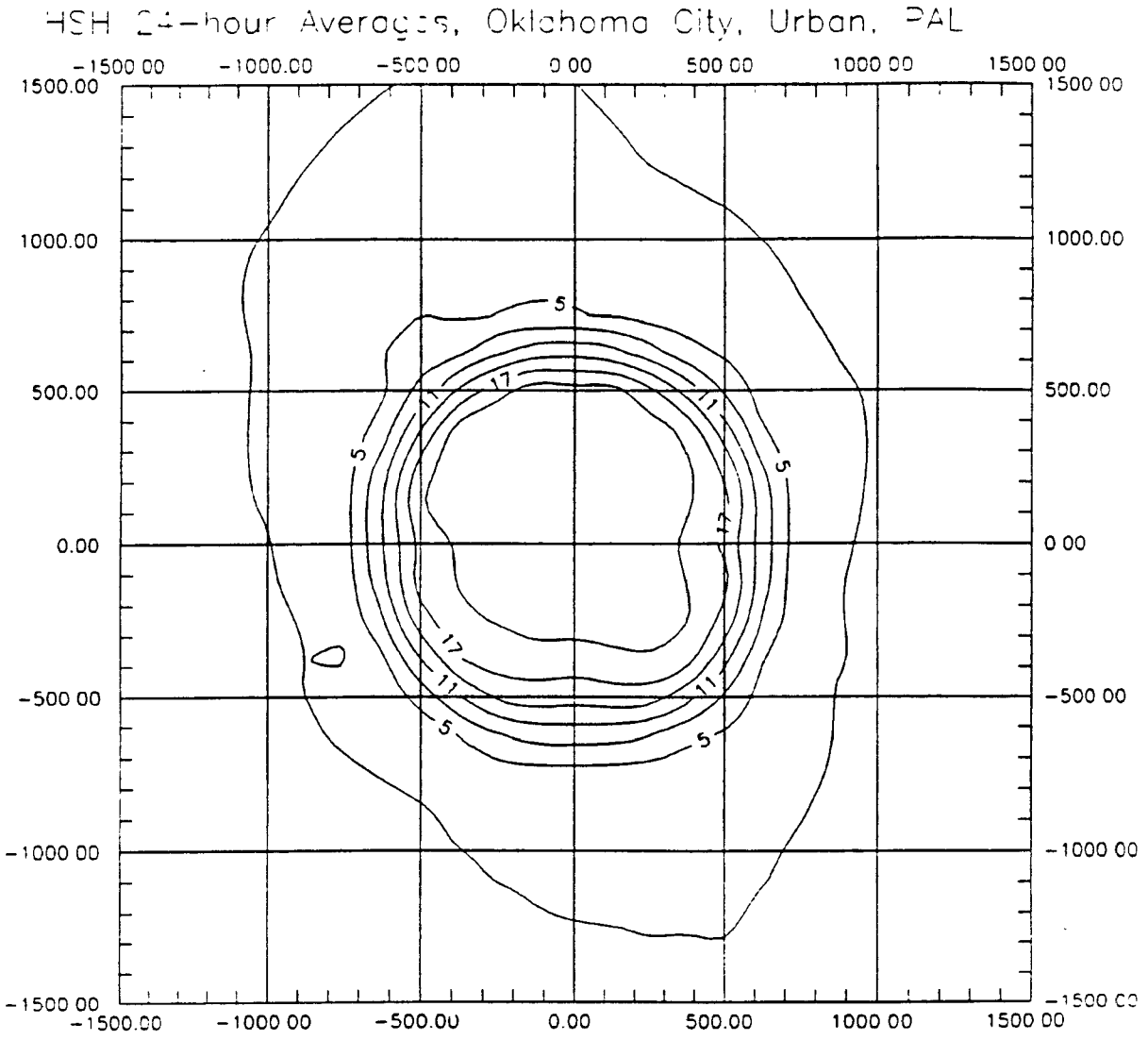

Figure 35. Contour Diagram of HSH 24-hour Average Urban Concentrations ($\mu g/m^3$) from the Numerical Integration Algorithm for the 1000 Meter Wide Ground Level Source with Close-in Receptors Using Oklahoma City 1988 Data.

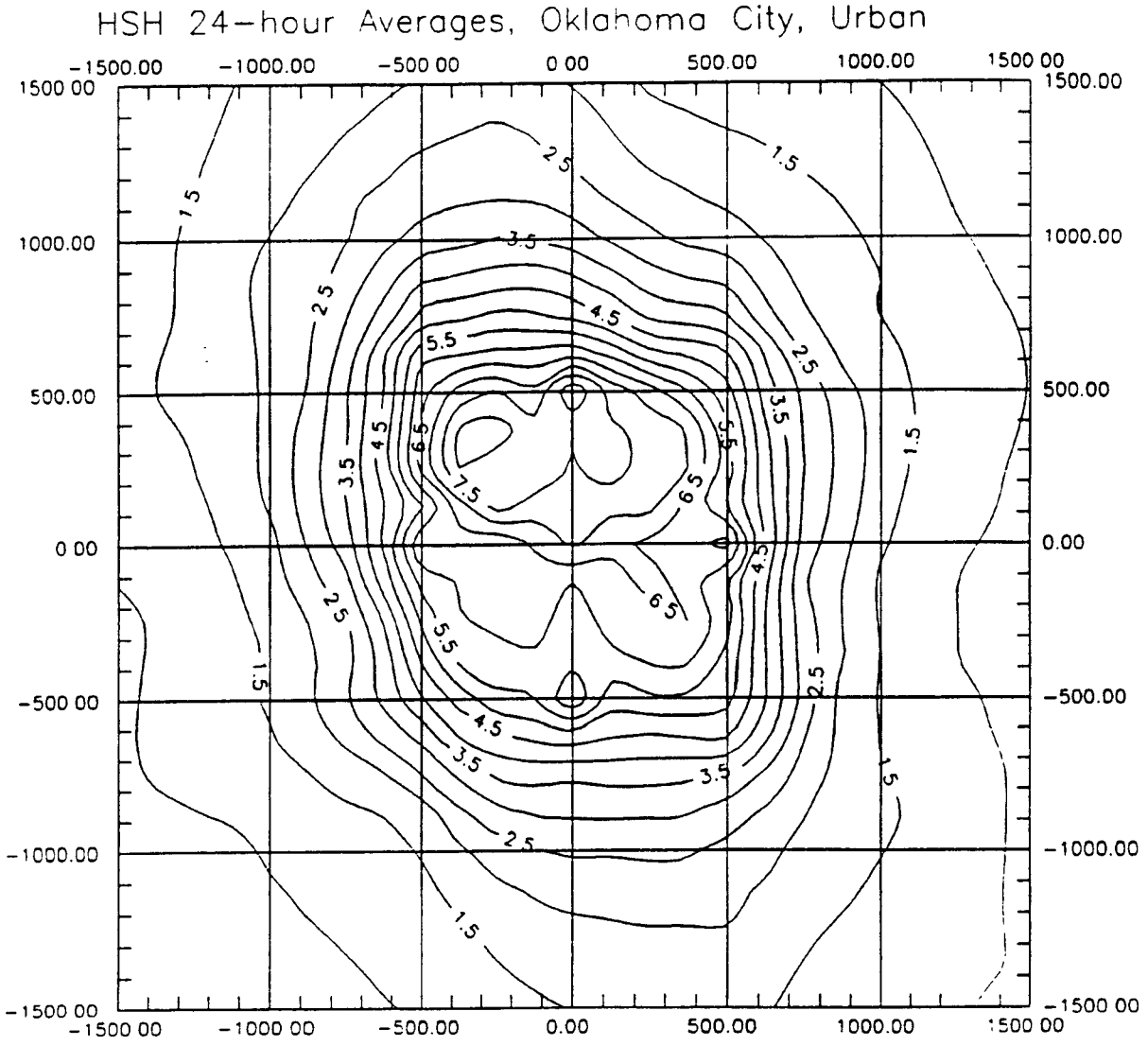

Figure 36. Contour Diagram of HSH 24-hour Average Urban Concentrations ($\mu g/m^3$) from the Finite Line Segment Algorithm for the 1000 Meter Wide Ground Level Source with Close-in Receptors Using Oklahoma City 1988 Data.

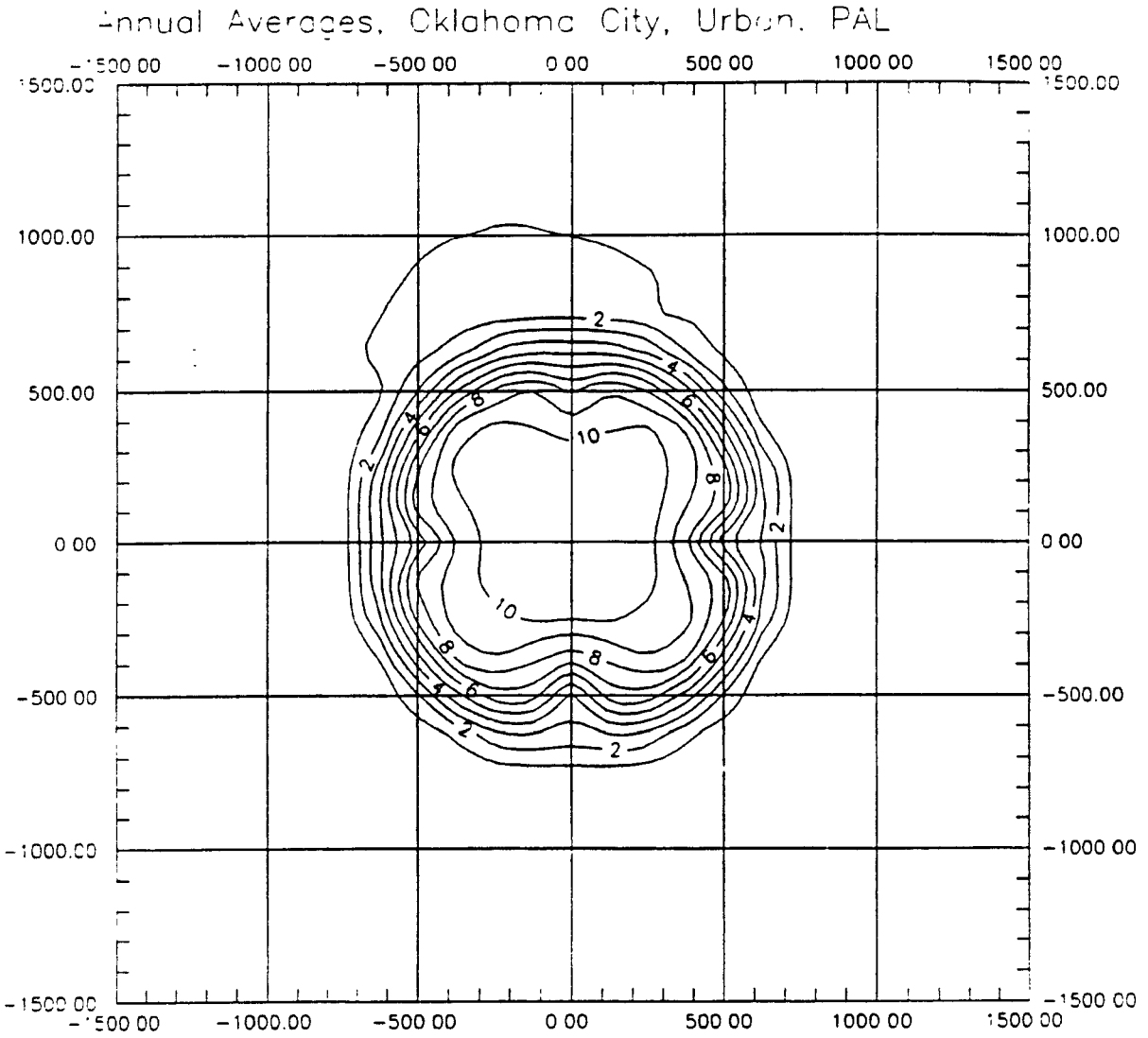

Figure 37. Contour Diagram of Annual Average Urban Concentrations ($\mu g/m^3$) from the Numerical Integration Algorithm for the 1000 Meter Wide Ground Level Source with Close-in Receptors Using Oklahoma City 1988 Data.

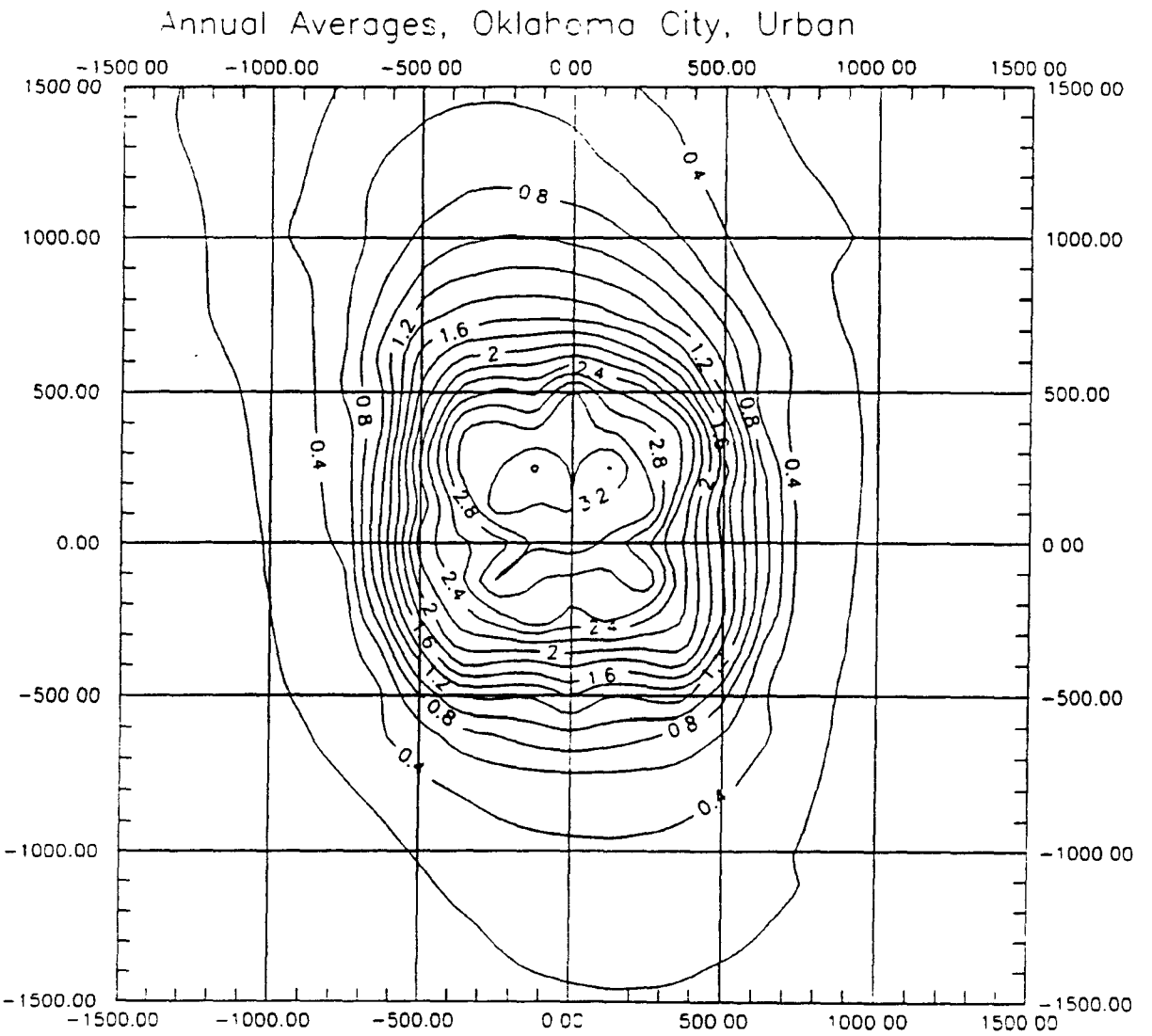

Figure 38. Contour Diagram of Annual Average Urban Concentrations ($\mu g/m^3$) from the Finite Line Segment Algorithm for the 1000 Meter Wide Ground Level Source with Close-in Receptors Using Oklahoma City 1988 Data.

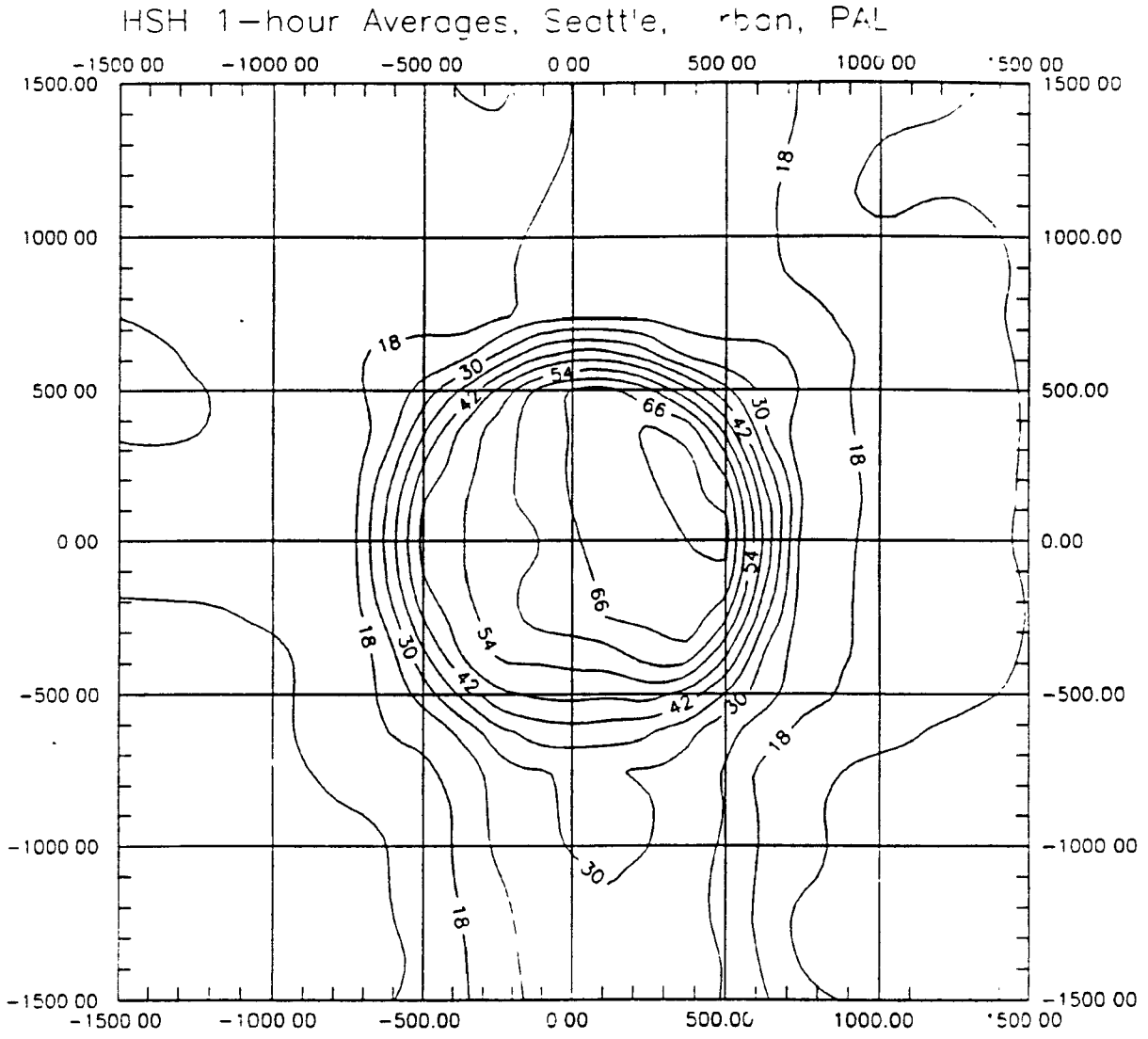

Figure 39. Contour Diagram of HSH 1-hour Average Urban Concentrations ($\mu g/m^3$) from the Numerical Integration Algorithm for the 1000 Meter Wide Ground Level Source with Close-in Receptors Using Seattle 1983 Data.

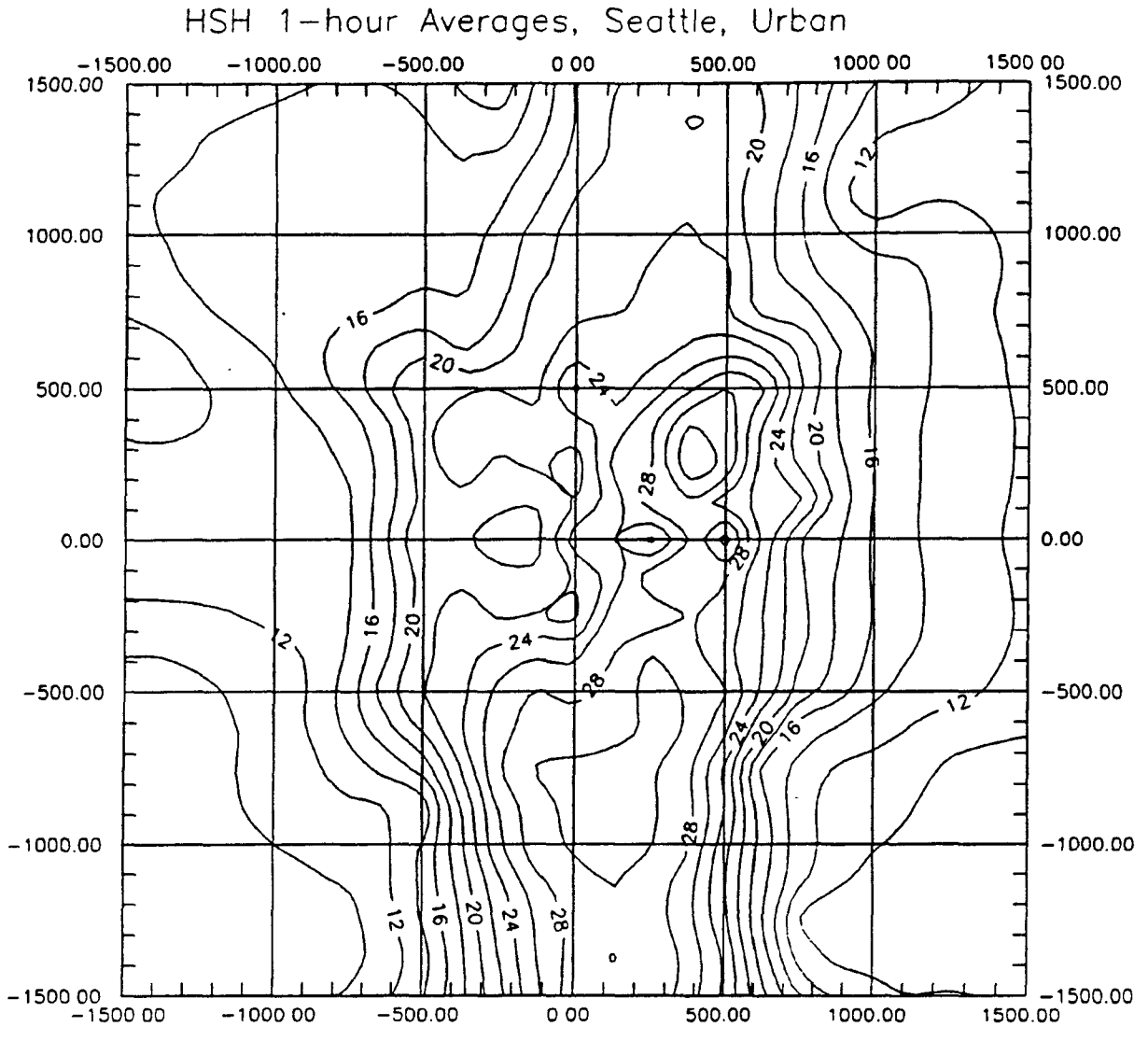

Figure 40. Contour Diagram of HSH 1-hour Average Urban Concentrations ($\mu g/m^3$) from the Finite Line Segment Algorithm for the 1000 Meter Wide Ground Level Source with Close-in Receptors Using Seattle 1983 Data.

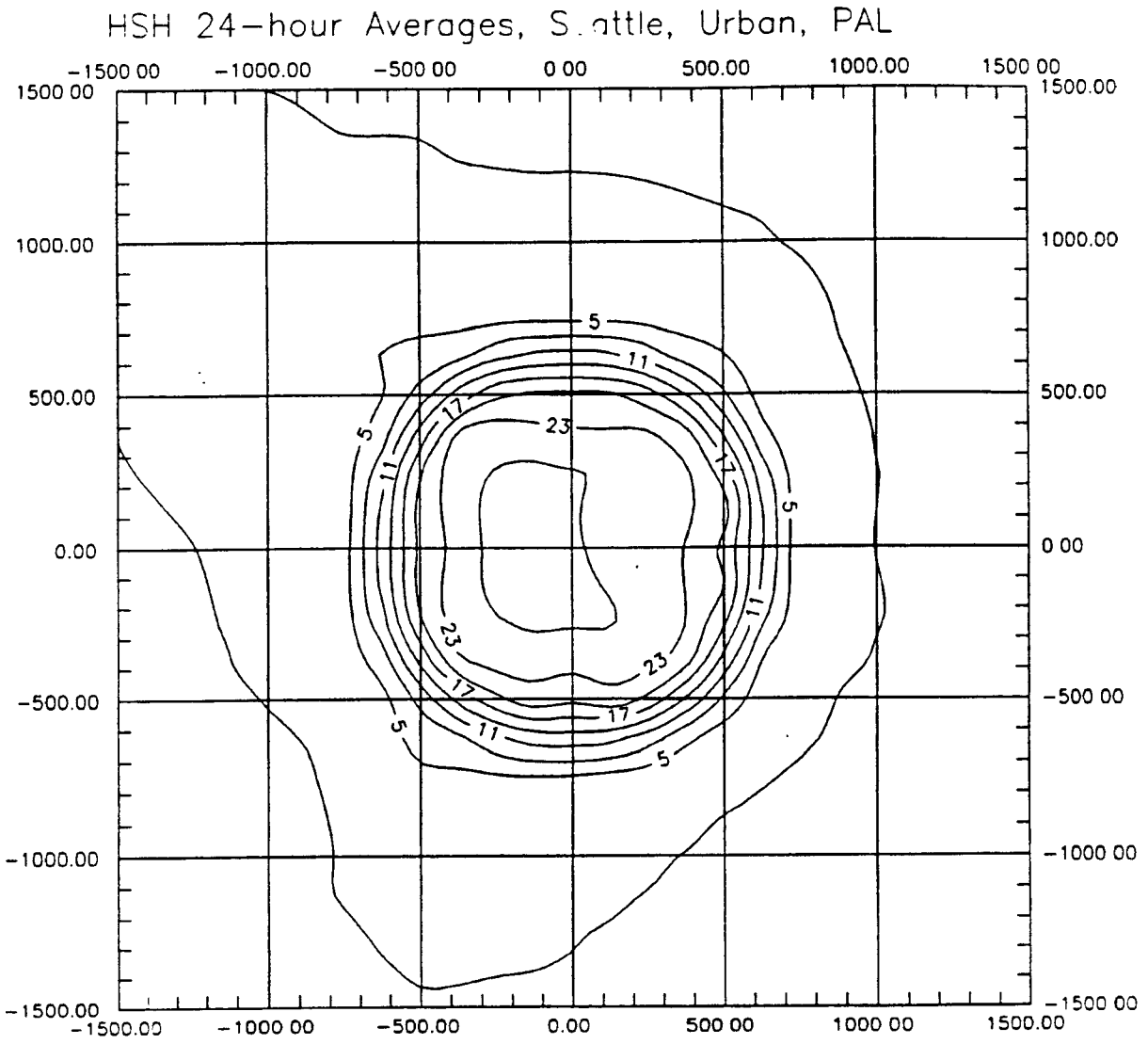

Figure 41. Contour Diagram of HSH 24-hour Average Urban Concentrations ($\mu g/m^3$) from the Numerical Integration Algorithm for the 1000 Meter Wide Ground Level Source with Close-in Receptors Using Seattle 1983 Data.

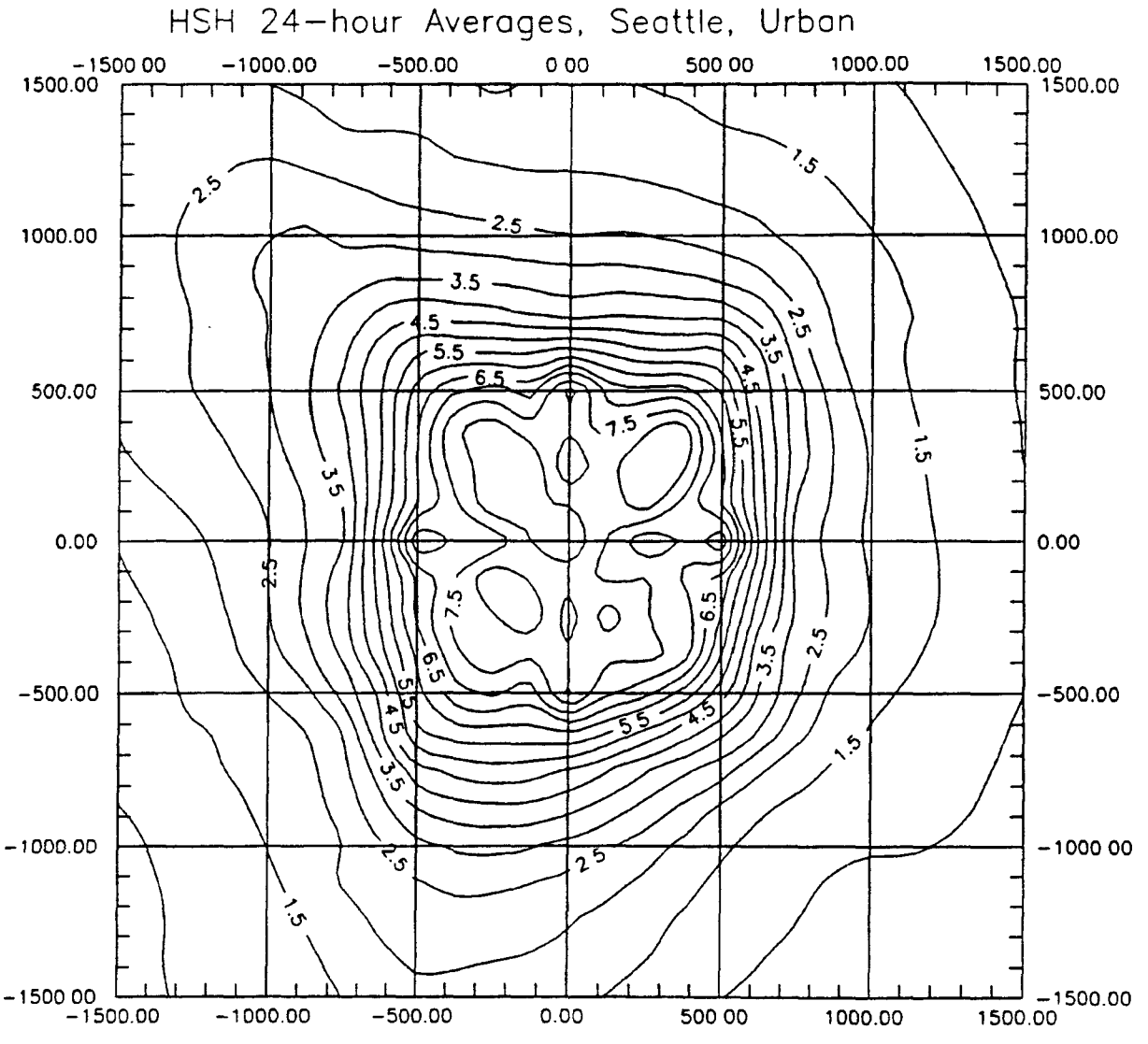

Figure 42. Contour Diagram of HSH 24-hour Average Urban Concentrations ($\mu g/m^3$) from the Finite Line Segment Algorithm for the 1000 Meter Wide Ground Level Source with Close-in Receptors Using Seattle 1983 Data.

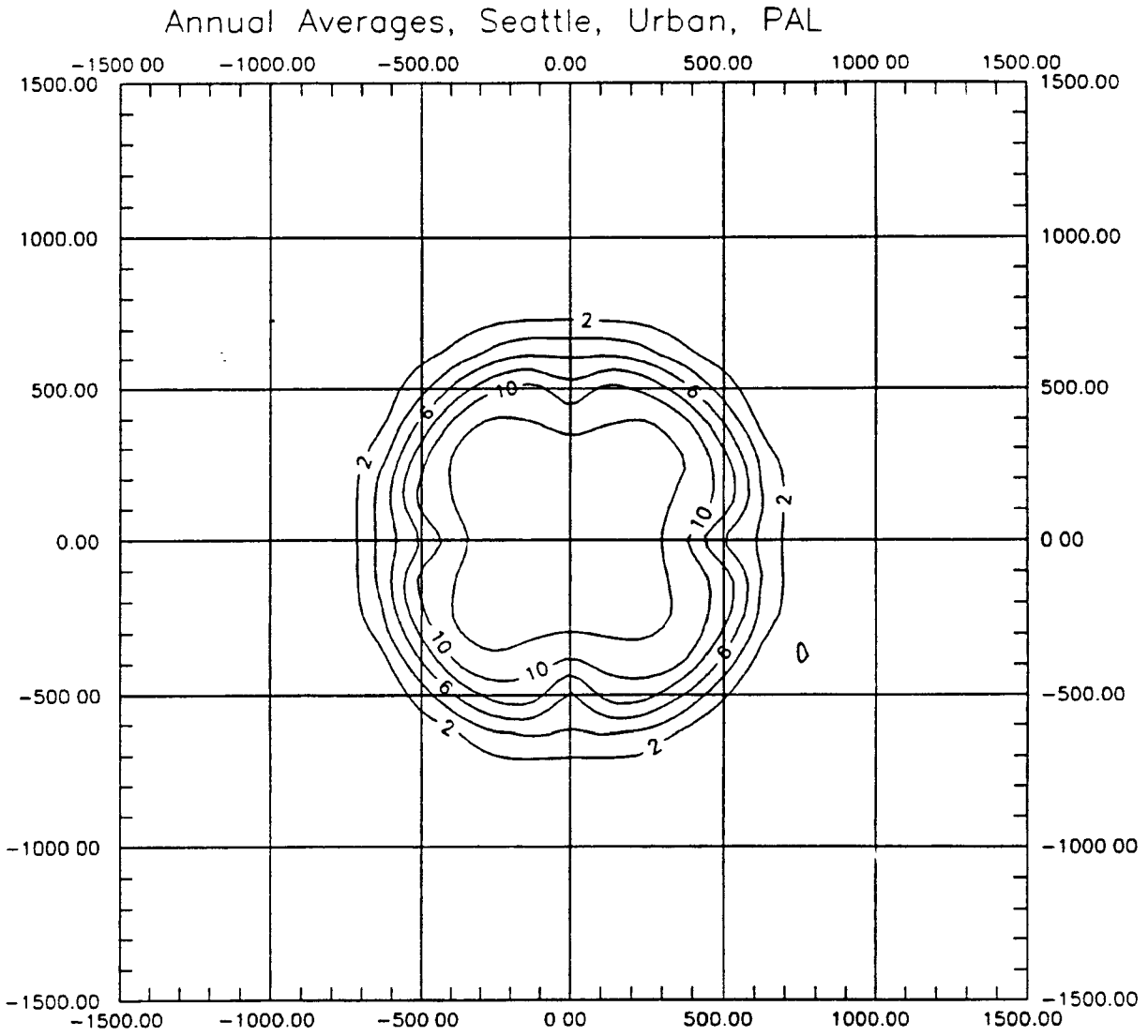

Figure 43. Contour Diagram of Annual Average Urban Concentrations ($\mu g/m^3$) from the Numerical Integration Algorithm for the 1000 Meter Wide Ground Level Source with Close-in Receptors Using Seattle 1983 Data.

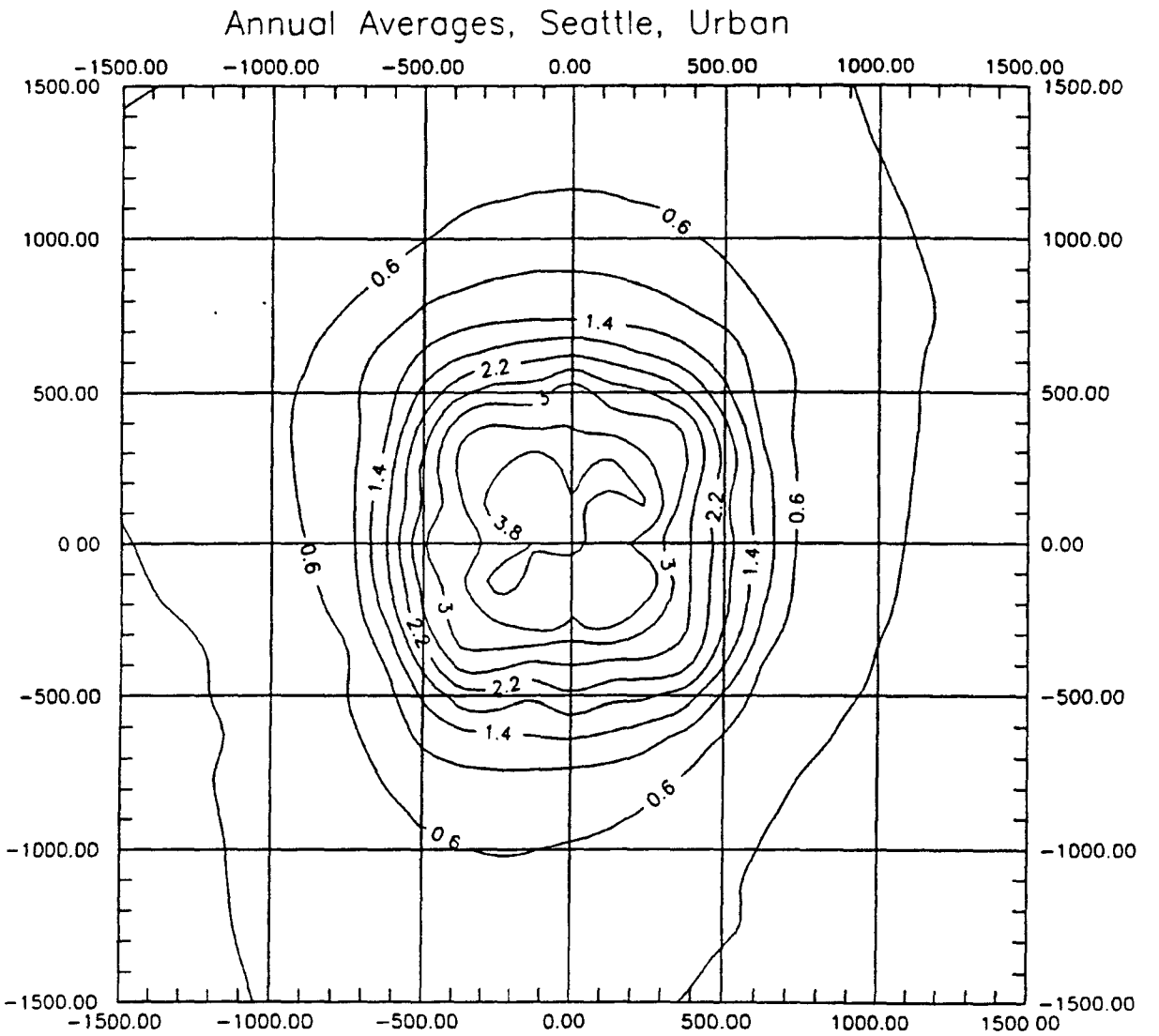

Figure 44. Contour Diagram of Annual Average Urban Concentrations ($\mu g/m^3$) from the Finite Line Segment Algorithm for the 1000 Meter Wide Ground Level Source with Close-in Receptors Using Seattle 1983 Data.

4. LIMITED COMPARISON WITH FDM RESULTS

The Fugitive Dust Model (FDM) also includes an integrated line source algorithm for modeling impacts from area sources (TRC, 1990). It was originally intended that the sensitivity analysis presented in this report would include results of the FDM model for the cases using rural dispersion coefficients (FDM does not include the option for using urban dispersion coefficients). However, comparison of the integrated line source results based on the numerical integration method used in the new ISCST2 model with initial FDM results generated by EPA Region X showed unexpectedly large differences. The ISCST2 numerical integration results were generally about 50 to 100 percent larger than the FDM results, with larger differences in a few cases. Upon further investigation, it was discovered that these differences were attributable to three assumptions made by FDM in its implementation of the integrated line source algorithm. Specifically, FDM assumes:

1) a minimum mixing height of 100 meters;

2) a minimum release height of 0.5 meters; and

3) that the rural dispersion coefficients are representative of a 10-minute averaging period and a surface roughness of 3 cm.

The FDM model uses the third assumption as the basis for adjusting the lateral and vertical dispersion coefficients. When the numerical integration algorithm in the new ISCST2 model was modified to use the first two assumptions, and the FDM model was modified to eliminate the third assumption (i.e., setting the sigma adjustments factors = 1.0), the corresponding results of the two models were very comparable, agreeing to within a few percent in most cases. Table 10 presents these results for the very small (10 meter wide) ground level area source case (with a release height = 0.5 meters).

The largest difference in Table 10 is about 10 percent for the Seattle 3-hour HSH. Upon further investigation it was discovered that the FDM model includes an error in the code that effects the calms processing routines for 3-hour averages. If one hour during a three-hour period is calm, then the FDM model sums the remaining two hours and divides by two for the average. The correct procedure is to divide by three in this case, since two hours is less than 75 percent of the 3-hour averaging period. This error leads to larger 3-hour averages for cases including calm hours from FDM than from ISCST2, and accounts for the larger differences in Table 10 for 3-hour averages.

Another difficulty in comparing ISCST2 results with FDM results is related to the fact that the FDM model includes two different modes of implementing the integrated line source algorithm. One mode uses a 5-line integration to approximate the area source, while the other mode "converges" to a more accurate representation of the area source. The convergent mode begins by comparing results for 5 lines versus 6 lines. If convergence is not indicated, then the model continues by comparing results for 10 lines versus 11 lines, and then for 15 lines versus 16 lines, and so on until convergence is reached, out to a limit of 901 lines. The 5-line and convergent algorithm were both executed for the 10-meter wide area source, and gave comparable estimates (to within a few percent difference). However, the convergent mode could not successfully be executed on the X-Large, Close-in case because of the extremely long execution time involved (it was estimated that it would take at least 45 days to complete a one year simulation with 180 receptors on a 33-MHz 486 computer, compared to about 6 hours using the numerical integration method implemented in the new ISCST2 model). Therefore, the FDM model was only run for selected receptors in order to compare FDM convergent results with results from the numerical integration algorithm in the ISCST2 model. Based on these limited comparisons it is concluded that the numerical integration algorithm gives results that are very comparable to the FDM convergent results, to within about one percent difference. This conclusion is based on comparisons for receptors located both within the area for the close-in case and downwind of the area for other ground level cases, and also includes the receptor locations for the highest impacts as well as receptors with relatively low impacts.

Comparisons were also made between the FDM convergent results and the FDM 5-line results for selected receptors located within the area. These comparisons show that the 5-line integration is not reliable for receptors located within the area. The 5-line results showed very large variations over relatively short distances, especially near the center of the area. Since FDM divides the area into 5 lines regardless of where the receptor is located, the impacts for receptors located within the area are estimated based only on the lines that are located upwind of the receptor for a given hour.

The conclusion from all of these comparisons between the ISCST2 numerical integration algorithm and the FDM integrated line source algorithm is that ISCST2 provides a much more efficient and reliable algorithm for modeling impacts at receptors located within and nearby the area, and that it gives comparable results to the FDM convergent algorithm when modeled based on the same assumptions for release height, mixing height, and dispersion parameters. Moreover, the current version of FDM includes an error in the implementation of the calms processing routines for 3-hour averages.

Table 10

Comparison of ISCST2* Numerical Integration Results With FDM** 5-Line Results for the Very Small Source (10m Width) - Rural

	ISCST2 Numerical Integration	FDM 5-Line Integration	Ratio ISCST2/FDM
Pittsburgh 1964			
1-hr High	112172	116993	0.96
1-hr HSH	95015	94148	1.01
3-hr High	66169	68600	0.96
3-hr HSH	62426	64601	0.97
24-hr High	28378	28745	0.99
24-hr HSH	21035	21311	0.99
Annual	3208	3205	1.00
Okla. City 1988			
1-hr High	113594	119314	0.95
1-hr HSH	113594	119314	0.95
3-hr High	68653	69308	0.99
3-hr HSH	51986	51419	1.01
24-hr High	25432	25442	1.00
24-hr HSH	20537	20456	1.00
Annual	5853	5891	0.99
Seattle 1983			
1-hr High	107377	108872	0.99
1-hr HSH	104723	105308	0.99
3-hr High	55576	61648	0.90
3-hr HSH	48897	52654	0.93
24-hr High	21933	22547	0.97
24-hr HSH	20231	20753	0.97
Annual	5014	5002	1.00

* ISCST2 results are based on a minimum mixing height of 100 meters and a release height of 0.5 meters.

** FDM results are based on a minimum mixing height of 100 meters, a minimum release height of 0.5 meters, and no sigma adjustment factors.

5. REFERENCES

Brode, R.W., 1992: Summary of the Quality Assurance and Equivalence Tests Performed on the Modified Area Source Algorithm for the ISCST2 Model. Internal Project Report, WA I-27, U.S. Environmental Protection Agency, Research Triangle Park, North Carolina.

Environmental Protection Agency, 1989: Review and Evaluation of Area Source Dispersion Algorithms for Emission Sources at Superfund Sites. EPA-450/4-89-020. U.S. Environmental Protection Agency, Research Triangle Park, North Carolina.

Environmental Protection Agency, 1992. User's Guide for the Industrial Source Complex (ISC2) Dispersion Models. EPA-450/4-92-008. U.S. Environmental Protection Agency, Research Triangle Park, North Carolina.

Petersen, W.B. and E.D. Rumsey, 1987. User's Guide for PAL 2.0 - A Gaussian-Plume Algorithm for Point, Area, and Line Sources. EPA/600/8-87/009. U.S. Environmental Protection Agency, Research Triangle Park, North Carolina.

TRC Environmental Consultants, 1990: User's Guide for the Fugitive Dust Model (FDM), (Revised). EPA-910/9-88-202R. U.S. Environmental Protection Agency - Region 10, Seattle, Washington.

TECHNICAL REPORT DATA
(Please read Instructions on reverse before completing)

1. REPORT NO.	2.	3. RECIPIENT'S ACCESSION NO.
EPA-454/R-92-015		

4. TITLE AND SUBTITLE	5. REPORT DATE
Sensitivity Analysis of the Revised Area Source Algorithm for the ISC2 Short Term (ISCST2) Model	October 1992
	6. PERFORMING ORGANIZATION CODE
7. AUTHOR(S)	8. PERFORMING ORGANIZATION REPORT NO.
9. PERFORMING ORGANIZATION NAME AND ADDRESS Pacific Environmental Services 5001 South Miami Boulevard Post Office Box 12077 Research Triangle Park, NC 27709-2077	10. PROGRAM ELEMENT NO.
	11. CONTRACT/GRANT NO. WA No. I-131 EPA Contract No. 68 D00124
12. SPONSORING AGENCY NAME AND ADDRESS U.S. Environmental Protection Agency Office of Air Quality Planning and Standards Technical Support Division Research Triangle Park, NC 27711	13. TYPE OF REPORT AND PERIOD COVERED Final Report
	14. SPONSORING AGENCY CODE

15. SUPPLEMENTARY NOTES
EPA Work Assignment Manager: Jawad S. Touma

16. ABSTRACT

This report includes information on an improved algorithm for modeling dispersion from area sources, which has been developed based on a numerical integration of the point source concentration function. A sensitivity analysis is presented of the algorithm as implemented in the short-term version of the Industrial Source Complex (ISC2) model. To examine the sensitivity of the design concentrations across a range of source characteristics, five ground-level area sources were modeled, with sizes varying from 10 meters to 1,000 meters in width. An elevated source scenario consisting of a 100-meter wide area with a release height of 10 meters was also modeled. An additional case involving 1,000 meter wide ground level area was also modeled with receptors located within and nearby the area. The high and high-second (HSH) 1-hour, 3-hour and 24-hour averages and high annual averages were determined for each of these source scenarios using a full year of real time meteorological data. All of the sources were modeled as square areas oriented N-S and E-W, since the original ISC algorithm was limited to handling that source geometry. Each scenario was run for one year of National Weather Service meteorological data from Pittsburgh, PA (1964); one year of NWS data from Oklahoma City, OK (1988); one year of NWS data from Seattle, WA (1983). This report is being released to establish a basis for reviews of the capabilities of this methodology and of the consequences resulting from use of this methodology in routine dispersion modeling of air pollutant impacts.

17. KEY WORDS AND DOCUMENT ANALYSIS

a. DESCRIPTORS	b. IDENTIFIERS/OPEN ENDED TERMS	c. COSATI Field/Group
Air Pollution Toxic Air Pollutants Air Quality Dispersion Models	Dispersion Modeling Meteorology Air Pollution Control	

18. DISTRIBUTION STATEMENT	19. SECURITY CLASS (Report)	21. NO. OF PAGES
Release Unlimited	Unclassified	
	20. SECURITY CLASS (Page) Unclassified	22. PRICE

EPA Form 2220-1 (Rev. 4-77) PREVIOUS EDITION IS OBSOLETE